SIMULATION OF HYDRODYNAMICS AND SOLUTE TRANSPORT IN THE PAMLICO RIVER ESTUARY, NORTH CAROLINA

By Jerad D. Bales and Jeanne C. Robbins

U.S. GEOLOGICAL SURVEY

Open-File Report 94-454

Albemarle-Pamlico Estuarine Study Report No. 94-10

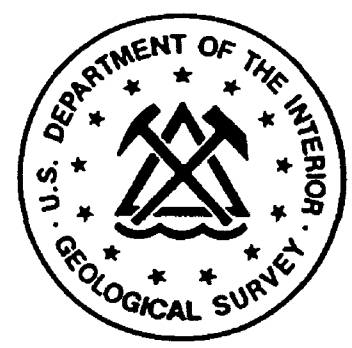

Prepared in cooperation with the

ALBEMARLE-PAMLICO ESTUARINE STUDY of the

NORTH CAROLINA DEPARTMENT OF ENVIRONMENT, HEALTH, AND NATURAL RESOURCES

Raleigh, North Carolina

1995

U.S. DEPARTMENT OF THE INTERIOR
BRUCE BABBITT, Secretary

U.S. GEOLOGICAL SURVEY
Gordon P. Eaton, Director

Any use of trade, product, or firm names is for descriptive purposes only and does not imply endorsement by the U.S. Geological Survey or the State of North Carolina.

For additional information write to:

District Chief
U.S. Geological Survey
3916 Sunset Ridge Road
Raleigh, North Carolina 27607

Copies of this report may be purchased from:

U.S. Geological Survey
Earth Science Information Center
Open-File Reports Section
Denver Federal Center, Box 25286, MS 517
Denver, Colorado 80225

CONVERSION FACTORS, TEMPERATURE, VERTICAL DATUM, AND ABBREVIATIONS

Multiply	By	To obtain
	Length	
centimeter (cm)	0.3937	inch
meter (m)	3.281	foot
kilometer (km)	0.6214	mile
	Area	
square meter (m^2)	10.76	square foot
square kilometer (km^2)	0.3861	square mile
	Volume	
cubic meter (m^3)	35.31	cubic foot
	Mass	
gram (g)	0.03527	ounce avoirdupois
kilogram (kg)	2.205	pound avoirdupois

Temperature: In this report, temperature is given in degrees Celsius (°C), which can be converted to degrees Fahrenheit (°F) by the following equation:

$$°F = 1.8\ (°C) + 32$$

Sea level: In this report, "sea level" refers to the National Geodetic Vertical Datum of 1929 (NGVD of 1929)—a geodetic datum derived from a general adjustment of the first-order level nets of both the United States and Canada, formerly called Sea Level Datum of 1929.

Abbreviations and acronyms used in this report in addition to those shown above:

cm/s	centimeter per second
m/d	meter per day
m/s	meter per second
m^2/s	square meter per second
m^3/s	cubic meter per second
ppt	parts per thousand
ppt/km	parts per thousand per kilometer

CONTENTS

ILLUSTRATIONS

ILLUSTRATIONS (Continued)

TABLES

SIMULATION OF HYDRODYNAMICS AND SOLUTE TRANSPORT IN THE PAMLICO RIVER ESTUARY, NORTH CAROLINA

By Jerad D. Bales *and* Jeanne C. Robbins

ABSTRACT

An investigation was conducted to characterize flow, circulation, and solute transport in the Pamlico River estuary. The study included a detailed field-measurement program and calibration, validation, and application of a physically realistic numerical model of hydrodynamics and transport to a 48-kilometer reach of the estuary.

Water level, salinity, water temperature, wind speed and direction, current velocity, and bathymetric data were collected during the study period March 1988 through September 1992. Additional data from pre-existing continuous-record streamflow gaging stations and meteorological stations also were used in the study. During the study period, the mean daily water-level range was 0.322 meter at the upstream end of the study reach and 0.179 meter at the downstream end. Mean near-surface salinities ranged from 2.2 parts per thousand near Washington, North Carolina, at the upstream end of the study reach to 11.0 parts per thousand at the downstream end of the study reach, and mean near-bottom salinities ranged from 4.7 parts per thousand near Washington to 11.4 parts per thousand at the downstream end of the study reach. Daily variations in salinity generally were less than 2 parts per thousand. Wind speeds generally were greatest during the winter months, when winds were from the west, northwest, and north. Current meters deployed for a 15-day period recorded velocities ranging from a maximum downstream velocity of 31 centimeters per second to a maximum upstream velocity of 34 centimeters per second, with a marked difference in velocity direction and magnitude across the estuary.

A two-dimensional, vertically averaged hydrodynamic and solute-transport model was applied to the study reach. The model domain was discretized into 5,620 computational cells, 200 x 200 meters each, bounded by the estuary shoreline. Model calibration was achieved through adjustment of model parameters for June 14-30, 1991. Additional simulations for the periods August 30-September 12, 1989, and July 4-28, 1991, were used to validate the model. The model was calibrated and validated for water levels ranging from -0.052 to 0.698 meter, for salinities ranging from 0.1 to 13.1 parts per thousand, and for wind speeds from calm to 22 meters per second. The model was tested for stratified and unstratified conditions. The mean difference between simulated and observed water levels was less than 2 centimeters. The mean differences between simulated and observed salinities at three interior checkpoints were less than 1 part per thousand.

Simulated results were sensitive to the value of the wind-stress coefficient but were relatively insensitive to changes in other model parameters. The presence of a lateral water-level gradient at the downstream open-water boundary changed the net transport because of an associated change in the overall longitudinal gradient. The addition of open-water boundaries at two tributary streams had little effect on simulated circulation and salinity patterns in the estuary.

Simulated flows for four periods in 1989 and 1991 ranged from 610 cubic meters per second in the upstream direction to 543 cubic meters per second in the downstream direction at the upper end of the study reach, and from 5,930 cubic meters per second in the upstream direction to 6,970 cubic meters per second in the downstream direction at the lower end of the study reach. Simulations showed the presence of topographic eddies and lateral differences in velocity, including concurrent upstream and downstream flow at a given cross section. Particle-track analyses

demonstrated that particles released at mid-estuary may not exit the estuary for as long as 25 days. Simulation of the transport of a conservative solute released at mid-estuary showed the solute to be diluted 500 times the original strength across the estuary after 5 days of continuous release; the solute was present over a 17-kilometer reach of the estuary after 19.3 days of continuous release.

INTRODUCTION

The Pamlico River was at one time considered to be one of the most productive estuaries in the eastern United States (North Carolina Department of Natural Resources and Community Development, 1989). Historically, the Pamlico River has supported major commercial and recreational fisheries, which have been described as the most important in the State (Rader and others, 1987). Primary and secondary nursery areas vital to a variety of estuarine-dependent finfish and shellfish are located along the shore and in tributary creeks of the eastern part of the estuary.

Symptoms of environmental stress are present, and in some cases increasing, in the Pamlico River. Environmental concerns include declining fish catches, finfish and blue crab diseases, algal blooms, low dissolved-oxygen levels, sedimentation, the alteration of the natural hydrology of nursery areas, and the disappearance of some species of benthic plants (Rader and others, 1987; North Carolina Department of Natural Resources and Community Development, 1989). Elevated levels of mercury, cadmium, copper, and other trace metals occur in Pamlico River bed sediments (Riggs and others, 1989). Total ammonia plus organic nitrogen and total phosphorus concentrations in the Pamlico River generally increased between 1970 and 1988 (Harned and Davenport, 1990). In 1989, the Tar-Pamlico River Basin was designated as Nutrient Sensitive Waters by the State Environmental Management Commission, resulting in more strict limits on the discharge of nutrients into the waters of the basin.

The hydrodynamic processes in natural water bodies are key components of the complex aquatic ecosystem. Water movements at different scales and of different types govern the distribution of salt, dissolved gases, nutrients, and sediment in estuaries, as well as the aggregation and distribution of microorganisms and plankton. The proper description of flows and circulation is critical to the understanding and management of water quality, productivity, and distribution and abundance of biota in estuaries.

Because of the complexities of estuaries, field measurements and numerical models are needed to understand and describe circulation processes. Field observations provide useful information for characterizing and understanding local physical and biochemical processes and for detecting trends. However, the expense of field measurements and the extreme heterogeneity of the estuarine environment limit the extent to which measurements can be extrapolated over space and time. According to Signell and Butman (1992), generalization of field measurements must be qualified by the specific conditions under which the data are collected.

Numerical models provide the capability to describe physical and biochemical processes with high spatial resolution throughout the entire estuary. Numerical models can also be used to conduct experiments by evaluating estuarine response to a wide range of imposed tidal, inflow, meteorological, and chemical loading conditions. The design of field-measurement programs can sometimes be improved through the application of a numerical model to identify important locations or processes that should be measured. Numerical models are limited, however, by the manner in which physical processes are represented by the model, the assumptions and simplifications included in the model, the numerical scheme used to solve the governing equations, and the availability of reliable field observations. Scientifically credible and effective modeling requires carefully collected field measurements for use in model calibration, validation, and application.

The development of numerical models to characterize water circulation was identified as a high-priority goal of the Albemarle-Pamlico Estuarine Study (North Carolina Department of Natural Resources and Community Development, 1987). Moreover, successful implementation of the State's innovative whole-basin approach to water-quality management requires the development and application of sophisticated numerical models to, among other things, assist in wasteload allocation (Creager and others, 1991). Issues such as the origin of depressed dissolved-oxygen levels, resuspension and movement of contaminated sediments, residence times of nutrients, and flushing of pollutants cannot be addressed fully without an understanding and documentation of water movement in the estuary.

To address the specific need for a reliable numerical model of flows and transport in the Pamlico River, the U.S. Geological Survey (USGS), in cooperation with the Albemarle-Pamlico Estuarine Study of the North Carolina Department of Environment, Health, and Natural Resources, conducted an investigation of hydrodynamics and transport in the Pamlico River. The investigation included a detailed field-measurement program and the calibration, validation, and application of a physically realistic numerical model of hydrodynamics and solute transport. The objectives of the modeling were to (1) provide a spatially detailed description of circulation and solute transport in the estuary, (2) develop the capability to compute flow rates, and (3) characterize the movement of passive materials in the estuary.

Purpose and Scope

This report documents development and application of a two-dimensional, unsteady hydrodynamic and solute-transport model for a reach of the Pamlico River which extends 48 kilometers (km) downstream (east) from the U.S. Highway 17 bridge near Washington, North Carolina. The model is based on vertically integrated equations of motion and transport solved by using the alternating-direction implicit (ADI) numerical scheme on a finite-difference grid. The governing equations solved within the model are nonlinear, time-dependent, and retain coupling of motion and transport.

A general description of the study area and an overview of previous investigations is followed by a summary of the data collection. Data collected during 1988-92 are used to provide a general characterization of the hydrologic conditions in and around the Pamlico River. The numerical model, including the governing equations, numerical solution scheme, and input requirements, is described in some detail in order to document model capabilities and limitations. Model construction, calibration, and validation are documented, along with the results of an analysis of model sensitivity to changes in various parameters. The model is then applied to the study reach to characterize flow, circulation patterns, and solute transport for different sets of hydrologic conditions.

Approach

The approach leading to the development and implementation of the hydrodynamic and solute-transport model consisted of data collection to characterize conditions in the study area and to implement and operate the model; model calibration, validation, and sensitivity testing; and model application. Data collection included measurements of water level, salinity, wind speed and direction, inflow from tributary streams, and channel bathymetry.

Model calibration is accomplished by adjusting model parameters until model results agree with observations (Ditmars and others, 1987). The model is considered to be validated if model results agree with observations distinct from those used for model calibration without further adjustment of model parameters (Ditmars and others, 1987). The model is assumed to be valid over the range of conditions used in the calibration and validation process. Sensitivity testing is the determination of the effects of small changes in model parameters or input data on model results.

The validated model was applied to the study reach to compute flows, circulation patterns, and solute transport for different hydrologic conditions. Model simulations also were used to track the movement of materials released at different locations within the study reach under different flow conditions.

Description of Study Area

The Pamlico River estuary lies within the Coastal Plain physiographic province of North Carolina (fig. 1). Much of the shoreline surrounding the estuary is composed of marshes, particularly near the mouth of the estuary (Bellis and others, 1975; Copeland and others, 1984). Land-surface elevations in the area are generally less than 8 meters (m) above sea level. Streams that drain to the Pamlico River have small drainage basins with little topographic relief, low sediment loads, and fairly acidic waters (Copeland and others, 1984).

The climate of the region is mild and moderately moist. The annual mean temperature is about 16 degrees Celsius (°C), and the mean annual precipitation is about 125 centimeters (cm) (Hardy and Hardy, 1971). Interannual variability in precipitation is large, ranging from 80 to 200 cm, but on the average, precipitation is relatively uniform throughout the year,

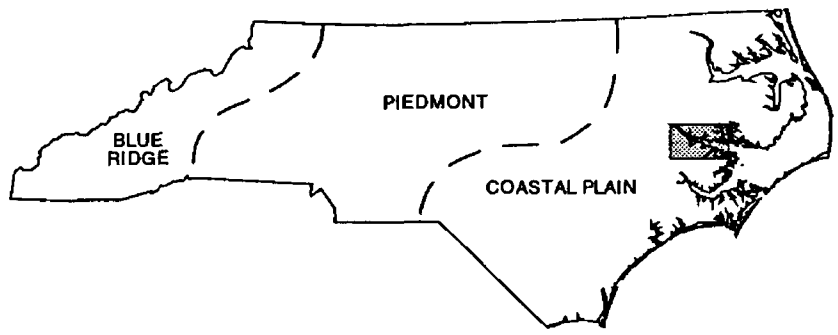

LOCATION OF STUDY AREA AND PHYSIOGRAPHIC PROVINCES IN NORTH CAROLINA

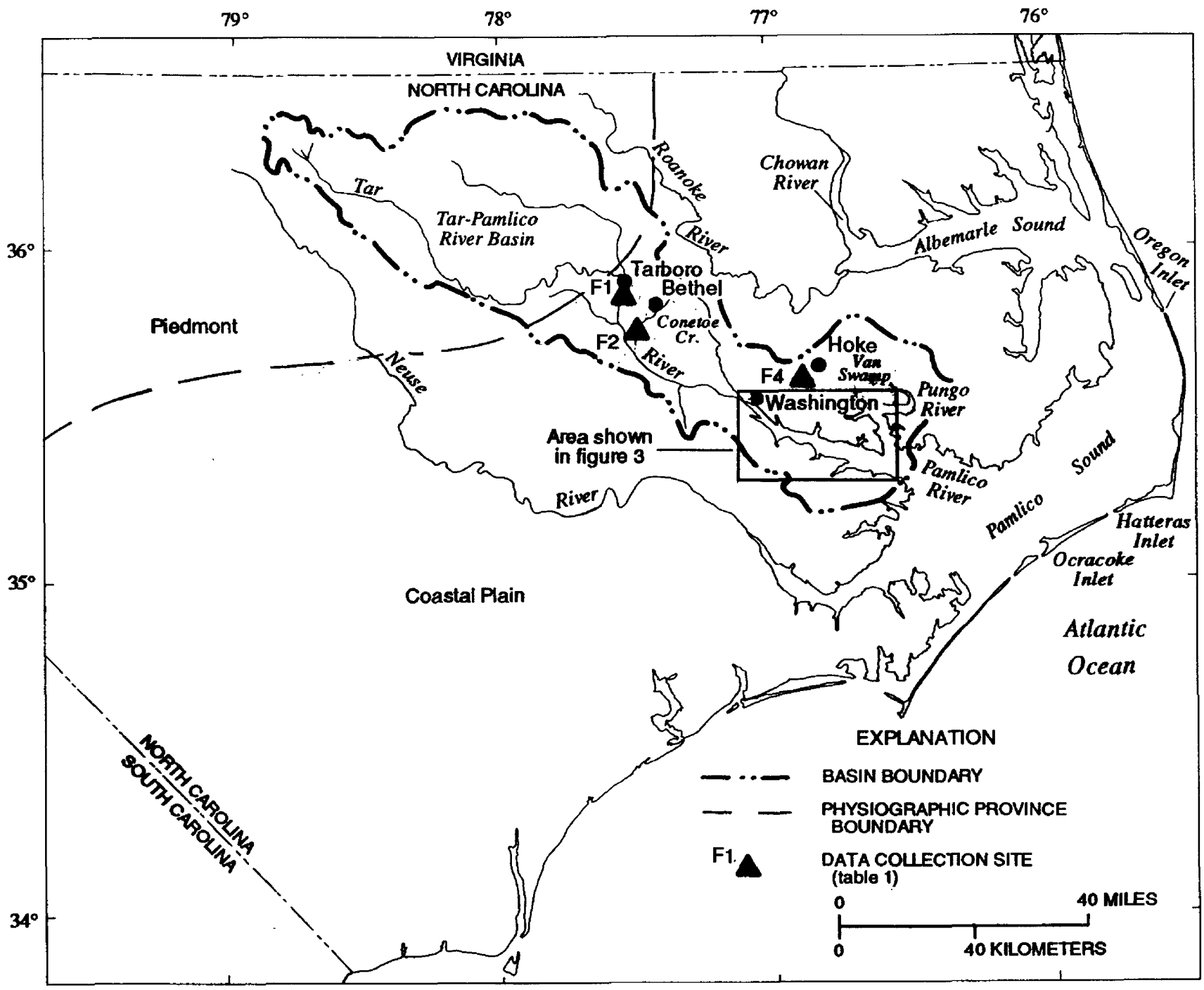

Figure 1. Location of the Tar-Pamlico River and data-collection sites outside of study reach.

although slightly higher rainfall amounts typically occur in July, August, and September. Evapotranspiration rates average about 85 cm per year and exhibit much less variability from year to year than precipitation (Wilder and others, 1978). Winds are typically from the south to southwest between April and August, and from the north to northwest between September and March.

Upstream from Washington, the Pamlico River is known as the Tar River and drains an 8,000-square-kilometer (km^2) rural area in the Piedmont and Coastal Plain Provinces (fig. 1). Between Washington and the confluence of the Pungo River with the Pamlico River (excluding the Pungo River Basin), an additional area of 1,230 km^2 drains

directly to the study reach. The drainage area for the entire Tar-Pamlico Basin is 11,150 km^2 (fig. 1).

The distance from Washington to the confluence of the Pamlico and Pungo Rivers is about 50 km. The Pamlico River estuary increases in width from about 300 m at Washington to more than 6 km just upstream of the Pamlico-Pungo confluence. Maximum depths range from about 3 m at Washington to between 5 and 6 m near the Pamlico-Pungo confluence (fig. 2). The bottom material near Washington is primarily organic-rich mud. In the lower reaches of the estuary, fine-grained materials occur mostly along the channel axis, and sand predominates near the shoreline (Wells, 1989).

The numerical model was developed for the reach of the Pamlico River bounded on the west by the U.S. Highway 17 bridge at Washington and on the east by a section just upstream of the confluence of the Pungo and Pamlico Rivers (figs. 1 and 2). The study reach is 48 km long, 300 m wide at the western (upstream) end, and 6 km wide at the eastern (downstream) end. Some data collection for the investigation occurred outside of this reach.

Previous Studies

There have been many investigations of the hydrology, characteristics, and water quality of the Pamlico River (Bales and Nelson, 1988). Pertinent information from some of these investigations is presented in the Hydrologic Conditions section of this report. There are, however, very little data or information on hydrodynamic and transport processes in the Pamlico River. Horton and others (1967) measured the movement of dye in the Pamlico River. During the 4-day measurement period, the dye cloud moved at an average rate of 915 meters per day (m/d). Horton and others (1967) also constructed a simplified tidal flushing model to estimate exchange rates in the estuary. For low inflow conditions, the predicted flushing time (time for water to move downstream through the entire estuary) was 587 days; the predicted flushing time was 65 days for average freshwater inflow conditions. Results from the tidal flushing model did not compare favorably with available dye and salinity data. Finally, at least two hydrodynamic models of Pamlico Sound have been published (Amein and Airan, 1976; Pietrafesa and others, 1986), but these models did not include the Pamlico River.

Acknowledgments

This study was conducted in cooperation with the Albemarle-Pamlico Estuarine Study of the North Carolina Department of Environment, Health, and Natural Resources. The support and assistance of former study directors D.N. Rader, R.E. Holman, and R.G. Waite are greatly appreciated. Staff from the North Carolina Division of Environmental Management and Division of Marine Fisheries assisted with the design of the data-collection network and with the collection of some data. The U.S. Coast Guard granted permission for the installation of instrumentation on Pamlico River multipile channel markers. The assistance of the U.S. Coast Guard in installing data-collection instrumentation on channel markers and in deploying and recovering current meters is also gratefully acknowledged. The cooperation of the following landowners, who allowed water-level recorders to be installed on their property, is appreciated: Mr. William M. Daniels, Jr., Pamlico Beach; Ms. Lorraine Shinn, South Creek; and Mr. Earl Sadler, Lowland.

DATA COLLECTION AND HYDROLOGIC CONDITIONS

Scientifically credible and effective modeling requires carefully collected, continuous records of boundary data for model application and short-term records for model calibration and validation. To provide the required information for the Pamlico River estuary hydrodynamic model and to better define the physics of flow in the Pamlico River, water level, salinity and water temperature, wind speed and direction, current velocity, and bathymetric data were collected from March 1988 through September 1992. Data from pre-existing continuous-record streamflow gaging stations and meteorological stations were also available during this period.

Water Level

Water-surface elevations were recorded at 15-minute intervals at five locations in the study reach (fig. 3; table 1). Elevations were referenced to sea level. Water-level records from sites WL1 and WL4 were used for model boundary data, and records from sites WL2, WL3, and WL5 were used for model calibration and validation. Data collection began in March 1988 and continued at some stations through September 1992 (fig. 4).

Because of the relatively small water-level gradients in the estuary and the importance of these gradients in affecting hydrodynamic conditions, efforts were made to ensure the highest possible accuracy in gage datums. The North Carolina Geodetic Survey conducted a ground survey in which all gage datums were tied to the national first-order network.

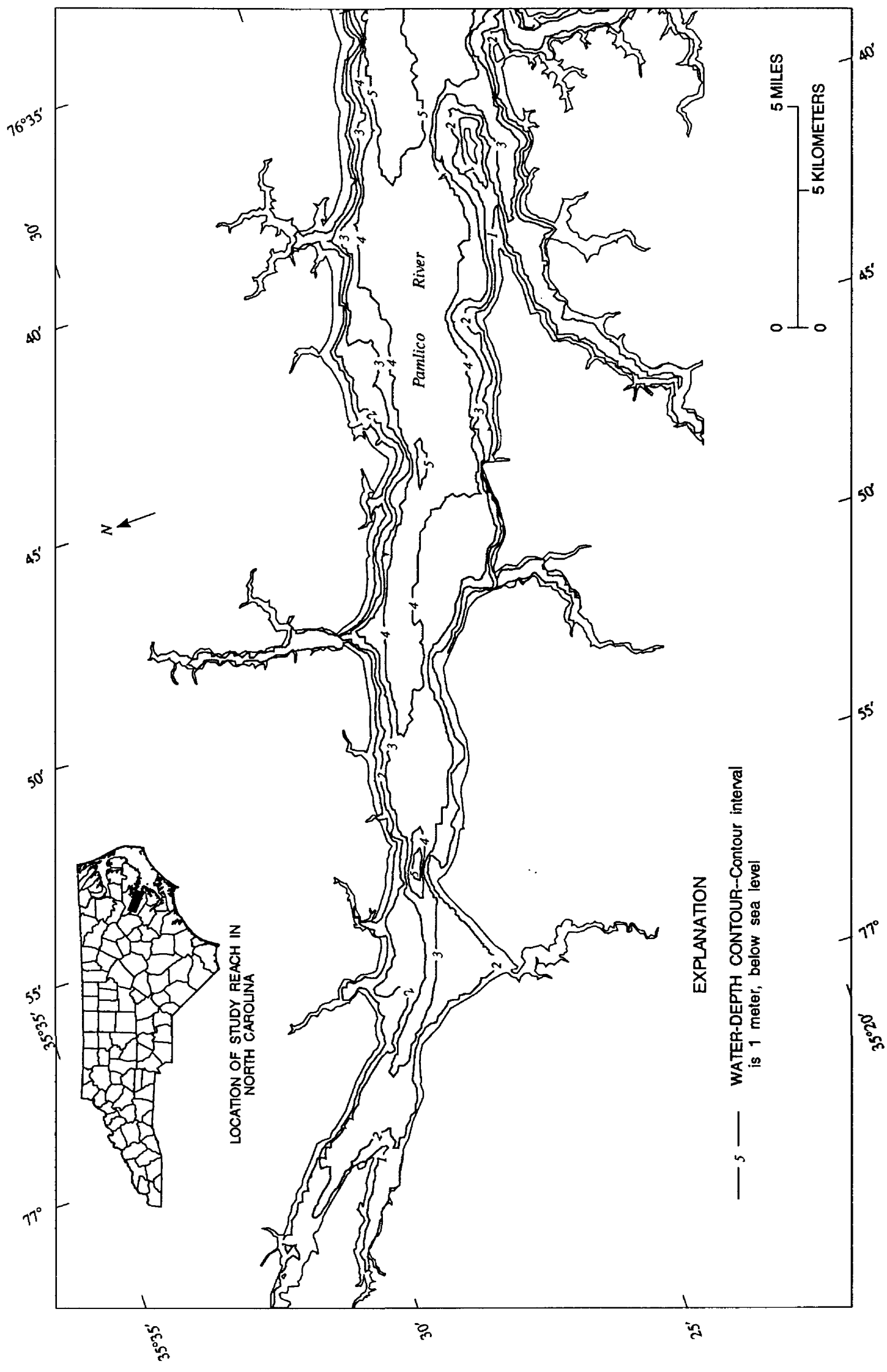

Figure 2. Pamlico River study reach showing bathymetry.

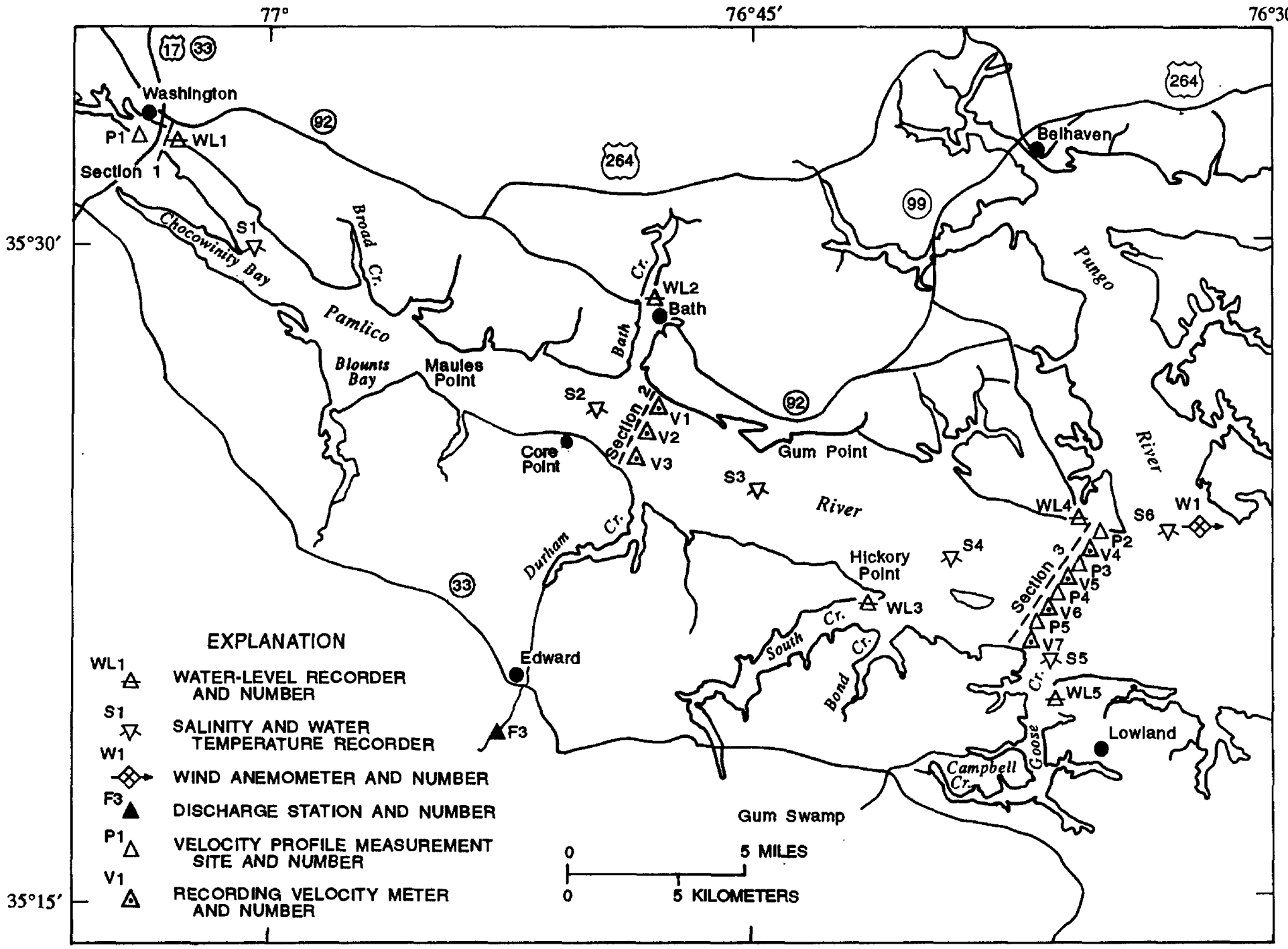

Figure 3. Location of Pamlico River data-collection sites, North Carolina.

Table 1. Description of Pamlico River data-collection sites
[USGS, U.S. Geological Survey; ---, no station number assigned]

Site no.	USGS station number	Latitude	Longitude	Measurement interval (minutes)
Water-level data (fig. 3)				
WL1	02084472	35°32'33"	77°03'43"	15
WL2	02084535	35°25'36"	76°45'54"	15
WL3	0208455120	35°21'34"	76°42'39"	15
WL4	02084555	35°23'37"	76°36'22"	15
WL5	0208455600	35°19'34"	76°36'35"	15
Salinity and temperature data[1] (fig. 3)				
S1	0208450705	35°30'30"	77°01'12"	15
S2	0208453300	35°28'48"	76°50'30"	15
S3	0208454253	35°24'47"	76°45'52"	15
S4	0208455155	35°21'24"	76°38'48"	15
S5	0208455615	35°19'54"	76°37'06"	15
S6	0208457700	35°22'42"	76°33'24"	15
Wind speed and direction data (fig. 3)				
W1	0208457700	35°22'42"	76°33'24"	30
Flow data (figs. 1 and 3)				
F1	02083500	35°53'38"	77°32'00"	60
F2	02083800	35°46'33"	77°27'45"	60
F3	02084540	35°19'25"	76°52'26"	60
F4	02084557	35°43'49"	76°44'49"	60
Velocity, salinity, and temperature data[2] (fig. 3)				
V1	---	35°25'00"	76°49'15"	5
V2	---	35°25'30"	76°49'02"	5
V3	---	35°26'01"	76°48'49"	5
V4	---	35°21'05"	76°37'09"	5
V5	---	35°21'48"	76°36'51"	5
V6	---	35°22'20"	76°36'37"	5
V7	---	35°22'55"	76°36'21"	5
Velocity and salinity data[3] (fig. 3)				
P1	---	35°32'33"	77°03'43"	120
Velocity, salinity, and temperature data[4] (fig. 3)				
P2	---	35°20'57"	76°37'12"	15
P3	---	35°21'28"	76°37'00"	15
P4	---	35°22'04"	76°36'46"	15
P5	---	35°22'40"	76°36'29"	15

[1]Salinity measured near the water surface and near the channel bottom; water temperature measured near the water surface.

[2]Data collected at a point about 1.5 meters above the channel bottom; salinity, water temperature, and current speed and magnitude recorded.

[3]Data measured at 11 locations across the channel and at 3 points in the vertical at each location; measurements made at about 2-hour intervals.

[4]Vertical profiles measured at about 0.3-meter intervals; current speed and direction recorded.

Second-order vertical accuracy (for example, between 4.2 and 5.7 cm in 50 km) was achieved during this survey. However, a difference in elevation of 5 cm over 50 km is approximately equal to the typical water-surface slope in the Pamlico River estuary, so small errors in gage datums can have significant effects on computed water-surface slope and, thus, on simulated flows.

Subsequently, the USGS evaluated the use of a global positioning system with three antennae for determining gage datums in the network of water-level recorders. In one 50-km loop, the error of closure was about 7 cm. These results are similar to those achieved by the North Carolina Geodetic Survey when using a global positioning system in other applications (G. Thompson, North Carolina Geodetic Survey, oral commun., 1989). Consequently, gage datums determined by the ground survey were used in the study.

Water-level fluctuations in Pamlico Sound, east of the study reach, have been examined extensively by Jarrett (1966) and Pietrafesa and others (1986). For periods of 1 to 7 days, water levels in the northern part of the sound were typically coherent and 180° out of phase with water-level oscillations in the southern part of the sound (Pietrafesa and others, 1986). Coherent wind fields for all periods greater than 1 day were generally aligned in the north-northeast to south-southwest direction, or along the major topographic axis of the sound (Pietrafesa and others, 1986). Hence, at all periods of 1 to 7 days, predominant winds blowing along the axis of the sound result in a rise in water level at one end of the sound and an associated lowering of water level at the other end. When the wind relaxes, a seiching (water-level oscillation in a closed basin) motion results. Pietrafesa and others (1986) also detected a strong sea breeze effect at periods of 24 hours. However, water levels in the sound responded relatively uniformly to the sea breeze in contrast to the 1- to 7-day period winds.

Characteristics of water-level fluctuations in the Pamlico River estuary study area have not been documented as thoroughly as have the characteristics of Pamlico Sound. It has generally been assumed that wind is primarily responsible for water-level fluctuations in the Pamlico River (Copeland and others, 1984) rather than astronomical tides. Jarrett (1966) analyzed 5 months of water-level data collected at 6-hour intervals at a location near Washington and concluded that the semi-diurnal tidal component, which has a period of 12.42 hours (M2 tide), accounted

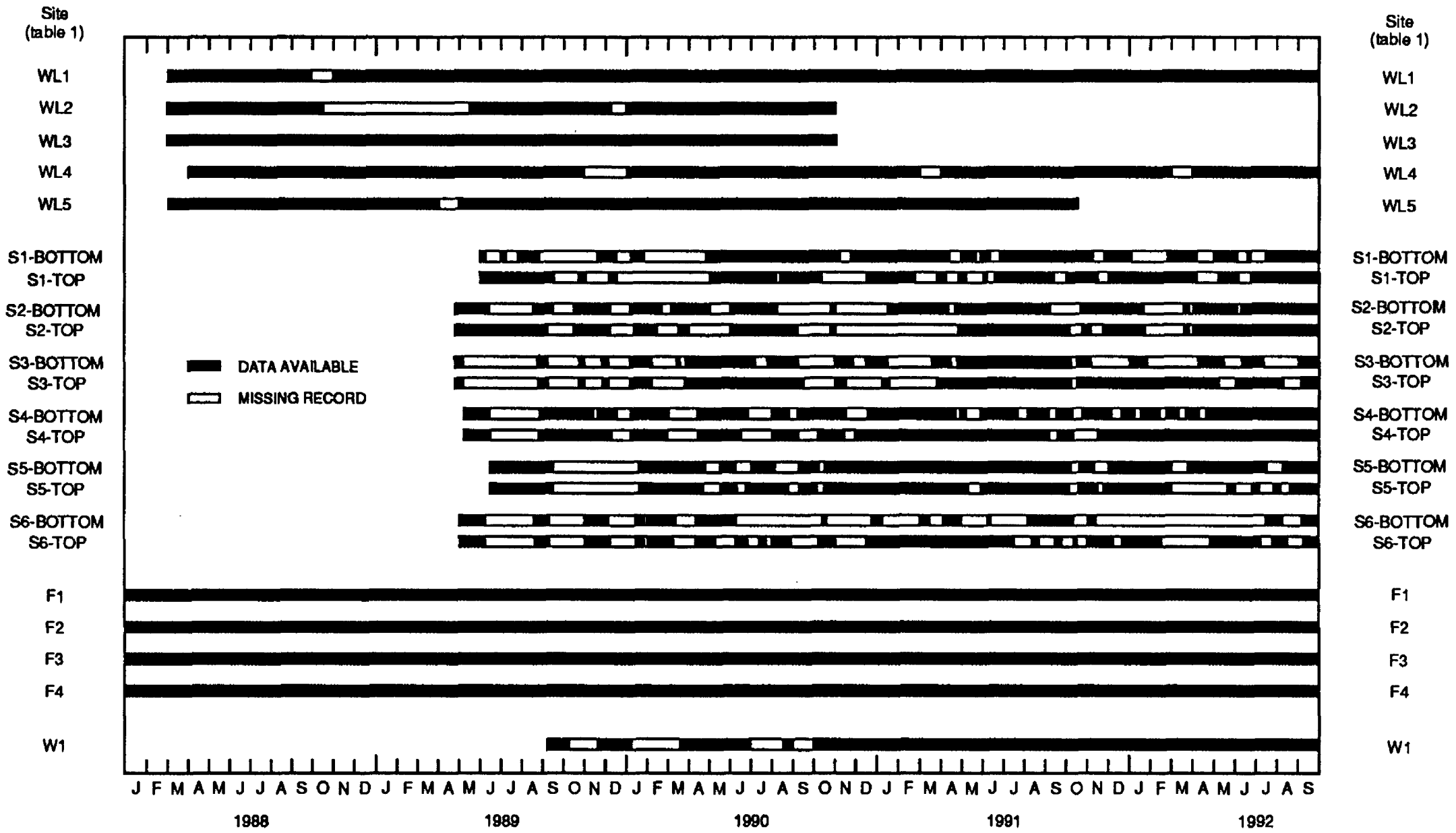

Figure 4. Period of record at selected data-collection sites in the Pamlico River.

for less than 3 percent of the variance in the water-level record. This result could be questionable, however, because of the data-collection interval (which was equal to one-half of the M2 period) and the length of record.

Harmonic analysis of water-level data from site WL1 generally agrees with the results of Jarrett (1966). The amplitude of the M2 tidal constituent was less than 5 cm. Nevertheless, there is a periodic variation in water levels in the Pamlico River. For example, during July 5-11, 1991, the period between minimum water levels at site WL4 was fairly constant (fig. 5); similar conditions prevailed at other sites throughout the study period. Figure 5 also illustrates the phase difference between the occurrence of high water at sites WL1 and WL4; high water at site WL4 was typically 1 to 2 hours prior to high water at site WL1.

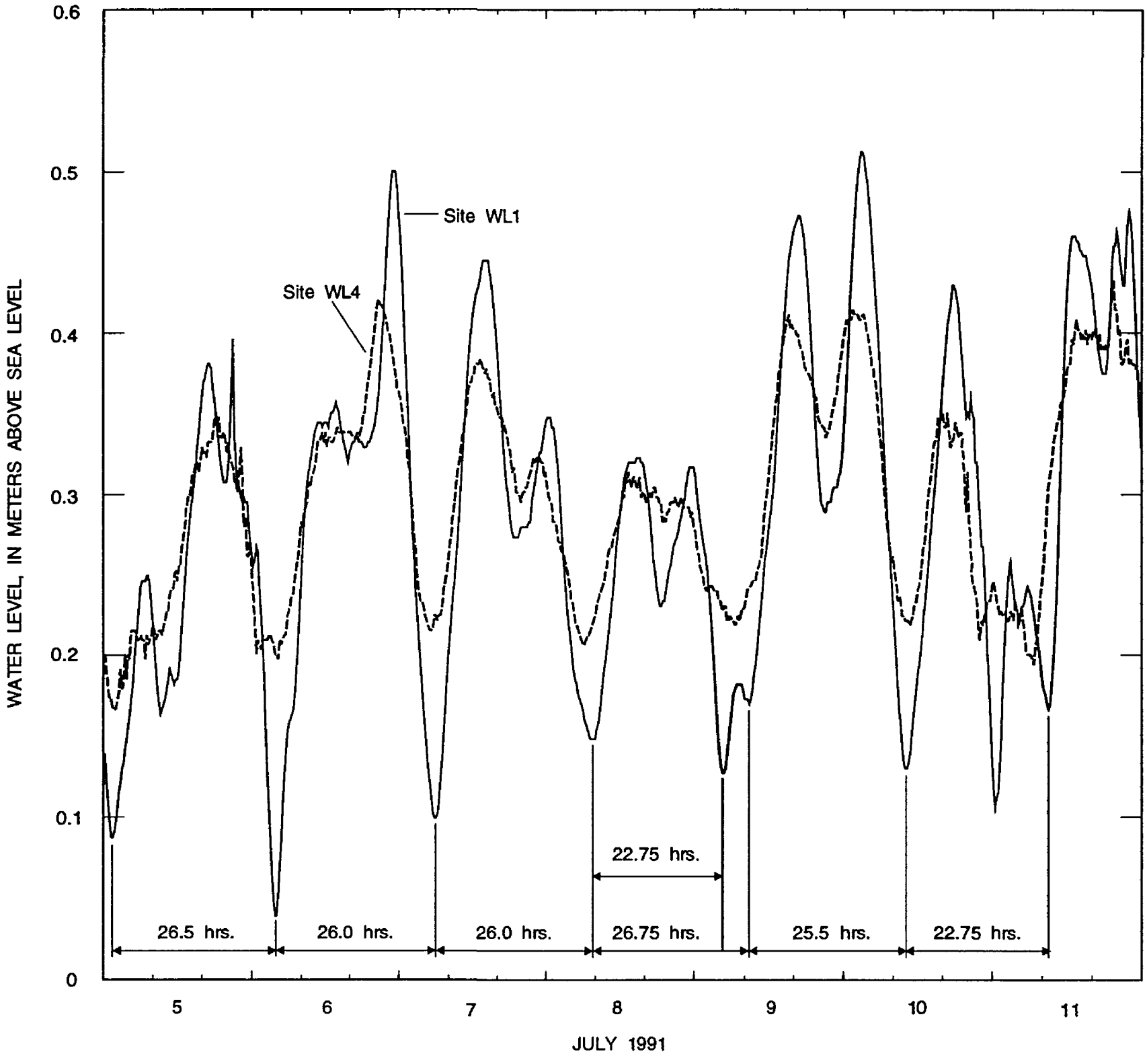

Figure 5. Water levels at sites WL1 and WL4 in the Pamlico River during July 5-11, 1991, showing time between minimum water levels at site WL1.

During the study period, the mean water level in the Pamlico River ranged from 0.226 m above sea level at site WL3 to 0.247 m above sea level at site WL2 (table 2). (Mean values are computed from available data; for some months, there may be periods of missing data, as shown in figure 4.) The highest and the lowest water levels were observed at the upstream end of the Pamlico River. Likewise, the largest daily water-level fluctuations occurred at the upstream end of the estuary.

Table 2. Observed water-level characteristics in the Pamlico River, 1988-92

Water-level characteristic	Site (fig. 3)				
	WL1	WL2	WL3	WL4	WL5
Mean water level[1]	0.232	0.247	0.226	0.238	0.241
Mean daily maximum[1]	.390	.372	.321	.324	.327
Maximum observed[1]	1.192	1.043	.912	.927	.948
Mean daily minimum[1]	.068	.119	.121	.145	.147
Minimum observed[1]	-1.128	-.661	-.326	-.399	-.329
Mean daily range[2]	.322	.253	.200	.179	.180
Total range[2]	2.320	1.704	1.238	1.326	1.277
Days of record	1,681	977	1,286	1,557	1,269

[1]Values are in meters above sea level.
[2]Values are in meters.

Water levels generally were highest in the late summer and early fall (August-October) and lowest during the winter (December-February) (table 3). As noted by Pietrafesa and others (1986), the water level in the coastal ocean is at a minimum during January and February when water temperature is lowest and water density is greatest. Likewise, water levels in the coastal ocean increase in the spring and summer as water temperature increases. The water level in the Pamlico River responds to these changes in the coastal ocean water level.

The observed difference in mean water levels between the upstream and downstream boundaries of the study reach was very small (tables 2 and 3). In fact, according to the results in table 2, the mean water level at sites WL1 and WL4 for the period 1988-92 differed by only 0.6 cm, which is probably much less than the accuracy achieved in establishing gage datums. Although instantaneous differences between upstream and downstream water levels were as great as 0.3 m, the water-surface slope in the Pamlico River was generally small, on the order of 10^{-6}, which again emphasizes the need for good vertical control of gage datums.

The mean water levels at sites WL4 and WL5 differed by 0.3 cm during the period of record (table 2). The magnitude of the lateral water-level gradient was not constant, however (table 3). For example, during August 30-September 3, 1989, water level at site WL5 exceeded that at site WL4 most of the time, but the difference in water levels at the two gages ranged from +1.0 cm (water level at site WL5 greater than at site WL4) to -0.5 cm. It can be said with some certainty, then, that a lateral water-level gradient does exist across the downstream end of the study reach (the lateral water-level difference would be constant if the difference were entirely due to differences in gage datums). However, there is some uncertainty about the magnitude of the gradient because of questions about the accuracy of gage datums.

The daily water-level range (difference between daily maximum and daily minimum water level) was generally the greatest during April and May, and typically at a seasonal minimum during the fall. Increased water-level fluctuations correspond to increased energy available for mixing and transport processes.

Salinity and Water Temperature

Continuous records of specific conductance and water temperature were collected at six sites in the Pamlico River (fig. 3; table 1). Salinity was computed from specific-conductance values standardized to 25 °C using the conversion given by Miller and others (1988). Salinity data from sites S1 and S5 were used for model boundary conditions; data from site S6 were available for boundary conditions when information was missing at site S5. Data from sites S2, S3, and S4 were used for model calibration and validation. These data, as well as data-collection procedures, were summarized by Garrett and Bales (1991) for April 1989 through September 1990, by Garrett (1992) for October 1990 through September 1991, and by Garrett (1994) for October 1991 through September 1992.

Table 3. Observed monthly mean water level and monthly mean of the daily water-level range at five Pamlico River water-level gages, 1988-92
[---, insufficient data]

Site (fig. 3)	Jan.	Feb.	Mar.	Apr.	May	June	July	Aug.	Sept.	Oct.	Nov.	Dec.
	Monthly mean water level (meters above sea level)											
WL1	0.160	0.143	0.221	0.231	0.259	0.256	0.198	0.294	0.344	0.310	0.237	0.089
WL2	.084	.119	.183	.253	.247	.225	.197	.284	.362	.336	.213	---
WL3	.143	.123	.226	.238	.237	.241	.191	.256	.343	.290	.210	.121
WL4	.171	.154	.215	.237	.260	.258	.200	.290	.337	.300	.268	.090
WL5	.150	.124	.254	.265	.258	.249	.204	.287	.356	.304	.223	.138
	Monthly mean daily water-level range (meters)											
WL1	0.326	0.327	0.336	0.355	0.348	0.318	0.312	0.304	0.299	0.297	0.316	0.308
WL2	.262	.269	.233	.295	.287	.254	.245	.236	.234	.230	.249	---
WL3	.196	.193	.201	.228	.225	.205	.192	.186	.189	.183	.196	.186
WL4	.183	.180	.178	.200	.198	.178	.178	.169	.168	.168	.180	.162
WL5	.179	.178	.186	.202	.199	.188	.175	.162	.170	.165	.177	.176
	Days of record											
WL1	124	119	155	149	155	148	154	154	150	104	117	124
WL2	27	33	62	60	70	90	93	93	90	83	30	16
WL3	92	86	124	118	124	120	121	97	120	109	90	85
WL4	123	117	99	137	155	150	155	155	150	124	96	96
WL5	93	84	93	104	124	120	121	124	120	109	90	87

Water-quality monitors were located on U.S. Coast Guard channel markers. Water temperature was measured near the water surface. Specific conductance was monitored near the surface and about 1 m above the channel bottom. Exact placement of sensors in the water column at each site was summarized by Garrett and Bales (1991). The underwater sensors were controlled by a single above-water unit, and data were recorded electronically at 15-minute intervals. Monitors were typically serviced once every 3 weeks.

Vertical profiles (measured at 0.3-m intervals) of salinity and water temperature were recorded each time the monitors were serviced. The difference between the near-surface and near-bottom water temperature was typically less than 1 °C. Top-to-bottom differences in salinity of more than 5 parts per thousand (ppt) were, however, sometimes observed.

Information on Pamlico River salinities has been published by several researchers, but data usually consisted of measurements made at biweekly or monthly intervals. Copeland and others (1984) characterized the segment of the Pamlico River between Washington and the mouth of Bath Creek as an oligohaline region where salinities usually varied between 0.5 and 5 ppt. The segment of the estuary between the mouth of Bath Creek and the mouth of the Pungo River was characterized as mesohaline, where salinities typically ranged from 5 to 18 ppt.

At least two hydrographic atlases of the Pamlico River have been published. Data collected in North Carolina estuarine waters north of the White Oak River by the University of North Carolina Institute of Marine Sciences were summarized by Williams and others (1967) for 1948 through 1966. Data collected near the water surface and near the channel bottom at eight sites in the Pamlico River were tabulated, and figures were presented showing monthly mean (1) surface and bottom isotherms and (2) surface and bottom isohalines. The number of observations per month at each site varied between 0 and 7, but was usually

less than 3. According to the somewhat limited data, salinities in the estuary are at a minimum in April and a maximum in November. Isohalines presented by Williams and others (1967) depicted the presence of a lateral salinity gradient in the estuary, with higher salinities on the north side. During winter months, the lateral difference for near-bottom measurements was as much as 5 ppt. The smallest lateral gradients were for near-surface conditions during the late spring and early summer. Schwartz and Chestnut (1973) presented data collected monthly during 1972 at four sites near the mouth of the Pamlico River. These data also seemed to indicate the presence of a lateral salinity gradient, with the maximum gradient occurring in November.

Giese and others (1985) analyzed about 1,800 salinity observations made near site WL1 between 1961 and 1967. These data were supplemented by 10 sets of salinity surveys in the Pamlico River between Washington and the mouth. Results of the salinity surveys indicated that salinities were generally higher on the north side of the estuary than on the south side, which agrees with the conclusions of Williams and others (1967) and Schwartz and Chestnut (1973). Giese and others (1985) also reported that there was a fairly consistent longitudinal salinity gradient equal to 0.2 part per thousand per kilometer (ppt/km) for the 75 km of the estuary upstream from the mouth. Daily observations of salinity at site WL1 were less than 0.1 ppt 50 percent of the time between 1961 and 1967. Near-surface salinities were greater than 3.0 ppt, and near-bottom salinities were greater than 5.6 ppt about 5 percent of the time at site WL1 between 1961 and 1967.

Harned and Davenport (1990) compiled available salinity data collected in the Pamlico River between 1967 and 1988; much of the information was from Stanley (1988). The estuary, from Washington to the mouth, was subdivided into 10 zones to expedite data analysis. The number of observations per zone ranged from 602 to 2,193. No distinction was made in the analysis between near-surface and near-bottom salinity. The median salinity ranged from 2 ppt in the upstream zone to 15 ppt in the downstream zone. If median salinity is used as the measure, then the characterization by Copeland and others (1984) of the segment of the estuary between Washington and Bath Creek as oligohaline and the segment between Bath Creek and the mouth as mesohaline is appropriate. However, the difference between the minimum observed and maximum observed salinity in each zone was between 15 and 20 ppt. Twenty-five percent of the observations were greater than 8 ppt in the upstream zone, and 25 percent were greater than 18 ppt in the downstream zone.

Near-surface and near-bottom salinities observed at sites S1-S6 during 1989-92 are summarized in tables 4 and 5. The number of days of record for site S6 was significantly less than at other sites, so results from site S6 in tables 4 and 5 are not directly comparable to results from other sites. Also, a pocket of extremely saline water, not representative of natural conditions, was detected at site S5 in July 1990; a similar, but less extreme, condition seems to have occurred again in August 1992.

Mean near-surface salinities ranged from 2.2 ppt at site S1 to 11.0 ppt at site S6, and mean near-bottom salinities ranged from 4.7 ppt at site S1 to 11.4 ppt at site S5 (table 4). The difference between maximum observed and minimum observed salinity at each site ranged from 13.2 ppt to 20.4 ppt, which generally agrees with the results reported by Harned and Davenport (1990). High salinities were observed at site S1 (13.2 ppt near the surface and 13.5 ppt near the bottom). Likewise, low salinities were observed at the downstream end of the estuary (2.1 ppt near the surface and 2.9 ppt near the bottom at site S5). Although overall observed variations in salinity were large at each site, daily variations were generally less than 2 ppt. Larger daily variations were observed near the bottom than near the surface at each site (table 4).

Minimum monthly mean salinities generally occurred in April or May (table 5). Minimum monthly means also typically occurred earlier in the year at sites S1 and S2, which were the two upstream stations. Maximum monthly mean salinities were generally in November or December (table 5). The difference between the maximum and minimum monthly mean salinity ranged from 5.4 ppt at site S6 (near surface) to 8.5 ppt at site S5 (near surface).

The difference between simultaneously observed near-surface and near-bottom salinities was computed for all observations at each site. Monthly means of the differences were then

Table 4. Observed salinity characteristics in the Pamlico River, 1989-92
[<, less than]

Site (fig. 3)	Salinity (in parts per thousand)							Complete days of record
	Mean	Mean daily maximum	Maximum observed	Mean daily minimum	Minimum observed	Mean daily range	Total range	
				Near surface				
S1	2.2	3.0	13.2	1.5	<0.1	1.5	13.2	756
S2	5.7	6.3	13.6	5.1	.1	1.2	13.5	768
S3	7.7	8.4	18.1	7.0	<.1	1.4	18.1	819
S4	9.6	10.2	16.2	9.0	.9	1.2	15.3	931
S5	10.4	10.9	17.9	9.8	2.1	1.1	15.7	843
S6	11.0	11.8	20.3	10.2	1.3	1.6	19.0	688
				Near bottom				
S1	4.7	5.4	13.5	3.8	<0.1	1.6	13.5	799
S2	8.0	8.9	16.9	6.7	<.1	2.2	16.9	851
S3	8.8	10.1	20.1	7.7	.4	2.4	19.7	654
S4	10.3	11.3	20.4	9.6	<.1	1.7	20.4	887
S5	11.4	12.2	50.7[a]	10.6	2.9	1.6	47.8[a]	905
S6	10.6	11.6	19.4	9.7	4.1	1.9	15.3	404

[a]Values not representative of natural conditions.

Table 5. Observed monthly mean salinity, in parts per thousand, for near-surface and near-bottom conditions at six salinity monitors in the Pamlico River, 1989-92
[---, fewer than 25 days of record; no mean computed]

Site (fig. 3)	Jan.	Feb.	Mar.	Apr.	May	June	July	Aug.	Sept.	Oct.	Nov.	Dec.
						Near surface						
S1	2.7	3.7	0.8	---	1.2	1.2	1.9	1.1	2.1	3.2	6.1	4.5
S2	4.9	---	4.3	4.9	4.5	4.4	5.7	5.8	6.9	7.3	6.9	11.2
S3	8.2	7.8	8.4	5.5	4.3	7.2	8.1	7.4	8.4	8.4	11.1	11.7
S4	10.2	10.8	11.3	8.1	7.0	8.1	10.5	9.4	10.1	9.4	10.1	13.5
S5	10.7	10.2	9.5	7.7	7.1	8.8	9.2	9.5	11.3	12.7	13.0	15.6
S6	13.2	11.9	12.4	8.3	9.1	8.3	9.7	9.6	12.1	14.2	12.1	13.7
						Near bottom						
S1	7.6	7.5	4.6	---	1.9	1.8	3.7	4.1	4.8	5.5	7.4	8.4
S2	9.6	7.5	7.5	5.2	5.3	6.3	8.7	9.4	8.6	8.9	9.9	12.2
S3	10.8	---	---	5.3	5.0	8.7	10.6	9.6	8.8	10.0	13.1	11.7
S4	11.0	11.4	12.8	8.6	7.0	8.4	10.6	10.0	10.8	10.8	12.1	13.6
S5	13.0	11.5	10.6	9.8	9.0	9.8	10.3	11.0	11.9	12.8	14.6	16.7
S6	---	---	11.6	8.8	7.1	8.0	---	12.5	12.6	---	13.4	13.1

determined (table 6). At sites S4 and S5, the monthly mean difference between near-surface and near-bottom salinity was typically less than 1 ppt, but ranged from 0.5 to 5.7 ppt at site S1 and 0.9 to 4.8 ppt at site S2. With the exception of site S6, where a smaller number of observations was available, the minimum vertical salinity gradient generally occurred between April and July, and the top-to-bottom difference in salinity was usually greatest from late summer through early winter. Monthly mean values mask much of the dynamics of the vertical mixing processes in the Pamlico River. For example, at site S1, water having a top-to-bottom salinity difference of 4 ppt was observed to become uniformly mixed in less than 1 hour; 2 days later, the water column went from uniformly mixed to having a top-to-bottom difference of 4 ppt in less than 3 hours (Giese and Bales, 1992).

Wind

Wind speed and direction were recorded at 30-minute intervals near the downstream boundary of the study reach at site W1 (fig. 3; table 1). The wind anemometer was located at an elevation of 10 m above the water surface and was serviced at approximately monthly intervals.

Winds were generally from the south, southwest, and west during late spring and summer months (table 7). Winds were typically from the northwest, north, and northeast during the fall and shifted to the west, northwest, and north during the winter. There is a general progression of winds back to the south until about June, when winds slowly begin to rotate back to the north. According to Weisberg and Pietrafesa (1983), the annual vector-average wind over the coastal ocean east of the study area is from the northeast.

Wind speeds were greatest during the winter months (table 7). During December through May, wind speeds were greater than 9 meters per second (m/s) at least 10 percent of the time. The high mean wind speed in September resulted primarily from the occurrence of Hurricane Hugo in 1989; otherwise, September wind speeds were comparable to those in August. Winds were typically light during June through August, with wind speeds less than 4.5 m/s about 37 percent of the time. Weisberg and Pietrafesa (1983) noted that the maximum mean and maximum variance in wind speeds occurred during the winter months in the coastal ocean east of the study area; minimum mean and minimum variance in wind speeds occurred during summer months.

Pietrafesa and others (1986) analyzed the frequency characteristics of winds measured at New Bern and Cape Hatteras during a 340-day period in 1978. A well-defined sea breeze oriented approximately north-northwest to south-southeast was detected. During periods longer than about 2 days, winds tended to be aligned in the northeast-southwest direction, or along the major topographic axis of Pamlico Sound and approximately perpendicular to the axis of the Pamlico River.

Freshwater Inflow

The Tar-Pamlico River system drains 11,150 km^2, but only about one-half (54 percent) of the basin is gaged. The downstream-most gaging

Table 6. Monthly mean of the difference between simultaneously measured near-bottom and near-surface salinity at six sites in the Pamlico River, 1989-92
[---, fewer than 25 days of record; no mean computed]

Site (fig. 3)	Monthly mean of the difference between simultaneously measured near-bottom and near-surface salinity (in parts per thousand)											
	Jan.	Feb.	Mar.	Apr.	May	June	July	Aug.	Sept.	Oct.	Nov.	Dec.
S1	5.7	3.6	3.6	0.5	1.0	0.7	1.6	2.9	2.7	2.3	3.0	3.7
S2	4.8	---	2.6	2.5	.9	1.7	1.7	3.5	2.0	1.3	2.5	1.6
S3	2.3	---	---	.6	.9	1.5	2.5	2.4	.4	1.6	2.5	---
S4	1.0	.9	1.3	.8	.4	.5	.4	.8	.6	1.2	1.3	.7
S5	1.4	1.3	.8	.5	.6	.2	1.0	1.3	.6	.1	1.6	1.2
S6	1.2	.3	.9	1.0	2.0	1.8	---	2.6	.2	---	2.2	.5

Table 7. Observed monthly wind statistics at site W1 in the Pamlico River, 1989-92
[m/s, meters per second]

Direction (degrees east of north)	Percent of time wind blew from stated direction												Annual
	Jan.	Feb.	Mar.	Apr.	May	June	July	Aug.	Sept.	Oct.	Nov.	Dec.	
338-22 (N)	18.8	16.3	12.4	8.8	10.6	8.3	2.6	6.4	8.6	16.5	18.5	20.6	12.3
23-67 (NE)	11.9	17.4	5.2	10.6	16.7	17.1	6.6	17.5	32.8	13.9	12.9	14.5	14.8
68-112 (E)	5.9	6.8	7.1	10.6	7.8	9.3	3.5	11.4	12.5	11.9	6.0	2.5	7.9
113-157 (SE)	6.9	9.1	11.8	14.3	13.9	14.7	7.1	13.2	11.8	15.0	9.8	4.5	11.0
158-202 (S)	7.1	8.4	8.9	15.4	13.0	12.1	16.5	12.9	9.0	9.3	11.1	7.9	11.0
203-247 (SW)	10.4	11.6	19.9	15.8	17.9	21.4	40.4	18.2	15.1	10.6	12.4	18.2	17.7
248-292 (W)	22.3	16.5	18.2	15.2	12.4	10.2	19.8	14.3	7.2	11.1	15.9	17.6	15.1
293-337 (NW)	16.7	13.9	16.5	9.3	7.6	6.1	3.5	6.1	3.0	11.7	13.4	14.3	10.3
Mean speed (m/s)	5.6	5.3	6.4	5.7	5.9	5.1	5.4	4.5	6.2	5.0	5.0	6.0	5.5
Percent of time speed is greater than 9 m/s	10	13	17	12	13	5	6	2	13	8	8	17	10
Percent of time speed is greater than 6.7 m/s	34	29	40	33	37	25	30	12	30	23	25	40	30

station on the mainstem of the Tar River is located at Tarboro (site F1, fig. 1; table 1) where the drainage area is 5,660 km^2, compared to a drainage area of 8,000 km^2 at the upstream boundary of the study reach near Washington.

Downstream from Tarboro, flows from three small basins (drainage areas between 37 and 126 km^2) are gaged (figs. 1 and 3; table 1). The only gaged tributary which flows directly into the study reach is Durham Creek. Site F3 on Durham Creek (fig. 3) is 10.9 km upstream of the confluence of the creek with the Pamlico River. Conetoe Creek (site F2, fig. 1) drains to the Tar River upstream of the study reach. Flows at Van Swamp (site F4, fig. 1) drain to the Pungo River, and then to the Pamlico River downstream from the study reach.

Much of the land around the Pamlico River consists of altered wetlands that have been ditched and drained to accommodate agriculture and other land uses. Water-control structures are widely used in these agricultural drainage ditches and can alter the natural seasonal distribution as well as the volume of runoff. Flows from these lands are not well documented, although Treece and Bales (1992) reported flows from three small agricultural drainage canals in Beaufort County on the south side of the Pamlico River.

The period between January 1988 and September 1992 was characterized by a 14-month low-flow period, a subsequent 18-month high-flow period, and then a 25-month low-flow period. Monthly mean flows at site F1 were below average from January 1988 through February 1989 (fig. 6). With the exception of September 1989, March 1990, and July 1990, monthly mean flows at site F1 were above average from March 1989 through

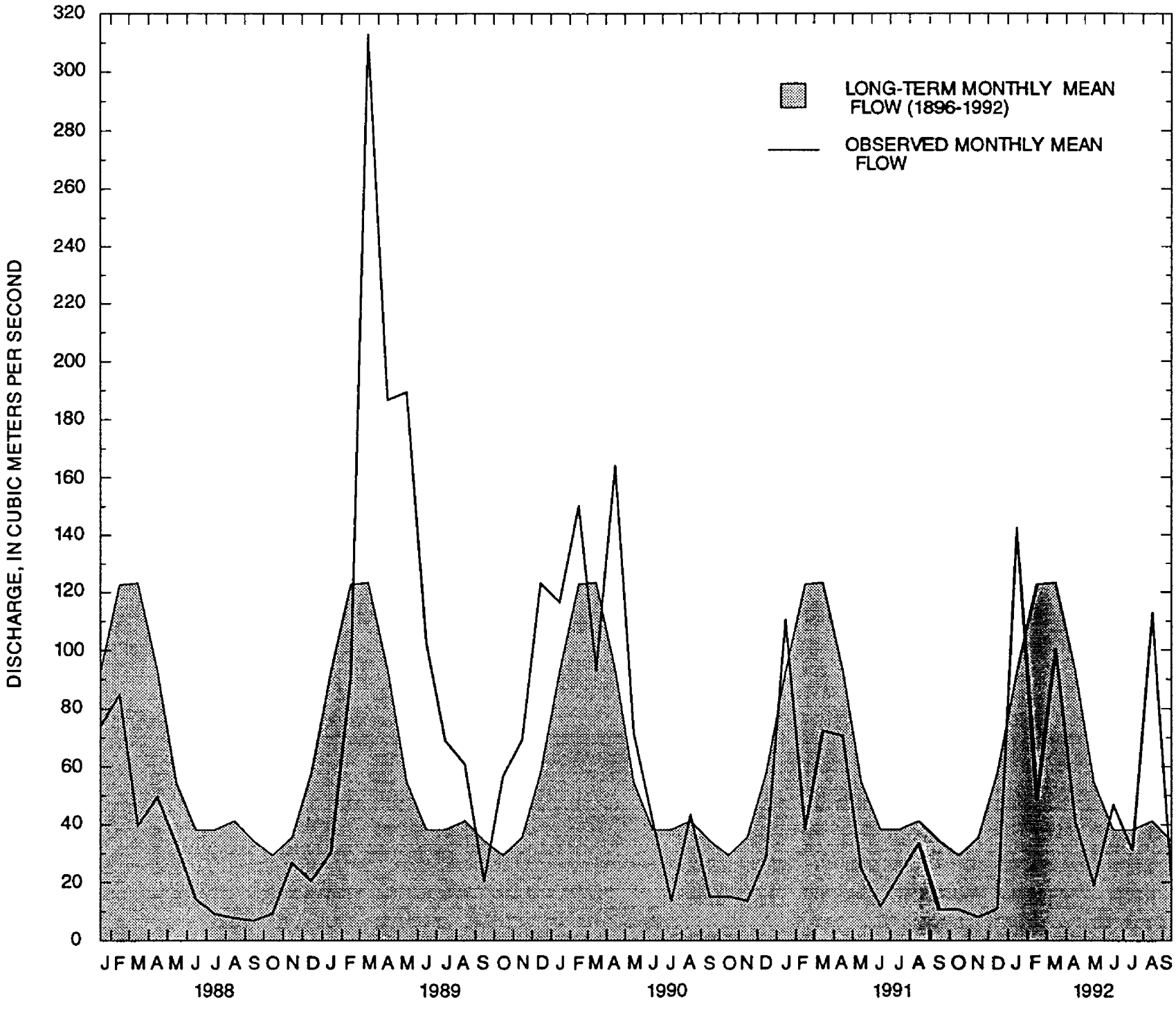

Figure 6. Long-term monthly mean and observed monthly mean flow at Pamlico River site F1 during January 1988 through September 1992.

August 1990. Monthly mean flows were then below average until September 1992, with the exception of January 1991 and January, June, and August 1992.

The long-term (1896-1992) annual average flow at site F1 is 63.2 cubic meters per second (m^3/s). Applying a drainage area ratio of 1.41 (8,000-km^2 drainage area at Washington divided by 5,660-km^2 drainage area at site F1) gives a long-term annual mean freshwater inflow of 89 m^3/s at Washington. Using observed annual mean flow at site F1 and the drainage area ratio, estimated annual mean freshwater inflows at Washington during the study period were 42.4 m^3/s in 1988; 132 m^3/s in 1989; 112 m^3/s in 1990; 53.2 m^3/s in 1991; and 70.0 m^3/s in 1992. Annual means are based on the water year, from October through September, determined by the calendar year in which it ends.

Data from sites F3, located on the south side of the study reach, and site F4, on the north side of the estuary, were used to estimate freshwater inflow from the 1,230-km^2 area, which drains directly to the study reach. For each month between January

1988 and September 1992, measured monthly mean flows at sites F3 and F4 were converted to mean flow per square kilometer of drainage area; the values for sites F3 and F4 were averaged, and the result was multiplied by the local inflow drainage area of 1,230 km^2 (table 8). Site F3 drains an area of 67 km^2, and site F4 drains a 60-km^2 area.

Estimated monthly mean inflows from this area ranged from less than 0.1 to 46.1 m^3/s, which is equal to about one-half of the estimated long-term mean annual freshwater inflow at Washington. Estimated monthly mean freshwater inflows were less than 10 m^3/s 46 percent of the time, and less than 20 m^3/s 66 percent of the time. The monthly mean flow per square kilometer of drainage area was higher 70 percent of the time at site F3 than at site F4. The drainage area upstream of site F3 has fewer field ditches and drainage canals than the basin upstream of site F4. The estimated long-term mean annual inflow from the 1,230-km^2 area to the Pamlico River is 17 m^3/s.

Currents

Seven Aanderaa RCM4 current meters were deployed during August 23-24, 1989, and recovered on September 6, 1989 (fig. 3; table 1). Initial plans were to collect data for about 30 days, but the meters were recovered early because of the approach of a hurricane. At each of the seven sites, current velocity and direction, water temperature, and specific conductance were recorded at 5-minute intervals at a point about 1.5 m above the channel bottom. Three meters were placed across the channel near the mouth of Bath Creek (sites V1, V2, and V3, fig. 3), and four meters were deployed across the channel near the downstream boundary of the study reach (sites V4, V5, V6, and V7, fig. 3).

Locations for meter deployment were selected and identified on topographic maps and nautical charts. The latitude, longitude, and horizontal distance from the shore were determined from the charts for each location. The compass heading for the line along which the meters were to be deployed (fig. 3) was also determined from the charts. In the field, locations for meter deployment were identified by starting near the shore at a pre-determined landmark, cruising along the proper compass heading, and using radar to determine the distance from the shore. Loran-C was insufficiently accurate to identify meter location in the field, so exact independent field determinations of meter latitude and longitude are unavailable. The latitude and longitude values given for each meter in table 1 are the values determined from the charts.

The longitudinal axis of the Pamlico River is oriented in the downstream direction at an angle of approximately 110° east of north. Consequently, in the subsequent discussions, downstream velocities are defined as those with a direction of between 21° and 200° east of north. Likewise, upstream velocities are those with a direction of between 201° and 20° east of north.

During the meter deployment period, velocities ranged from a maximum downstream velocity of 31 centimeters per second (cm/s) at site V4 to a maximum upstream velocity of 34 cm/s at site V1 (table 9). Highest mean and maximum velocities were generally observed on the north side of the estuary (sites V1, V4, and V5), although the mean upstream velocities were higher near the middle of the channel at the downstream measurement section (table 9). Higher currents, and associated greater salt flux, on the north side of the estuary partially explain the higher salinities that typically occur along the north shore.

Magnitude and direction of currents were measured at the moored current meters during August 30-September 6, 1989 (fig. 7). Although data were recorded at 5-minute intervals, data are plotted at hourly intervals for clearer visualization of results. The *y*-axis of each plot in figure 7 is aligned with the longitudinal axis of the Pamlico River, so that a velocity which is at an angle of 110° east of north is shown as a line perpendicular to and below the *x*-axis. The length of each line is proportional to the velocity magnitude.

Even at the relatively narrow section of the estuary where meter sites V1, V2, and V3 were located (fig. 3), there was a marked difference in velocity direction and magnitude across the estuary (fig. 7). Velocities were generally lower on the south side of the estuary than on the north side (fig. 7; table 9). Cross-channel, or nearly cross-channel, currents occurred more frequently at site V3 than at sites V1 or V2. In general, currents were most nearly aligned with the longitudinal axis of the estuary at site V2. At sites V1 and V3, the current tended to be aligned with the local shoreline (fig. 3),

Table 8. Measured monthly mean flow at sites F3 and F4 and estimated monthly mean local inflow to the Pamlico River study reach, 1988-92

[$(m^3/s)/km^2$, cubic meter per second per square kilometer; <, less than; ---, no data]

Month	1988			1989			1990			1991			1992		
	Monthly mean flow		Estimated monthly mean local inflow (m^3/s)	Monthly mean flow		Estimated monthly mean local inflow (m^3/s)	Monthly mean flow		Eatimated monthly mean local inflow (m^3/s)	Monthly mean flow		Estimated monthly mean local inflow (m^3/s)	Monthly mean flow		Estimated monthly mean local inflow (m^3/s)
	F3 [$(m^3/s)/km^2$]	F4 [$(m^3/s)/km^2$]		F3 [$(m^3/s)/km^2$]	F4 [$(m^3/s)/km^2$]		F3 [$(m^3/s)/km^2$]	F4 [$(m^3/s)/km^2$]		F3 [$(m^3/s)/km^2$]	F4 [$(m^3/s)/km^2$]		F3 [$(m^3/s)/km^2$]	F4 [$(m^3/s)/km^2$]	
January	0.031	0.023	33.2	0.0047	0.0003	3.1	0.023	0.026	30.1	0.026	0.011	22.8	0.022	0.018	24.6
February	.016	.016	19.7	.011	.0049	9.8	.0091	.013	13.6	.012	.011	14.1	.0083	.0076	9.8
March	.016	.012	17.2	.040	.035	46.1	.014	.019	20.3	.019	.020	30.0	.0066	.0042	6.6
April	.023	.026	30.1	.026	.032	35.7	.014	.020	20.9	.030	.034	39.4	.0054	.0039	5.7
May	.0064	.0070	8.2	.013	.040	32.6	.0056	.018	14.5	.011	.0056	10.2	.0045	.0017	3.8
June	.0037	.0016	3.3	.0019	.0036	3.4	.0050	.011	9.8	.012	.0015	8.3	.011	.0091	12.4
July	.0009	.0002	.7	.0088	.026	21.4	.0011	.0001	.7	.0084	.0047	8.0	.0080	.0015	5.8
August	.0003	.0001	.2	.015	.014	17.8	.0064	.0054	7.3	.038	.012	30.8	.018	.019	22.8
September	.0001	.0001	.1	.029	.007	22.1	.0054	.0008	3.8	.0035	.0025	3.7	.017	.0023	11.9
October	<.0001	<.0001	<.1	.025	.021	28.3	.0017	.0002	1.2	.0032	.0039	4.2	---	---	---
November	.0001	.0001	.1	.0099	.018	17.2	.010	.0011	6.8	.0034	.0021	3.4	---	---	---
December	.0001	<.0001	<.1	.031	.027	35.6	.012	.0012	14.8	.0059	.0030	4.2	---	---	---

which is at a slight angle to the longitudinal axis. Net water movement at each of the three mid-estuary sites was upstream during the measurement period.

Table 9. Summary of current velocities measured at moored current meters in the Pamlico River during August 23-September 6, 1989
[m, meter; cm/s, centimeters per second]

Site (fig. 3)	Approximate depth of flow (m)	Downstream velocities			Upstream velocities		
		Mean (cm/s)	Median (cm/s)	Maximum (cm/s)	Mean (cm/s)	Median (cm/s)	Maximum (cm/s)
V1	4.5	8.2	8	27	9.9	9	34
V2	3.9	5.7	5	25	5.3	4	22
V3	3.5	4.6	3	23	5.2	4	21
V4	5.4	9.4	7	31	5.5	4	25
V5	5.1	6.7	6	24	6.9	6	22
V6	4.5	4.6	4	26	6.1	5	20
V7	4.1	5.7	5	17	5.4	4	20

At the downstream meters (sites V4, V5, V6, and V7, fig. 3), however, net water movement was downstream at sites V4 and V5 on the north side of the estuary, and net movement was upstream at sites V6 and V7 on the south side of the estuary (fig. 7). Cross-channel currents were observed at sites V5, V6, and V7, but were seldom present at site V4. As with the mid-estuary sites, there were significant differences in current from the north to the south side of the estuary near the mouth.

The measured velocity vectors (magnitude and direction) were reformulated in terms of north-south and east-west components to further illustrate the characteristics of the velocity. Each point in figure 8A represents the north-south and east-west components of one velocity measurement. Points falling on the longitudinal axis indicate currents in the upstream or downstream direction. As shown in figure 7, current at site V2 was in the upstream direction the majority of the time (fig. 8A and B). Upstream current at site V2 was directed in three predominant directions—along the channel axis, about 45° north of the axis, and about 45° south of the axis (fig. 8B). These upstream currents oriented north and south of the channel axis could reflect the effects of Bath Creek and the orientation of the shoreline. The magnitudes of the currents at site V2 oriented generally in the cross-channel direction were typically much smaller than the along-channel currents. At site V5, currents were fairly evenly distributed between upstream and downstream, although the net current was in the upstream direction. Currents oriented across the channel were generally more prevalent and stronger than at site V2 (fig. 8A and B).

Vertical profiles of horizontal velocity, water temperature, and specific conductance were measured at 15-minute intervals at four locations near the downstream boundary (sites P2, P3, P4, and P5, fig. 3) for about 32 hours during August 28-29, 1989. Measurements were made at 0.3-m vertical intervals using a Neil Brown Instrument Systems Direct Reading Current Meter System. These data were primarily used to determine the vertical structure of the flow at locations near the recording current meters, which were measuring velocities at a single point in the water column. The vertical and lateral distribution of velocity also was measured near the upstream boundary (site P1, fig. 3) during August 28-29, 1989.

Measured currents near the downstream boundary exhibited great vertical and lateral variations. As an example, on August 29 at 1130 (fig. 9A), currents on the south side of the estuary were directed upstream and currents on the north side were downstream. Top-to-bottom differences in currents were generally greater on the south side of the estuary, but the lateral components of the currents were greater on the north side. Top-to-bottom differences in current magnitude were also relatively small at all sites on August 30 at 0015 (fig. 9B). As in figure 9A, the lateral component of the currents near the bottom at sites P2 and P3 were strong. At site P5, currents were weak but were generally downstream near the surface and upstream near the bottom.

Bathymetry

Bathymetric data for the Pamlico River were obtained from the National Ocean Survey (NOS). Approximately one million soundings were recorded for the study reach. Additional depth points were digitized from the 1:40,000-scale NOS chart for the Pamlico River (chart number 11554).

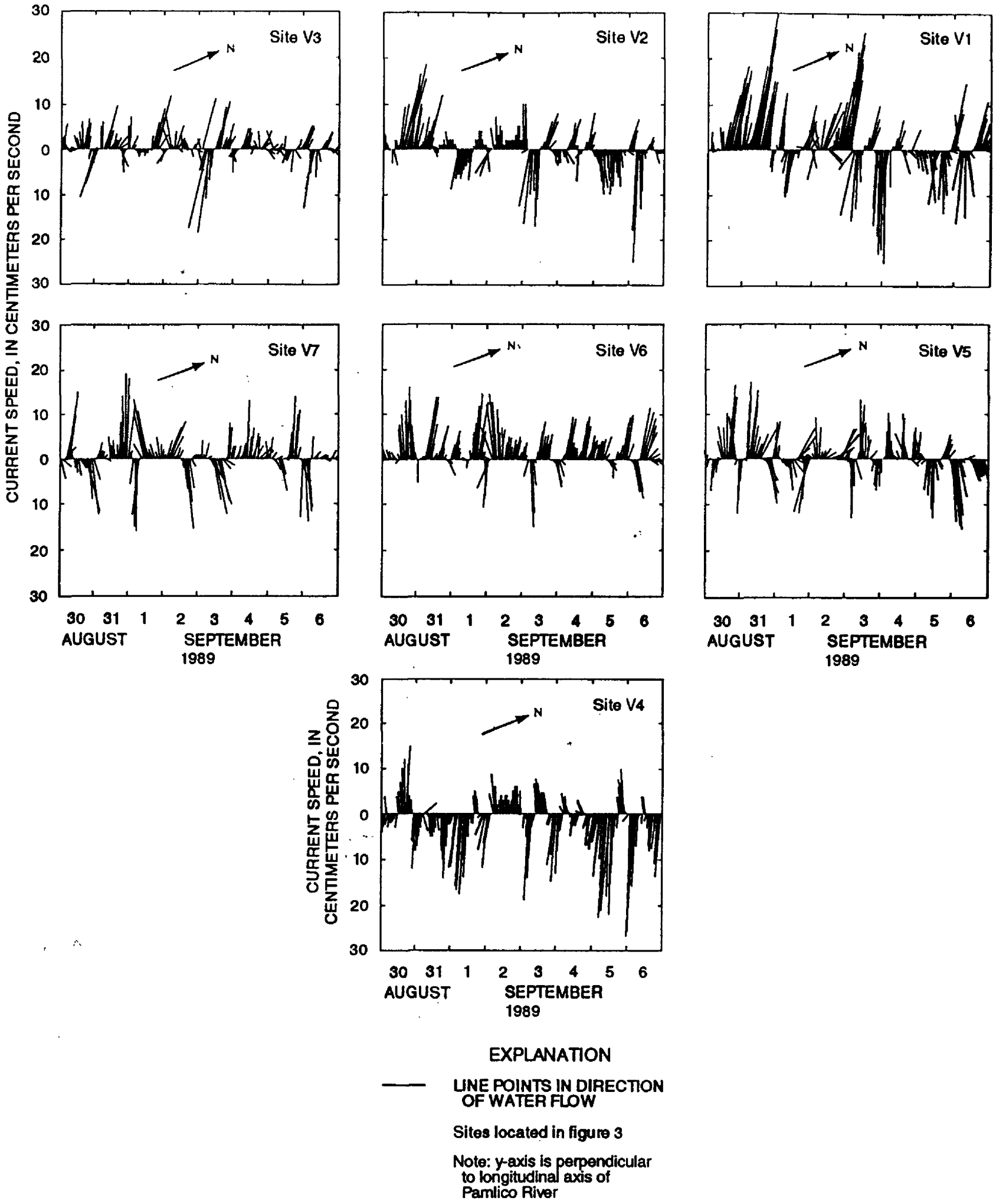

Figure 7. Observed velocity at seven moored current meter sites in the Pamlico River during August 30-September 6, 1989.

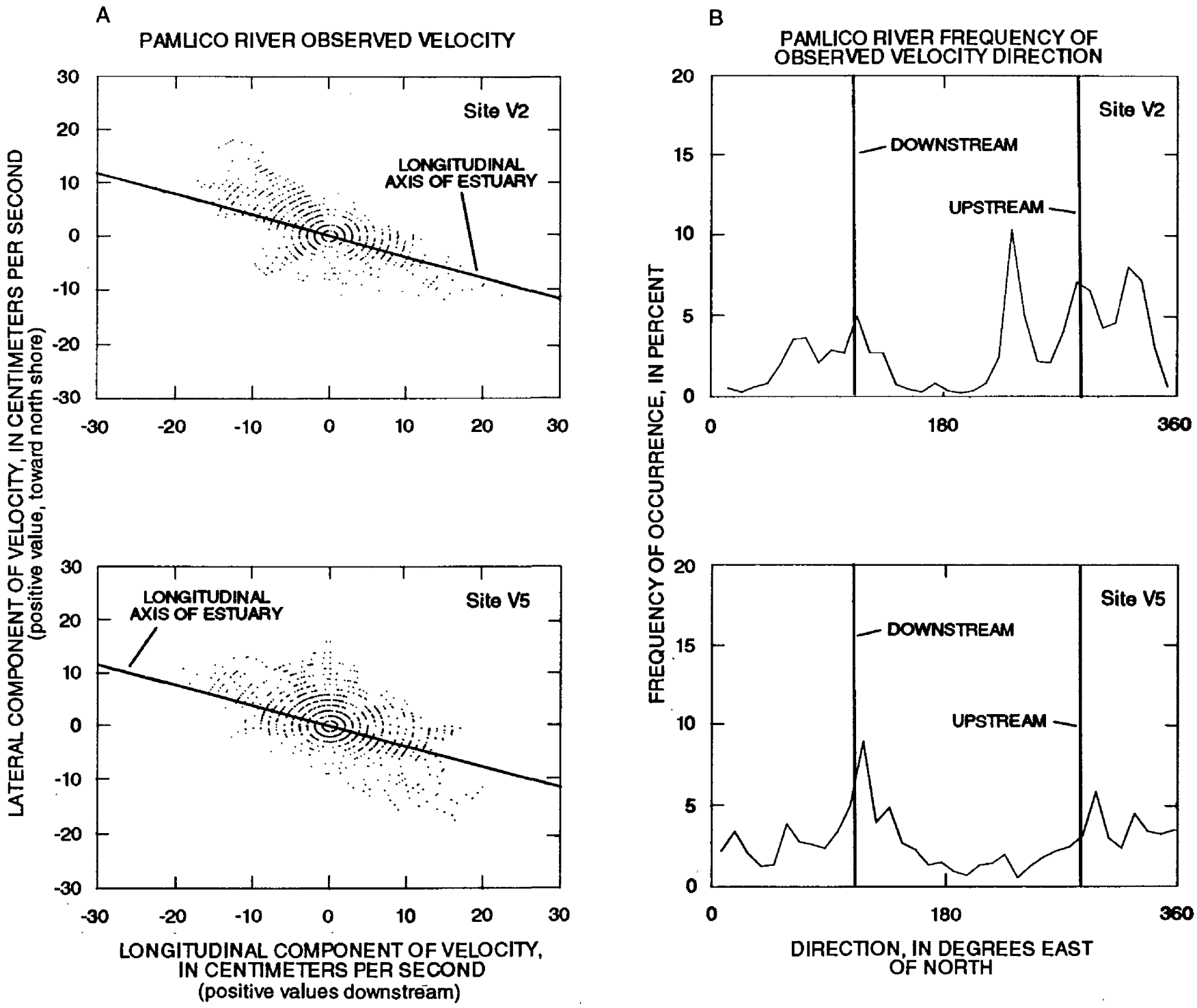

Figure 8. (A) Longitudinal and lateral velocity components and (B) frequency of occurrence of observed velocity direction at sites V2 and V5 in the Pamlico River during August 23-September 6, 1989.

NOS data, which were referenced to mean low water, were adjusted to the sea-level datum.

The 0-, 1.5-, and 3.0-m (0-, 5-, and 10-ft) elevation contours around the study reach were digitized from 1:24,000-scale USGS topographic maps. Spot elevations which were below the 3.0-m (10-ft) contour were also digitized from the topographic maps to complete the bathymetry data base.

The bathymetry was used to compute the volume of the study reach. At a level water-surface elevation of 0.0 m, the total water volume in the study reach is 6.555×10^8 cubic meters (m^3), and the surface area is 224.8 km^2. Assuming a long-term freshwater inflow of 106 m^3/s into the study reach (see Freshwater Inflow section), the ratio of the study reach volume to the inflow rate is about 72 days. Retention or residence time has no precise meaning for estuaries. During the 1988-92 study period, this ratio varied between 51 days (1989) and 138 days (1988).

MODELING APPROACH

The modeling approach chosen for the Pamlico River was based on the objectives of the investigation, the observed physical characteristics of the estuary, and the time and funding constraints

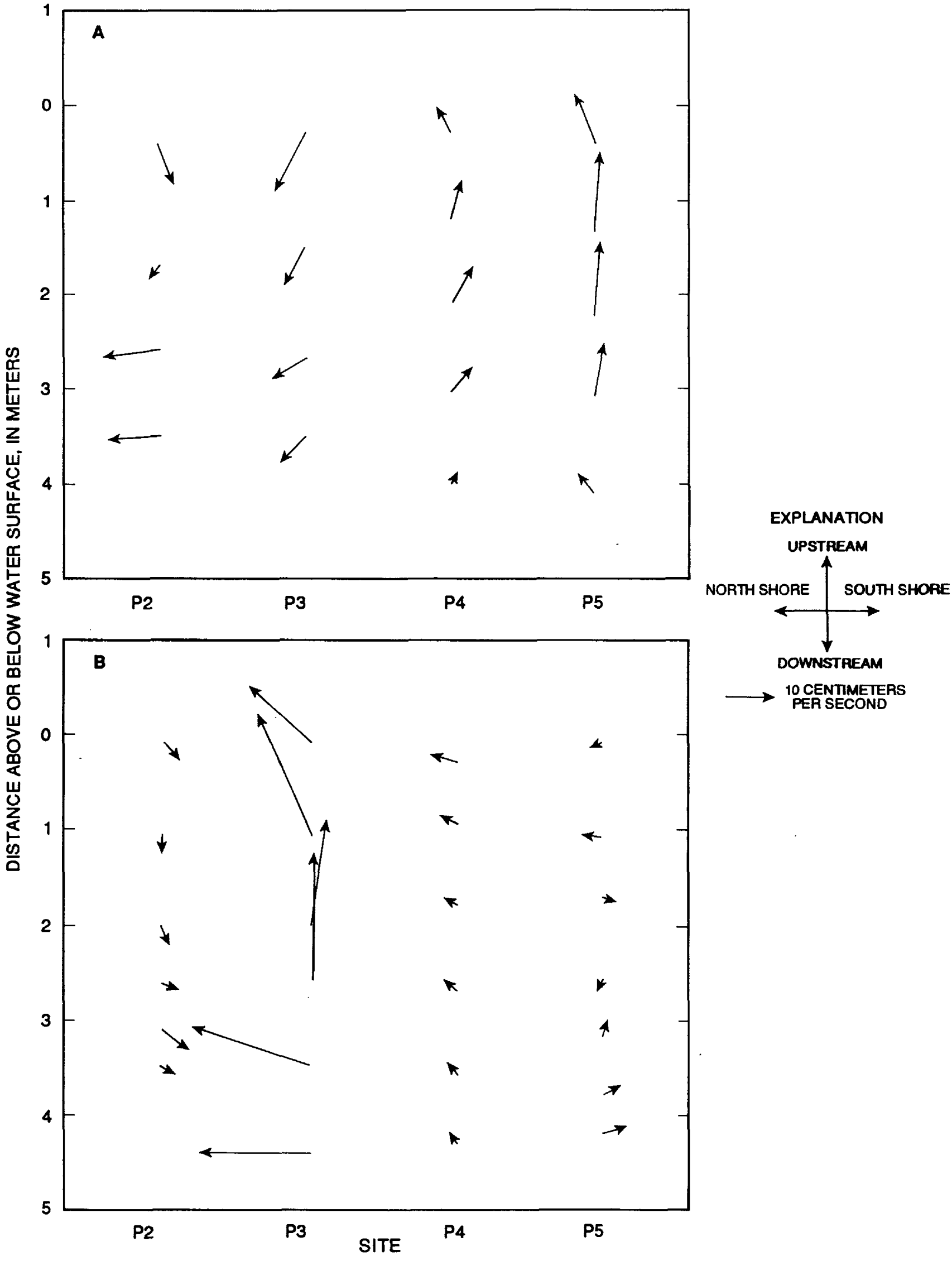

Figure 9. Measured currents at sites P2, P3, P4, and P5 in the Pamlico River on (A) August 29, 1989, at 1130 and (B) August 30, 1989, at 0015.

of the study. Pertinent physical characteristics of the estuary included water-level fluctuations, wind effects, freshwater inflow, and salinity regime. The amplitude of astronomical tides in the estuary and Pamlico Sound is small, and wind has a significant effect on water levels in the sound. The daily water-level range is typically less than 0.3 m, and the daily salinity range is about 2 ppt. The longitudinal salinity gradient in the estuary varies, but is about 0.2 ppt/km. Although the estuary is shallow, vertical salinity gradients do occur. The vertical gradients are, however, relatively small and do not generally persist for extended periods of time. Lateral water-level gradients appear to exist in the estuary; large differences in velocity magnitude and direction occur across the estuary. Because of the weak astronomical tides and low inflow-to-volume ratio, flow velocities are usually small.

Previous investigations also provide insight useful in selecting the modeling approach. Hunter and Hearn (1987) evaluated lateral and vertical variations in the wind-driven circulation of long shallow lakes and concluded that for most natural bathymetries, lateral circulation was predominant over vertical circulation. Signell (1992) also noted that estuarine flushing by wind is often adequately represented using a depth-averaged model, particularly when variations in bathymetry exist. Garvine (1985) investigated the effects of local and remote wind forcing on estuarine circulation. He concluded that (1) water-level and barotropic current variations are dominated by remote wind forcing and (2) the water-surface slope is generated in response to local wind and is in phase with the local wind stress. As previously discussed, water-level fluctuations at the downstream boundary of the study reach are the result of wind-induced water-level fluctuations in Pamlico Sound. Consequently, water-level fluctuations in the Pamlico River are likely dominated by barotropic wind forcing in Pamlico Sound.

With regard to spatial averaging, available modeling options included (1) one-dimensional, (2) two-dimensional, vertically averaged, (3) two-dimensional, laterally averaged, and (4) three-dimensional approaches. Each of these approaches could include time-varying (unsteady) conditions or steady flow. Moreover, complete nonlinear governing equations could be simplified to include only linear partial differential terms.

Steady-flow and linear models were judged to be too simplistic to realistically characterize the circulation and transport regime of the estuary. Likewise, one-dimensional approaches would provide information only on the longitudinal variation in flow and transport, and would not adequately characterize circulation. At the time the investigation began (1988), nonlinear, unsteady three-dimensional models, which included coupled flow and transport equations, were not widely used to provide spatially detailed simulations of estuarine circulation and transport. In addition, computing power at that time made long-term simulations of flow and transport with such models somewhat impractical. Since 1988, improvements in computer hardware, enhanced visualization techniques, and declining costs, as well as additional experience with nonlinear, unsteady three-dimensional models, which include barotropic and baroclinic forcing, have resulted in increased application of these models for simulation of estuarine circulation and transport. Nevertheless, spatially detailed (computational grid sizes of 100-200 m) three-dimensional modeling continues to require significant computing resources.

A two-dimensional, vertically averaged modeling approach was selected. This approach allowed discretization of the estuary into small computational cells so that spatially detailed information on velocity, circulation, and transport could be simulated. Longitudinal and lateral movement of materials within the estuary can be simulated, including the mixing across and along the estuary of substances discharged at one shoreline. The effects of lateral water-level and salinity gradients, both of which have been observed, are included in the model. The vertically averaged approach, however, does not permit the direct simulation of vertical salinity gradients or the effects of these gradients on flow and transport. Additionally, gravitational circulation, which is the long-term net movement of water upstream along the channel bottom in response to the longitudinal salinity gradient, is not directly simulated by the vertically averaged approach, although the gravitational circulation can be included using empirical methods. Recognition of these assumptions inherent in the modeling approach is important for interpretation of model results, as well as to maintain scientific credibility of the investigation.

NUMERICAL MODEL DESCRIPTION

The two-dimensional, vertically integrated, unsteady flow and transport model SIMSYS2D (Leendertse, 1987) was applied to the study reach. The model was first developed for applications in Jamaica Bay, New York (Leendertse and Gritton, 1971). Since that time, the model has undergone numerous revisions and updates and is now probably the most widely applied, best-documented model of vertically integrated hydrodynamics presently in use. Among its many applications, the model was used to investigate flooding and drying of tidal flats in Port Royal Sound, South Carolina (Schaffranek and Baltzer, 1988), to quantify the effects of dredge and fill on circulation in Tampa Bay, Florida (Goodwin, 1987), and to aid in the design of the Dutch Delta Works (Leendertse and others, 1981). In an application of the model to Puget Sound, Chu and others (1989) reported that the model was capable of reproducing the major tide and current characteristics in the sound. A modified version of the model was used by Ridderinkhof and Zimmerman (1992) to evaluate mixing and chaotic stirring in the Dutch Wadden Sea.

Westerink and Gray (1991) described the model as "a very comprehensive modeling package which is based on a staggered ADI [alternating-direction implicit] solution *** and includes many features such as various time stepping options, advective term discretization options, transport of passive tracers, coupled salinity transport, flooding and drying, the ability to include hydraulic structures, two forms of the bottom friction term including a form based on the subgrid scale energy level, a parametric expression for turbulence effects, various formulations for horizontal dispersion, and reactions and local inputs for transport."

The full three-dimensional equations of motion are reduced to a set of two-dimensional equations by assuming that vertical accelerations are negligibly small and by integrating the equations throughout the depth of flow. The resulting equations are nonlinear, time-dependent, and retain coupling of motion and transport so that time-varying horizontal density gradients are included in the equations of motion. Because the nonlinear advective and bottom stress terms are retained in the governing equations, the presence of eddies can be simulated and residual circulation can be computed. The governing equations are applied at specified, equally spaced computational points within the study reach and are solved at successive time steps to provide a close approximation of the time history of water level, current velocity, and constituent transport in the estuary. The following sections describe the governing equations, the numerical procedures to solve the equations in the model, and the model input requirements.

Governing Equations

Estuarine flows are unsteady, nonuniform, and turbulent. Unsteady flows are those in which velocity at a point varies with time. Nonuniform flows vary spatially. In turbulent flows, the instantaneous value of velocity varies randomly with respect to space and time about some mean value.

The basic equations of unsteady, nonuniform, turbulent fluid motion are formulations of the law of conservation of mass and Newton's second law of motion. Conservation of mass for the fluid is given by the equation of continuity, and mass conservation for dissolved or suspended substances is expressed by a transport equation. The law of conservation of momentum is given by the Navier-Stokes equation, which is the basic relation expressing Newton's second law for a viscous fluid. These equations apply to the turbulent flow of a minute parcel of fluid at an instant in time.

A deterministic description of turbulent flow at all points in time and space is not feasible. Consequently, following the original idea of Osborne Reynolds, the governing equations are simplified by decomposing quantities (velocity, pressure, and mass) into mean components and turbulent fluctuations. The equations are then averaged throughout a time interval, which is long relative to the time scale of the turbulent fluctuations. The mean quantity can also vary slowly with time, in which case the flow is characterized as unsteady turbulent flow.

The vertically integrated equation is obtained by integrating the three-dimensional continuity

equation throughout the depth of flow. The kinematic boundary conditions are applied at the water surface, where the vertical velocity is equal to the temporal rate of change of the water-surface elevation, and at the channel bottom, where the vertical velocity is zero, to give:

$$\frac{\partial z_1}{\partial t} + \frac{\partial (HU)}{\partial x} + \frac{\partial (HV)}{\partial y} = 0 \qquad (1)$$

where z_1 = water-surface elevation relative to a horizontal reference plane;
t = time;
x = longitudinal coordinate direction;
y = lateral coordinate direction;
H = $(z_1 + h)$, where h = distance from the channel bottom to the reference plane;
U = vertically integrated longitudinal velocity =

$$\frac{1}{H}\int_h^{z_1} u\,dz \qquad (2)$$

where u = point velocity in the longitudinal, or x-, direction; and

V = vertically integrated lateral velocity =

$$\frac{1}{H}\int_h^{z_1} v\,dz \qquad (3)$$

where v = point velocity in the lateral, or y-, direction.

The vertically integrated equation for conservation of longitudinal momentum is:

$$\frac{\partial U}{\partial t} + U\frac{\partial U}{\partial x} + V\frac{\partial U}{\partial y} - fV = -g\frac{\partial z_1}{\partial x} - \frac{g}{2}\frac{H}{\rho}\frac{\partial \rho}{\partial x} - RU$$

$$+ \frac{C_d \rho_a W^2 \sin\theta}{\rho H} + k_x\left[\frac{\partial^2 U}{\partial x^2} + \frac{\partial^2 U}{\partial y^2}\right] \qquad (4)$$

and the vertically integrated equation for conservation of lateral momentum is:

$$\frac{\partial V}{\partial t} + U\frac{\partial V}{\partial x} + V\frac{\partial V}{\partial y} - fU = -g\frac{\partial z_1}{\partial y} - \frac{g}{2}\frac{H}{\rho}\frac{\partial \rho}{\partial y} - RV$$

$$+ \frac{C_d \rho_a W^2 \cos\theta}{\rho H} + k_y\left[\frac{\partial^2 V}{\partial x^2} + \frac{\partial^2 V}{\partial y^2}\right] \qquad (5)$$

where f = Coriolis parameter, which is computed from the latitude of the estuary,
g = acceleration of gravity,
ρ = density of water,
R = bottom stress term,
ρ_a = density of air,
W = wind speed,
C_d = wind-stress coefficient,
θ = angle between wind direction and the positive y-direction,
k_x = longitudinal mixing coefficient, and
k_y = lateral mixing coefficient.

The terms on the left side of equations 4 and 5 describe the acceleration of the fluid. The first term is often called the local acceleration, and the second and third terms, which describe the advection of momentum, are called the advective terms. Because the equations are written with respect to a coordinate system which is fixed to the Earth's surface, the Coriolis acceleration term must be included in the momentum equations. The Coriolis parameter, f, is assumed to be constant for a given model application, which is reasonable if the model domain is confined to a small range in latitude. The Coriolis parameter is typically written as:

$$f = 2\Omega \sin\varphi \qquad (6)$$

where

Ω = angular velocity of the Earth, and
φ = the latitude of the estuary being described.

The terms on the right side of equations 4 and 5 describe the forces acting on the fluid. The first two terms on the right side of the equations represent the horizontal pressure gradients. The pressure gradient consists of the water-surface gradient (first term on the right side of the equations), and the vertically integrated density gradient (second term on the right side of the equations), which results from horizontal variations in density. Because of the dependence of the momentum balance on salinity, the horizontal density gradient terms couple the momentum equations to the transport equation. Consequently, salinity distribution within the estuary affects the flow field through the presence of the horizontal density gradient, and the flow field affects the salinity distribution by transporting mass. The horizontal gradient of atmospheric pressure is not included in the model, which is a reasonable assumption for the 48-km long Pamlico River study reach.

Stresses applied at the channel bottom, the water surface, and within the fluid are described by the last three terms, respectively, in equations 4 and 5. The bottom stress is related to the flow velocity using the following formulation:

$$R = \left[\frac{g}{H}\left(U^2+V^2\right)^{\frac{1}{2}}\right]\left[\frac{H^{\frac{1}{6}}}{\eta}\left(1+\alpha\frac{U\frac{\partial S_s}{\partial x}+V\frac{\partial S_s}{\partial y}}{\left(U^2+V^2\right)^{\frac{1}{2}}}\right)\right]^{-2} \quad (7)$$

where

η = a resistance coefficient analogous to the Manning coefficient for steady flow,
S_s = salinity in grams per kilogram (or parts per thousand), and
α = an empirical value relating the bottom stress to the time-varying horizontal density and velocity gradients.

The quadratic formulation given in equation 7 is essentially a depth-dependent friction relation based on the assumption of a vertical logarithmic profile of horizontal velocity in a steady flow. In this case, the equivalent drag coefficient increases with decreasing depth and the correct vorticity is produced at land boundaries if the shoreline is adequately resolved by the computational grid (Signell and Butman, 1992).

In the presence of horizontal density gradients, the magnitude of the bottom stress appears to be a function of the direction of the current. The term α in equation 7 represents a simple relation, described by Leendertse (1987), which increases the effects of bottom stress during flood flows and decreases the effects of bottom stress during ebb flows as a function of the horizontal density gradient.

The shear stress exerted by the wind at the water surface is typically described as a function of the square of the wind speed. For example, Thomas and others (1990) listed six formulations for computing shear stress at the water surface, five of which are a function of the square of the wind speed. The uncertainty in all the formulations, including the one used in equations 4 and 5, is in the determination of the value of the empirical coefficient relating stress to wind speed.

The last term in equations 4 and 5, which Leendertse (1987) calls a horizontal diffusion term, can be written for the x-direction as:

$$k_x\left[\frac{\partial^2 U}{\partial x^2}+\frac{\partial^2 U}{\partial y^2}\right] = \text{sum of viscous stresses, turbulent stresses, horizontal gradient of the cross product of vertical deviations from the vertical mean, and subgrid-scale momentum transfer.} \quad (8)$$

Viscous stresses oppose relative movement between adjacent fluid particles but are small compared to turbulent stresses in estuarine flows. The vertically integrated viscous stress term for the x-momentum equation is written as:

$$\nu\left[\frac{\partial^2 U}{\partial x^2}+\frac{\partial^2 U}{\partial y^2}\right] \quad (9)$$

where ν = coefficient of kinematic viscosity.

The viscous stress term for the y-momentum equation is analogous to equation 9, with V replacing U in each term. The relation for horizontal diffusion (eq 8) was originally developed by assuming that turbulent diffusion is analogous to viscous diffusion (eq 9). As shown in equation 8, however, the horizontal diffusion term includes processes other than turbulent diffusion.

The turbulent stresses result from the Reynolds decomposition of the nonlinear Navier-Stokes equation and represent a turbulent momentum flux. The unsteadiness of the tidal flow affects the turbulence mechanisms and structure (Gordon and Dohne, 1973; Anwar and Atkins, 1980). Partch and Smith (1978), in studies in a salt-wedge estuary, and Anwar (1983), in studies in a well-mixed and in a stratified estuary, reported turbulent mixing to be highly time dependent, with the most intense turbulent exchange occurring at the time of maximum current during ebb flow. Consequently, methods of predicting turbulent momentum flux should include temporal variability.

The turbulent shear stresses for the vertically integrated x-momentum equation are:

$$-\frac{1}{\rho}\frac{\partial}{\partial x}(\tau_{xx}H) - \frac{1}{\rho}\frac{\partial}{\partial y}(\tau_{xy}H) \qquad (10)$$

where

τ_{xx} = the vertically integrated turbulent shear stress acting in the x-direction on a plane normal to the x-direction, and

τ_{xy} = the vertically integrated turbulent shear stress acting in the x-direction on a plane normal to the y-direction.

The shear stresses are related to the turbulent velocity fluctuations by

$$\tau_{xx} = -\rho(\overline{u'u'}) \qquad (11)$$

and

$$\tau_{xy} = -\rho(\overline{u'v'}) \qquad (12)$$

where the cross products ($\overline{u'u'}$ and $\overline{u'v'}$) are the vertically integrated local temporal mean of the turbulent velocity fluctuations. Similarly, for the vertically integrated y-momentum equation, the turbulent shear stresses are:

$$-\frac{1}{\rho}\frac{\partial}{\partial x}(\tau_{yx}H) - \frac{1}{\rho}\frac{\partial}{\partial y}(\tau_{yy}H) \qquad (13)$$

The third component of the so-called horizontal diffusion term results from the vertical integration of the advection terms in the three-dimensional horizontal momentum equations. The velocity at any point in the vertical ($u(z)$) is equal to the sum of the vertically integrated velocity (U) and the deviation of the point velocity from the vertically integrated value ($u_d(z)$), or for the x-direction

$$u(z) = U + u_d(z) \qquad (14)$$

When the three-dimensional horizontal momentum equations are vertically integrated, horizontal gradients of the cross products of $u_d(z)$ and $v_d(z)$ result. These gradients have been included in the horizontal diffusion term, as is the normal procedure for models in which dimensionality has been reduced by integration over the depth of flow, across the channel, or through a cross section.

Momentum (or energy) transfers that occur at horizontal scales greater than the model computational grid length are resolved by the model through computation of the velocity field. However, momentum transfers that occur at the subgrid scale must be described empirically and also are included in the horizontal mixing term. Within the model, the subgrid-scale turbulent energy is computed as a constituent using the transport equation (eq 18). The subgrid-scale energy source is the energy loss from the main flow resulting from bottom stress, and the energy sink is the decay of turbulent energy. Using this model of turbulent energy, the vertically integrated energy is dependent on previous conditions (the system has memory), is related to the square of the velocity,

The final equation required by the model is an equation of state relating water density to water temperature and salinity. The equation of state used in the model is the relation derived by Eckert (1958):

$$\rho = \frac{\left[(5,890 + 38T) - (0.375T^2 + 3S_s)\right]}{\left[(1,779.5 + 11.25T - 0.0745T^2) - (3.8 + 0.01T)\,S_s + 0.698\,(5,890 + 38T - 0.375T^2 + 35S_s)\right]} \quad (21)$$

where

T = water temperature in degrees Celsius, and
S_s = salinity in grams per kilogram (or parts per thousand).

Because density varies only slightly with temperature, temperature is assumed to be uniform throughout the model domain. Density and the horizontal density gradients are computed at every computational point and for every time step during a simulation.

In summary, the governing equations are: (1) vertically integrated continuity equation (eq 1), (2) vertically integrated longitudinal momentum equation (eq 4), (3) vertically integrated lateral momentum equation (eq 5), (4) vertically integrated transport equation (eq 18), and (5) equation of state (eq 20). These equations are solved simultaneously for the five unknowns: (1) water level (z_1), (2) vertically integrated longitudinal velocity (U), (3) vertically integrated lateral velocity (V), (4) vertically integrated constituent concentration (S), and (5) vertically integrated density (ρ).

Numerical Solution Scheme

The governing differential equations (eqs 1, 4, 5, and 18) cannot be solved analytically for the complex conditions that exist in the Pamlico River estuary. Instead, the equations are solved using a procedure that replaces the continuous differentials in the equations by finite differences. Hence, each differential equation is reduced to an algebraic equation which can be solved for values at defined locations within the model domain.

The finite-difference equations are formulated on a space-staggered grid (fig. 10). According to Leendertse (1987), the space-staggered grid results in an efficient solution because velocity points are located between depth points on the grid for solution of the momentum equations (eqs 4 and 5) and because velocity points are located between water-level points for solution of the continuity equation (eq 1). A complete description of the finite-difference formulation of the continuity, momentum, and transport equations on the space-staggered finite-difference grid is given by Leendertse (1987).

The ADI finite-difference method is used to solve the governing equations. The ADI method was first introduced by Douglas (1955) and Peaceman and Rachford (1955), and uses a splitting of the time step to obtain a multidimensional implicit method which provides second-order accuracy. The x-momentum equation is solved during the first half of the time step, and the y-momentum equation is solved during the second half of the time step. The advantage of the ADI method over other implicit schemes is that solution of each set of algebraic finite-difference equations requires only the inversion of a tridiagonal matrix (Roache, 1982). The stability and convergence

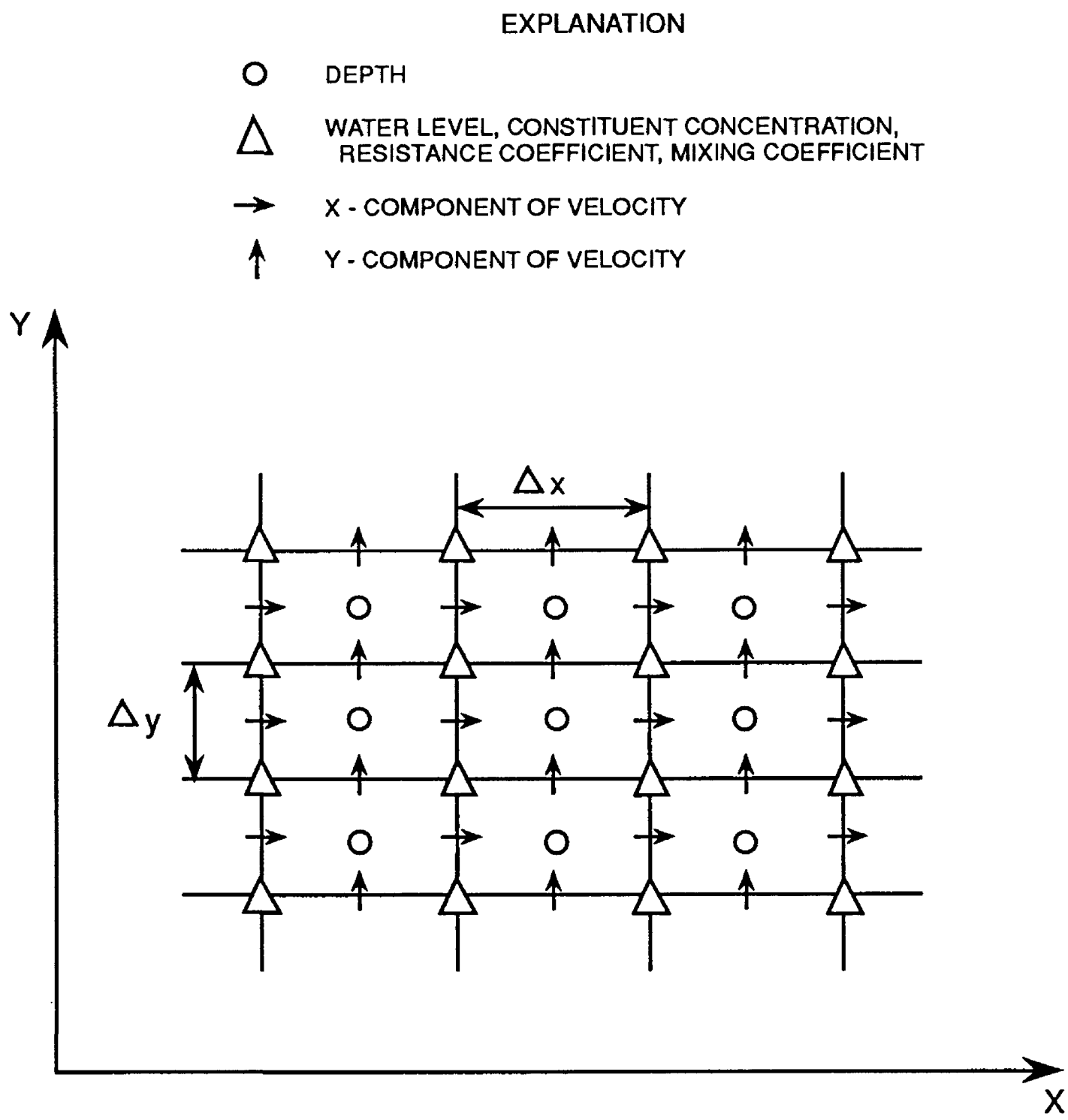

Figure 10. Location of variables on staggered finite grid.

characteristics of the ADI technique as applied to the governing equations were discussed by Leendertse (1987). Although the method is theoretically unconditionally stable, there are some practical limitations to the magnitude of the time step (Roache, 1982), particularly for model domains having irregular boundaries (Weare, 1979) or complex bathymetries (Benque and others, 1982).

Model Input Requirements

Four types of input are required to operate the numerical model: (1) initial conditions, (2) boundary conditions, (3) value of various model parameters, and (4) selection of model options.

Initial conditions are required to define the water level, velocity, and constituent concentrations in each computational cell prior to initiation of a simulation. Except as noted below, the initial water surface must be level, and initial velocities are usually set to zero. Initial constituent concentrations can be uniform throughout the computational domain, or can vary from computational cell to computational cell. Better results are obtained more quickly when the initial conditions specified in the model closely match prototype conditions. The model can also be restarted using previous simulation results for water level, velocity, and constituent concentration in each computational cell as initial conditions for a subsequent

simulation. When the model is restarted in this manner, the initial water surface need not be level.

Information on boundary conditions is required at each computational time step throughout a simulation, whereas initial conditions are required only at the beginning of a simulation. Boundary conditions must be specified at the channel bottom, at the water surface, and at all lateral boundaries. The bottom boundary is described by the elevation of the streambed and a resistance coefficient (eq 7) in each computational cell. The resistance coefficient can be adjusted during model calibration, and bottom boundary conditions subsequently remain constant throughout the remainder of the simulations.

The water-surface boundary condition consists of the time-varying wind blowing over the estuary. The model will accept spatially varying wind or wind that is uniform over the estuary. In the absence of any information, wind is usually assumed to be uniform in the model domain.

Lateral boundary conditions can consist of either time-varying water level (tide opening) or time-varying flow (inflow or outflow). Time-varying water constituent concentrations also must be specified at each lateral boundary. The Pamlico River model includes two tide openings where measured water levels and salinities are used as boundary conditions. Boundary conditions at each discharge point are described by time-varying flow and constituent concentrations.

Several model parameters must be specified prior to each simulation. These parameters include the wind-stress coefficient, C_d (eq 5); air density, ρ_a (eq 5); latitude of the estuary, φ (eq 6); the resistance coefficient for each computational cell, η (eq 7); α (eq 7); kinematic viscosity of water, ν (eqs 15 and 16); the unadjusted horizontal mixing coefficient, k' (eqs 15 and 16); the isotropic mass dispersion coefficient, D_i (eq 19); and D_c, which relates mass dispersion to flow properties (eq 20). The air density, latitude of the estuary, and kinematic viscosity of water are easily defined for the Pamlico River, assuming that the air and water temperature do not vary significantly during the simulation period. Other parameters are known with less certainty and can require some adjustment during model calibration. Following calibration, these parameters are not adjusted for any subsequent simulations.

The orientation of the coordinate system must be specified by the user. At long, open boundaries, the governing equations are solved by assuming that the velocity parallel and adjacent to the boundary is zero, and that the gradient of velocity perpendicular to the boundary is zero. Consequently, to improve model performance near the open boundaries, the x-axis is usually aligned with the longitudinal axis of the estuary so that the y-axis is parallel to the downstream boundary.

The model includes three primary user-specified options. The user can specify the type and frequency of model output. The numerical scheme for solution of the advective terms in equations 4 and 5 can also be selected. Options include (1) omitting the advective terms; (2) the Arakawa method (1966), which results in the conservation of vorticity and squared vorticity in the simulation; and (3) the Leendertse (1987) method, which is computationally more simple than the Arakawa method, but does not conserve vorticity. The Arakawa method is used in this application. The third user-specified option defines the procedure used to integrate the continuity (eq 1) and momentum (eqs 4 and 5) equations. The options define the time level at which the approximation of velocity and water-level terms are made in the finite-difference equations, as well as the spatial representation of these terms. The option recommended by Leendertse (1987), in which the velocity terms become essentially centered in time, was used in this application.

MODEL IMPLEMENTATION

Implementation of the hydrodynamic and transport model for the Pamlico River included (1) development of the computational grid, (2) specification of model boundary conditions, (3) identification of initial conditions, and (4) selection of model parameters. This section of the report provides a description of the model domain, computational grid, and results of convergence tests. Procedures and associated assumptions for specification of boundary and initial conditions are given, and model parameters are identified.

Computational Grid and Time Step

The model domain extends from Washington, North Carolina, downstream to a section of the estuary just downstream from Goose Creek (fig. 11). The domain encompasses most of the major tributary streams, including Chocowinity Bay, Broad Creek, Bath Creek, Goose Creek, South Creek, Durham Creek, and Blounts Creek, as well as some smaller embayments. The distance from the upstream to the downstream boundary is 48 km (240 computational cells), and the maximum width of the computational domain is 21 km (105 computational cells).

A finite-difference solution to a partial-differential equation, such as is used in this model, is spatially convergent if the numerical solution approaches the true solution of the differential equation as the finite-difference mesh size approaches zero (Roache, 1982). Spatial convergency can be tested by repeatedly running the model with a fixed set of boundary conditions for successively smaller computational grid sizes. The model is spatially convergent if no further change in model results is observed as the grid size is refined (Thompson, 1992). Likewise, a model is temporally convergent if model results remain substantially unchanged as the computational time step is decreased. To determine the effects of grid size and time step on model results, convergence testing should be included in modeling investigations and be conducted prior to model calibration.

Simulations of flow and transport in the Pamlico River were performed for three computational grid sizes: (1) 100 m x 100 m, (2) 200 m x 200 m, and (3) 400 m x 400 m. A 4-day simulation was made using the same set of boundary conditions, initial conditions, and model parameters for each of the three grid sizes. Water level, salinity, transport, and circulation patterns from each simulation were compared to determine if model results were significantly different for the three grid sizes.

Simulated water levels were only slightly affected by changes in grid size (table 10). Likewise, the mean and maximum simulated salinity at site S2 did not change appreciably with grid size. However, changes in the distribution of salinity within the estuary were noted (fig. 12). For example, the 2 ppt line of equal salinity was at approximately the same location within the estuary for the 100-m and the 200-m grid simulation results, but was about 1 km further downstream for the 400-m grid (fig. 12). This difference was considered to be significant given the relatively short simulation period. In general, the lines of equal simulated salinity for the 100-m and 200-m grids were in agreement with each other but differed from the results for the 400-m grid simulation.

Table 10. Results of convergence tests for computational grid and time step

	Grid size for time step=1 minute		
Water level at site WL3 (fig. 3)	**100 meters**	**200 meters**	**400 meters**
Mean	0.108	0.111	0.110
Maximum	.256	.281	.286
Minimum	-.049	-.049	-.054
Salinity at site S2 (fig. 3)	**Parts per thousand**		
Mean	2.4	2.4	2.3
Maximum	2.7	2.7	2.6
Flow near the downstream boundary	**Cubic meters per second**		
Mean	-61	-54	-40
Maximum	2,630	2,590	2,360
Minimum	-3,510	-3,270	-2,990
	Time step for grid size=200 meters		
	0.5 minute	**1.0 minute**	**3.0 minutes**
Mean salinity	**Parts per thousand**		
Site S2 (fig. 3)	7.6	7.6	7.6
Site S3 (fig. 3)	8.9	8.9	8.9
Site S4 (fig. 3)	10.7	10.7	10.7
Mean flow	**Cubic meters per second**		
At upstream boundary	-9.9	-9.8	-9.5
Near site V1 (fig. 3)	2.7	2.8	3.2
At downstream boundary	25.2	25.1	24.4

Differences also were evident in the simulated flow rates for the three grid sizes. The simulated mean flow increased in magnitude with a decrease in grid size (table 10). The mean flow for the 200-m grid was 35 percent greater than that for the 400-m grid. The mean flow for the 100-m grid

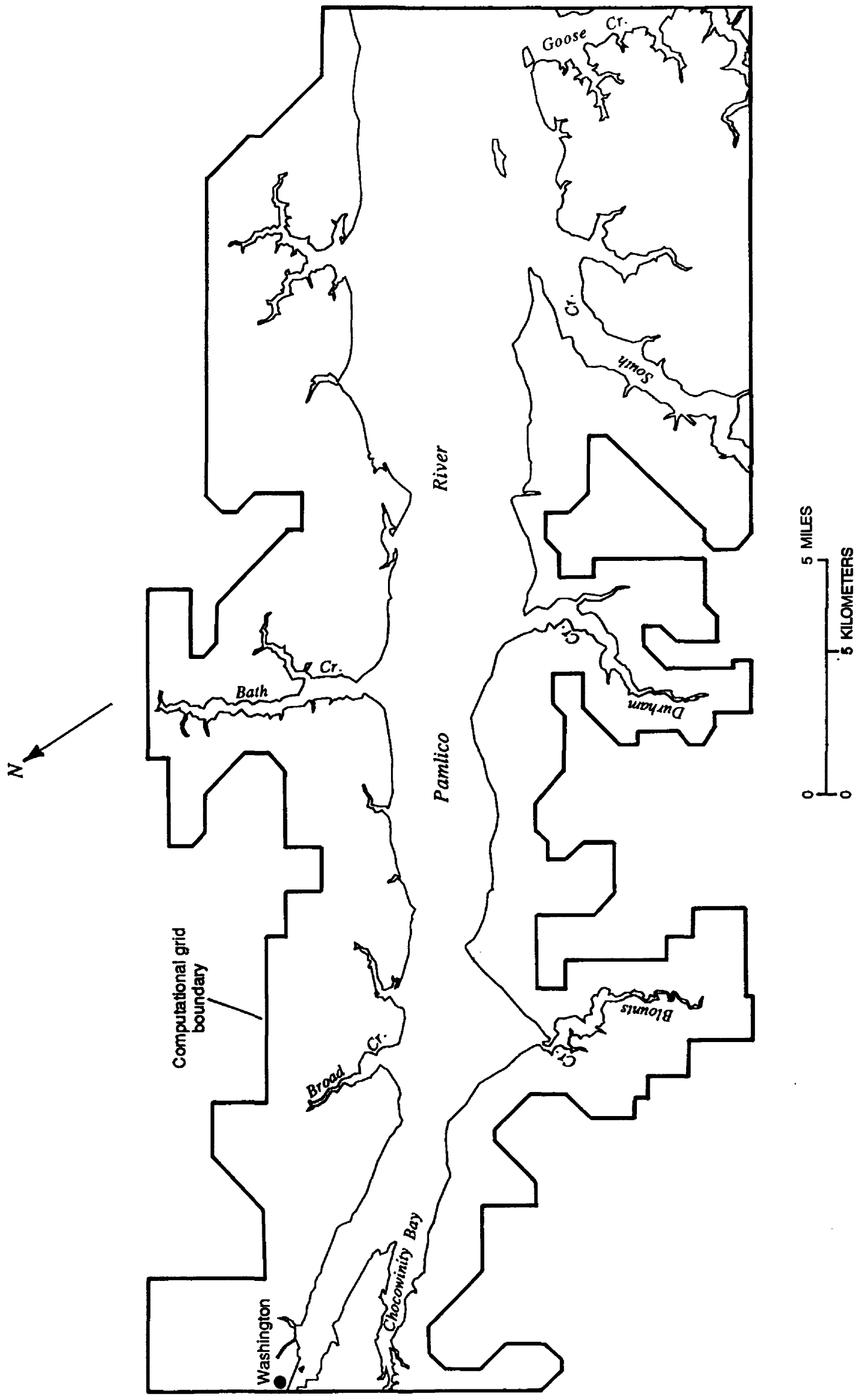

Figure 11. Computational domain for Pamlico River model.

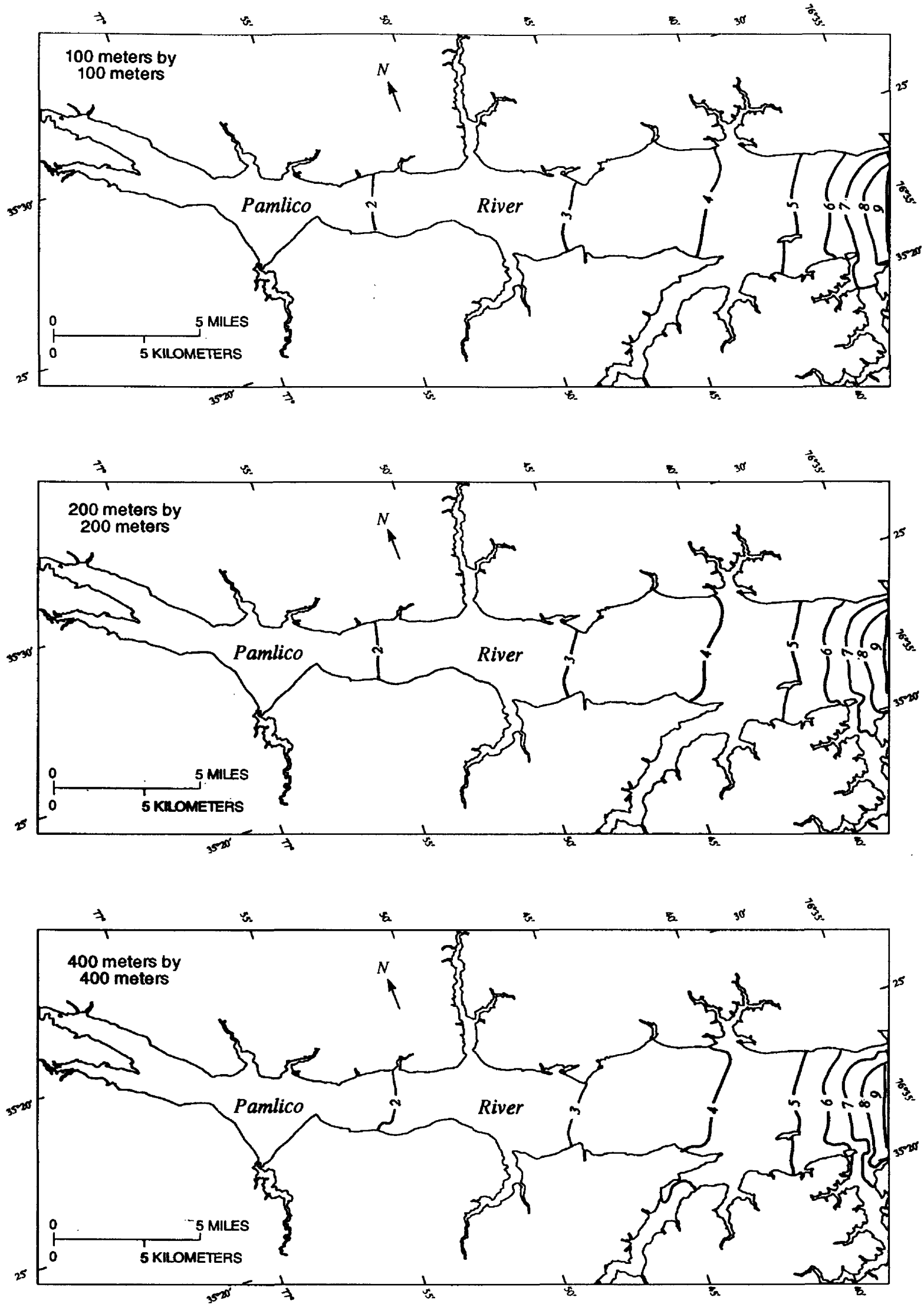

Figure 12. Lines of equal simulated salinity 59.33 hours after start of simulation for three computational grid sizes.

was 13 percent greater than the mean flow for the 200-m grid and 53 percent larger than for the 400-m grid.

All hydrodynamic components of the natural system having a wave length less than twice the selected grid size cannot be resolved by the model. Components which cannot be resolved by the grid are essentially filtered (or aliased into lower frequency components) from the description of the hydrodynamics of the estuary (Abbott and others, 1981). Hence, smaller grids permit better spatial resolution of hydrodynamic and transport processes.

Processes which occur at length scales smaller than the size of the grid spacing, or at the subgrid scale, must be described empirically in the model. Hence, increased resolution results in more direct simulation of hydrodynamic processes and less empiricism in the model. In addition, small-scale flow features, which may be important for mixing and transport processes, can be simulated with spatially detailed grids. For example, the gyre present just west of the mouth of Broad Creek (fig. 13) is resolved by the 100-m and the 200-m grids, but is not depicted with results from the 400-m grid simulation. Likewise, the circulation near the mouth of Chocowinity Bay (fig. 13) is not resolved using the 400-m grid. Because SIMSYS2D requires that flow channels be at least two computational cells wide, the smaller grid size also permits simulation of flow and transport into and out of the tributary streams and embayments (for example, Broad Creek, fig. 13).

Results from simulations with the 200-m grid provide very good spatial resolution of the hydrodynamics in the Pamlico River. Because of the relatively small differences in simulated results for the 100-m and the 200-m grids, and to minimize computational time based on the total number of computational cells in the model domain, the 200-m by 200-m grid size was selected for the Pamlico River model.

Simulations were made using the 200-m computational grid and time steps of 0.5, 1.0, and 3.0 minutes. Boundary data collected during June 14-30, 1991, (see following section on Pamlico River Model Calibration) were used for the simulations. Simulated salinities were unaffected by changes in computational time step (table 10). Simulated mean flows using the 0.5- and 1.0-minute time steps were essentially the same (table 10), and a 1.0-minute time step was subsequently used.

For the 200-m grid, there are 5,620 active computational cells bounded by the Pamlico River shoreline. Water level, velocity, and salinity are computed for each of these cells at 1-minute intervals during model simulations. Additional computational cells lie between the shoreline and the boundary of the model (fig. 10), but these cells do not generally enter into the computations.

Boundary Conditions

Boundaries of the Pamlico River model include the channel bottom, the shoreline and tributary streams, a downstream (or eastern) open-water boundary, an upstream (or western) open-water boundary near Washington, and the water surface. Lateral model boundaries are delineated in figure 11. A description of the assumptions and data used to describe conditions at each boundary follows.

Bottom Boundary

The channel bottom is assumed to be an impermeable boundary so that there is no discharge of ground water to the estuary within the model domain and no loss of water from the estuary to the ground-water system. Streams and estuaries in eastern North Carolina are typically discharge areas for ground water (Winner and Coble, 1989). However, results from a model of the North Carolina Coastal Plain aquifer system indicate that part of the Pamlico River is a recharge area (Giese and others, 1991) as a consequence of high ground-water pumpage at a mining operation near South Creek. The magnitude of recharge (or discharge) from the Pamlico River is unknown but probably small relative to the flow in the estuary.

The channel bottom is assumed to be immobile. In the Pamlico River, fine-grained sediments occupy the main channel of the estuary, and sands are confined to the nearshore region (Wells, 1989). Hence, it is unlikely that the large, mobile, sand bedforms that occur in alluvial streams and open seas exist in the Pamlico River, and the assumption of an immobile channel bottom is reasonable.

The channel bottom is assumed to cause resistance to the flow and thereby extract energy

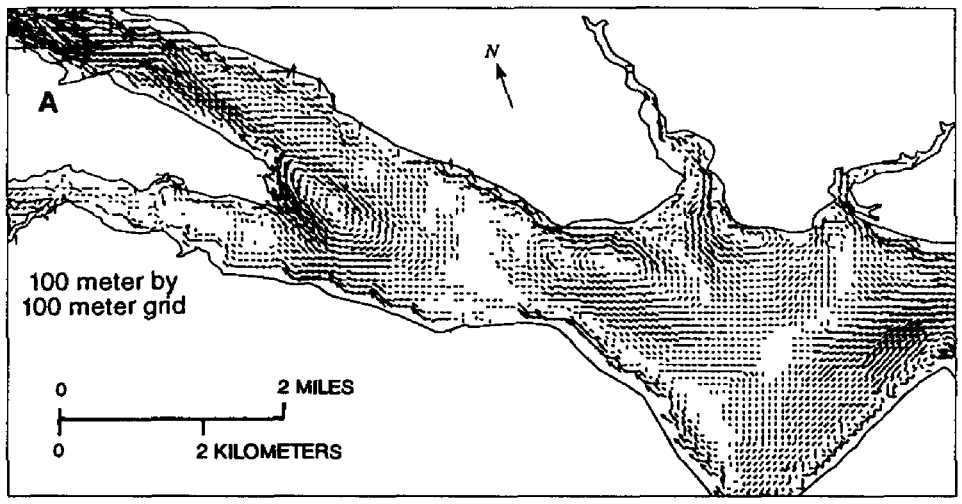

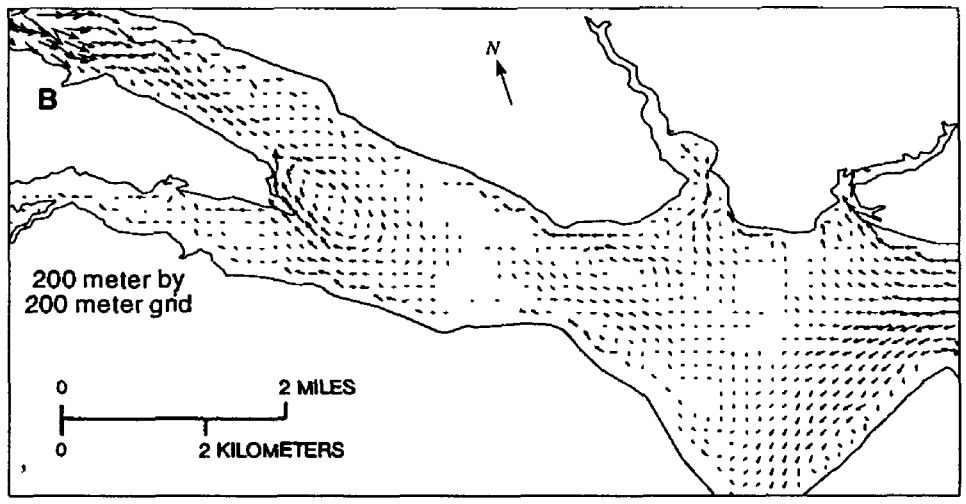

EXPLANATION

← VECTOR--Head points in flow direction. Greater vector length represents greater relative velocity

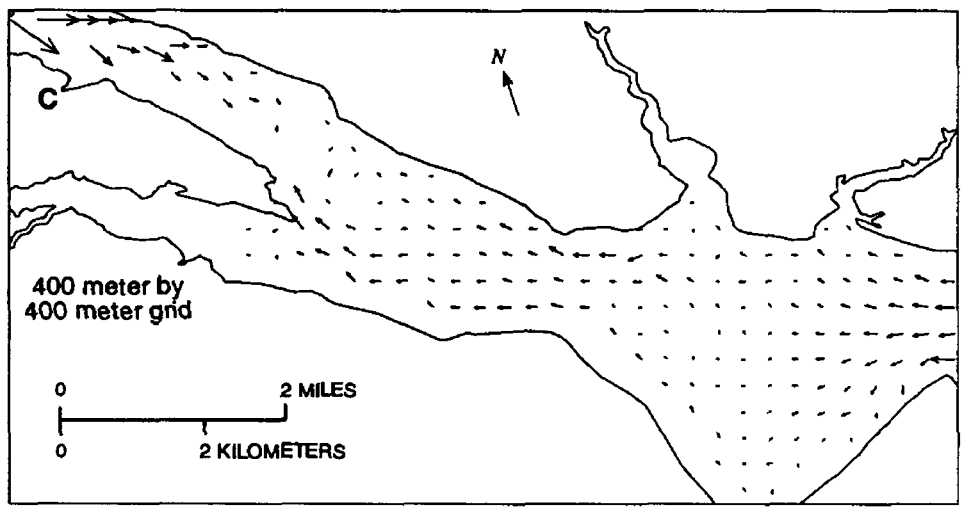

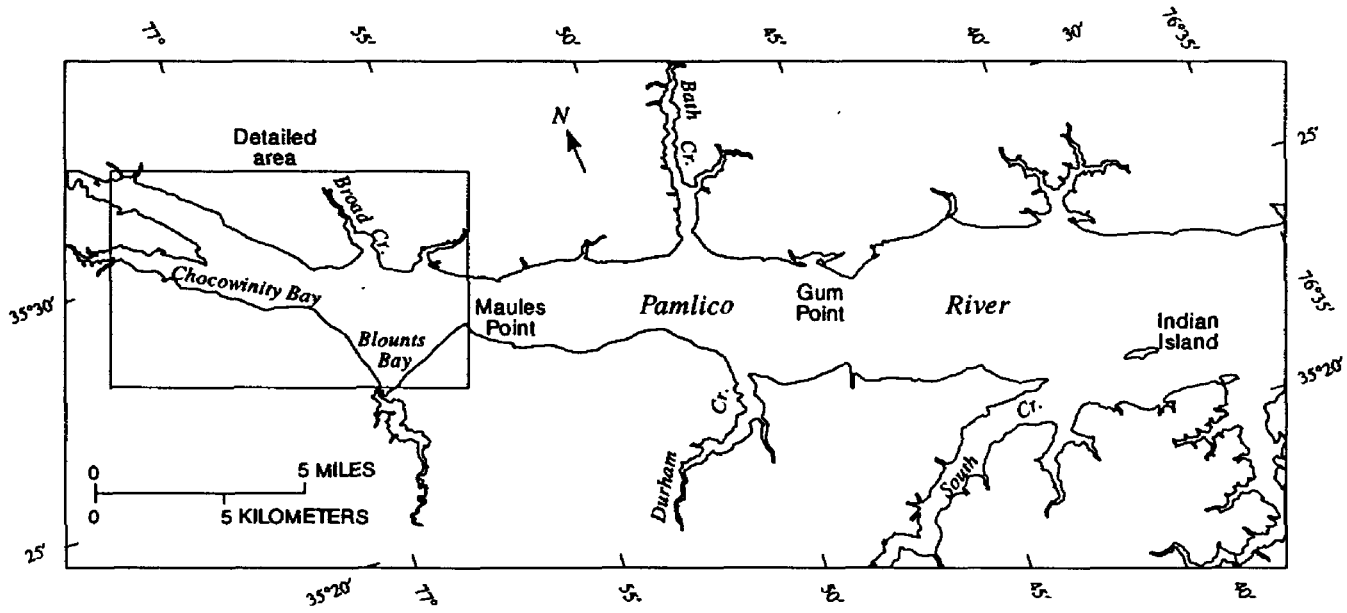

Figure 13. Simulated circulation patterns in the western end of the Pamlico River 67.75 hours after start of simulation for three computational grid sizes.

from the mean flow. Resistance increases as the roughness of the bottom material increases. A resistance coefficient, η, analogous to Manning's n, was assigned to each computational cell. (Manning's n applies to steady-flow conditions only.) The resistance coefficient, which is an empirical value that cannot be directly measured, can vary from cell to cell throughout the model domain.

Several formulations for the bottom stress term (eq 7) in the momentum equations (eqs 4 and 5) have been proposed and used in two-dimensional, vertically hydrodynamic models. Hence, the value of the resistance coefficient used in any given estuarine hydrodynamic model is somewhat dependent on the formulation of the bottom stress term in the model. Moreover, the resistance coefficient is directly dependent on the configuration of the channel bottom, as well as the material which forms the bottom. Nevertheless, values of the resistance coefficient used in other studies were used as a general guide in selecting appropriate values for the Pamlico River model.

Some examples of previously used resistance coefficients in vertically integrated hydrodynamic models include the following: (1) 0.015 to 0.030 for Stefansson Sound, Alaska (Hamilton, 1992); (2) 0.017 to 0.033 for Singapore Strait (Shankar and others, 1992); (3) 0.018 to 0.035 for Masonboro Inlet, North Carolina (Masch and Brandes (1975); (4) 0.02 for Pamlico Sound (Amein and Airan (1976); (5) 0.0235 for Tampa Bay, Florida (Goodwin, 1987); (6) 0.0264 for Boston Harbor (Signell and Butman, 1992); (7) 0.028 for Long Island Sound and adjacent waters (Beauchamp and Spaulding (1978); (8) 0.030 for Providence River, Rhode Island (Mendelsohn and Swanson, 1992); and (9) 0.030 for Cleveland Bay, Australia (King, 1992). During application of an earlier version of SIMSYS2D, Leendertse (1972) used resistance coefficient values of between 0.026 and 0.034 in a study of Jamaica Bay, New York.

For the Pamlico River model, a resistance coefficient value of 0.028 was initially assigned to all computational cells. The resistance coefficient was varied between 0.025 and 0.030 during model calibration and testing. The model also offers the option of increasing the resistance at the open-water boundaries to improve model performance. Resistance was increased slightly at the open-water boundaries, but no change in simulated results was noted.

Shoreline and Tributary Streams

The shoreline is defined as a boundary across which there is no flow. The exact position of the shoreline can change during a model simulation because of flooding or drying of computational grid cells in response to water-level changes.

A "leak test" was performed to ensure that there were no unintentional openings in the shoreline boundary through which flow could leave the model domain. The test was performed by (1) prescribing an initially level water surface throughout the estuary, (2) assuming that water level at the upstream and downstream open boundaries did not vary from the initial conditions, (3) assuming that there was no salt in the estuary or at the boundaries, and (4) assuming that there was no wind at the water surface. For the assumed conditions, flow would be generated within the model domain if there were openings in the shoreline. No leaks were found.

Boundary conditions also are required for computation of flow adjacent to the shoreline. The computation of the component of flow perpendicular to the shoreline requires the assumption that the gradient of velocity perpendicular to the shoreline is zero. For computation of the component of flow parallel to the shoreline, the velocity at the shoreline and the differential of the velocity at the shoreline are assumed to be zero. Additional information on computation of flow adjacent to closed boundaries, along with examples, is given by Leendertse (1987).

Tributary streams were treated as closed-end embayments. Water and salt movement into and out of these streams was simulated by the model, but no additional freshwater was added to the estuary through these tributaries. For most months, the freshwater inflow volume from tributary streams is small relative to the inflow from the Tar River (table 8). Moreover, the tributary streams inflow volume is quite small relative to the total volume of the Pamlico River. Tests were performed (and are described in the section on sensitivity tests) to determine if this assumption affected simulated hydrodynamics in the estuary.

If the model is subsequently used for simulation of water-quality processes, constituent loadings from the tributary streams should be included in the model. This could be done by treating the tributary streams as open-water boundaries and prescribing a time series of water level (or flow), salinity, and constituent concentrations at the upstream, open-water boundary of the tributary streams.

Open-Water Boundaries

Time series of observed water level and salinity are required at the open-water boundaries. (The salinity boundary data are used in the computations only for the condition of flow across the open boundary and into the model domain.) At the upstream, or western, boundary, observed water levels at site WL1 and observed salinities at site S1 (fig. 3) are used as boundary conditions. Observed water levels at site WL4 and salinities at site S5 are used as boundary conditions for the downstream, or eastern, boundary. Observed near-surface and near-bottom salinities are averaged to provide a vertical mean salinity for the boundary condition. Boundary conditions at the 1-minute computational interval are linearly interpolated from the data observed at 15-minute intervals.

Assumptions about velocities at the boundary are required for the condition of flow into the model domain. The longitudinal gradient of the velocity component perpendicular to the boundary is assumed to be zero. Likewise, the second derivative of the velocity, which is just inside and perpendicular to the boundary, is assumed to be zero. Finally, for the component of flow parallel to the open boundary, the advection terms in the momentum equations (eqs 4 and 5) are assumed to be zero. Hence, the open-water boundaries for the Pamlico River were oriented to be perpendicular to the topographic axis of the estuary so that the flow at the boundary was typically perpendicular to the boundary.

These or similar assumptions are generally required for the solution of a system of nonlinear, boundary-value equations, such as those solved by this numerical model. Moreover, the magnitude of each of these velocity terms assumed to be zero at or near the boundary is typically quite small. Consequently, these assumptions should have a negligible effect on the simulation results, and the effects should be confined to the region very near the boundary. Additional information on computations near open-water boundaries, along with examples, is given by Leendertse (1987).

Water-Surface Boundary

The "rigid lid" assumption is used in the description of the water surface. That is, the water surface in each computational cell moves vertically, but no deformation of the level water surface within the cell occurs. The rigid lid assumption implies that high-frequency, wind-generated waves are not included in the model. Inputs from precipitation and losses from evaporation are neglected for the relatively short simulation periods used in this investigation.

Momentum is transferred to the estuary by wind blowing over the water surface. Wind speed and direction measured at site W1 (fig. 3) is used for the water-surface boundary condition. It was assumed that the wind was spatially invariant over the entire model domain but that the wind varied with time. Wind-speed and direction data at the 1-minute computational interval are linearly interpolated from the data observed at 30-minute intervals.

Initial Conditions

Initial velocity, water-level, and salinity conditions must be described for each computational cell prior to model simulations. The velocity in each computational cell was assumed to be zero at the beginning of each simulation. The water surface was assumed to be initially level throughout the model domain. The initial water level was set equal to the average of the observed water level at sites WL1 and WL4 (fig. 3) at the beginning of the simulation. The upstream and downstream boundary water levels were measured at sites WL1 and WL4, respectively.

Initial salinity concentrations were determined from measured data at sites S1, S2, S3, S4, and S5 (fig. 3). Initial values for computational cells between the five measurement sites were linearly interpolated from the mean of the observed near-surface and near-bottom salinities. For some simulations, observed salinity did not vary linearly

along the longitudinal axis of the estuary, so some adjustment of the linearly interpolated initial values was required. The initial salinity conditions did not include lateral variations in salinity.

As expected, model results during the first several days of simulation are very sensitive to estimated initial salinity conditions. Simulation results indicated that the effects of initial conditions were generally transported out of the model domain within 4 to 6 days after the beginning of the simulation. However, the amount of time for solute to move through the estuary is variable and is also a function of the initial position of the solute.

Model Parameters

Five model parameters must be chosen prior to model simulations. These parameters include: (1) the wind-stress coefficient, C_d; (2) α in equation 7, which is used in the determination of the resistance coefficient; (3) the unadjusted horizontal momentum mixing coefficient, k' (eq 15); (4) the isotropic mass dispersion coefficient, D_i (eq 19); and (5) D_c (eq 20), a coefficient used to compute mass dispersion in the direction of flow. Because these parameters are generally empirical representations of a physical process, the parameters are not known with certainty and, thus, required some adjustment and testing during the calibration process.

The wind-stress coefficient seems to be a complex function of the roughness of the air-water interface, the fetch, the stability of the air mass above the water, the relative temperatures of the air and water, and the topography of the land upwind of the water body (Watanabe and others, 1983). Some sophisticated formulations are available for the computation of the wind-stress coefficient, and two of the most widely used are those of Garratt (1977) and Large and Pond (1981), both of which are based on measurements in the ocean. The wind-stress coefficient also is often assumed to be constant for estuarine model applications, which is the approach taken for the Pamlico River model. A value of 0.001 was initially selected for C_d. This is in general agreement with coefficient values suggested by Wu (1969). According to Wu, for example, $C_d = 0.001$ for a wind speed of 4 m/s, and $C_d = 0.0015$ for a wind speed of 9 m/s. In other applications, Schmalz (1985) used $C_d = 0.001$ in a two-dimensional, vertically averaged model of the Mississippi Sound; Leendertse and Gritton (1971) and Goodwin (1987) used a value of 0.0008; and Svendsen and others (1992) used $C_d = 0.0012$.

The term α is used to relate the resistance coefficient to the strength of the horizontal salinity gradients and to the direction of flow (eq 7). In the Pamlico River, flow velocities are generally low, and horizontal salinity gradients are typically small. Consequently, α was set to zero in all Pamlico River simulations. Subsequent tests indicated that nonzero values of α made no noticeable difference in simulation results.

The parameter k' is used in the computation of the horizontal exchange of momentum (eq 15). Horizontal momentum exchange, or mixing, depends primarily on the combined effects of spatial variations in the longitudinal and lateral velocities (eq 8; Ridderinkhof and Zimmerman, 1990). Consequently, for models with spatially detailed computational grids (such as the Pamlico River model), currents which dominate horizontal mixing are directly computed by the model, and the so-called horizontal diffusion term (eq 8) becomes relatively small in comparison to other terms in the momentum equation. In fact, Signell and Butman (1992) neglected horizontal momentum exchange in an application of a two-dimensional, vertically averaged model of Boston Harbor, which used 200-m x 200-m computational-grid cells. Ridderinkhof and Zimmerman (1990) used a value of $k_x = k_y = 7$ square meters per second (m^2/s) in a two-dimensional, vertically averaged model with 500-m x 500-m computational cells.

A value of $k' = 10$ m^2/s was initially used in the Pamlico River. Tests with a simplified model, described in a subsequent section, demonstrated the sensitivity of model results to the magnitude of k'.

As with horizontal mixing of momentum, horizontal mass exchange is well represented in the spatially detailed Pamlico River model. Hence, there is less need to focus on calibrating the model to D_i and D_c because the processes represented by the parameters are small relative to the other terms in the transport equation (eq. 18). Initially, D_i was set at 20 m^2/s, and D_c was set at 14 m^2/s, which is near the value given by Elder (1959). For the velocities and depths typically in the Pamlico River, D_f (which is computed from D_c, eq 20) is much

smaller than D_i. Tests with the Pamlico River model demonstrated that model results were relatively insensitive to changes in these two parameters.

SIMULATION OF HYDRODYNAMICS AND SOLUTE TRANSPORT

Prior to calibration and validation of the Pamlico River model, simulations were made for simplified conditions. Following these preliminary simulations, the Pamlico River model was calibrated using data collected during June 14-30, 1991. Model validation was conducted using data from August 30 through September 12, 1989, when current meters were in place, and July 4-28, 1991. The sensitivity of simulated results to small changes in various model parameters was then documented. Finally, the model was applied to simulate flow rates, circulation patterns, salinity distributions, and transport for several different forcing conditions.

Preliminary Simulations

Although the SIMSYS2D model has been widely used, documentation of model response to varying model parameters and simplified boundary conditions is difficult to find in scientific literature, as is the case for many other published models. Consequently, preliminary simulations were made for two geometric configurations to evaluate model characteristics and response. First, a model of a uniform channel with a rectangular cross section was used to characterize model response to changes in model parameters under steady-flow conditions. The model of the rectangular channel was used to analyze the effects of (1) three different treatments of the advection terms in equations 4 and 5, (2) changes in the unadjusted horizontal mixing coefficient (k' in eqs 15 and 16), and (3) wind. Second, idealized boundary conditions were applied to the Pamlico River model to characterize the individual effects of various forcing mechanisms on Pamlico River flow processes.

Rectangular Channel

Within SIMSYS2D, there are three options for treating the advection terms in the solution of the momentum equations. These options are: (1) omission of the terms, (2) the Leendertse (1987) method, and (3) the Arakawa (1966) method. The Leendertse method conserves momentum, and the Arakawa method conserves momentum and vorticity. Simulations were made using each of the three methods with values of the unadjusted horizontal mixing coefficient, k', of 0, 10, and 100 m^2/s.

A 2,100-m-long and 1,100-m-wide channel with a uniform rectangular cross section was used for the simulations. Computational cells for the test model were 100 m x 100 m. A groin, which was 100 m wide and extended 500 m across the channel, was placed in the channel 600 m downstream from the upstream boundary so that circulation patterns around the barrier, as documented by Lean and Weare (1979) and by Yeh and others (1988), could be examined. The model was run to steady state with constant inflow of 450 m^3/s at the upstream boundary and a constant water depth of 3 m at the downstream boundary.

Simulations made without the advection terms did not produce any circulation in the lee of the groin (fig. 14). Results from the simulations made using the Leendertse and the Arakawa methods for solution of the advection terms in the momentum equation did show the expected eddy downstream from the groin (fig. 14). As the unadjusted horizontal mixing coefficient, k', was increased, the circulation pattern was smoothed and became less distinct (fig. 14), although an order of magnitude increase in k' was required before this smoothing became apparent. The results indicate that the Arakawa solution method with a small value of k' (10 m^2/s) should reproduce circulation patterns in the Pamlico River, where topographic changes are less abrupt than in the test model.

Wind seems to significantly affect circulation in the Pamlico River. Consequently, the rectangular channel test model was used to evaluate changes in simulated flows in response to varying wind speed as a function of the wind-stress coefficient C_d, wind direction, and depth of flow. The groin was removed from the channel for these simulations. Simulations were made using a steady water level at each boundary and a water-surface slope of 2.4×10^{-6}.

For $C_d = 0.001$ and a water depth of 3 m, flow was increased 6 percent relative to the no-wind

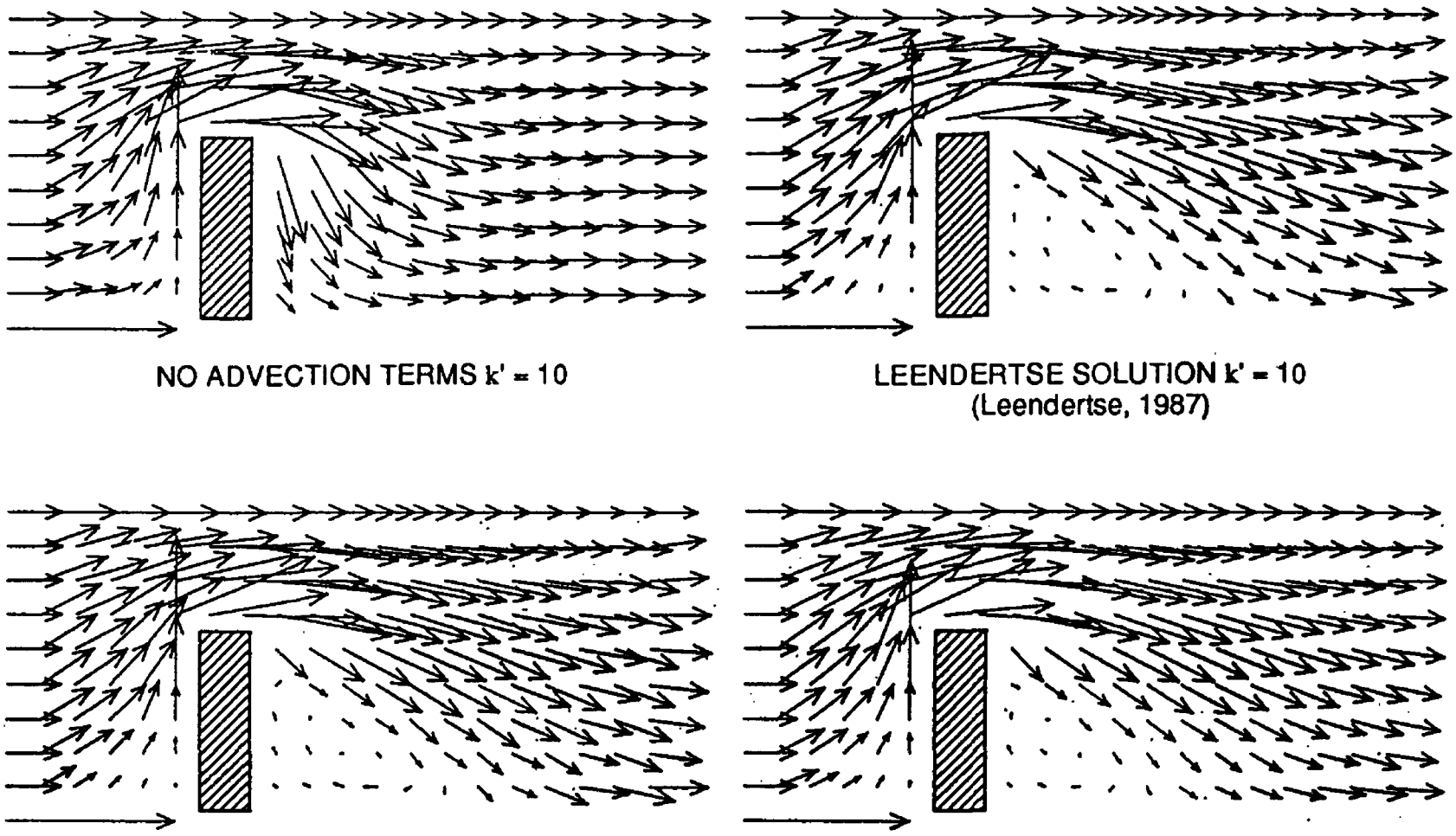

Figure 14. Circulation patterns in rectangular channel test model with steady flow for three treatments of advection terms and two values of k'.

ondition by a 2.5-m/s wind blowing downstream long the channel axis, and 24 percent by a 5-m/s vind blowing down the channel. For a wind lowing upstream along the channel axis, flow was ecreased 7 percent relative to the no-wind ondition by a 2.5-m/s wind and 31 percent by a -m/s wind. An increase in C_d of 50 percent esulted in a 3-percent increase in flow for a 2.5-m/s vind and a 10-percent increase in flow for a 5-m/s vind. As indicated by the wind-stress term in the nomentum equations, the flow is more sensitive to hanges in wind speed than to changes in C_d. The ffects of wind on flow increased with increased low depth. For $C_d = 0.001$ and a wind speed of 5 m/s, the flow increased by an order of magnitude for a five-fold increase in depth of flow.

Pamlico River Bathymetry

Simplified boundary conditions were applied to the 240- x 105-, 200-m Pamlico model grid to evaluate individual effects of various forcing mechanisms. The first simulation was for a constant inflow of 180 m^3/s at the upstream boundary, or about twice the annual mean flow, and a constant water level of 0.5 m at the downstream boundary. Salinity was zero throughout the model; no wind was prescribed, and the Coriolis force was

neglected. Initial conditions included zero flow and a level water surface at an elevation of 0.5 m. Using a 1-minute time step, a steady state was reached 6,000 minutes after starting the simulation. Water-level oscillations of more than 4 cm were observed prior to steady-state conditions. After steady-state conditions were reached, streamlines showed little or no curvature. Mass was conserved throughout the simulation. Inclusion of the Coriolis force in a second simulation having the same boundary conditions as the first resulted in some slight curvature of the streamlines in the lower 2 km of the estuary.

A sinusoidal tide with an amplitude of 0.3 m, or about 60 percent greater than the mean daily water-level range at sites WL4 and WL5 (table 2; fig. 3), and a period of 12.48 hours was prescribed at the downstream boundary for the next simulation. Conditions at the end of the previous simulation were used as initial conditions for this test. The model reached steady state within three tide cycles, or about 2,000 minutes after beginning the simulation. Streamlines showed some curvature, which appeared to be related to bathymetry. Flow remained in the downstream direction at the upstream boundary, as prescribed by the applied boundary condition. Flow at the downstream boundary ranged between about 10,000 m^3/s upstream and 10,000 m^3/s downstream.

Instantaneous differences in water level of as much as 7 cm were observed in the data collected at sites WL4 and WL5. To evaluate the effects of a lateral water-level gradient at the downstream boundary on circulation patterns, a simulation was performed using the same boundary conditions as the first simulation (constant inflow of 180 m^3/s at the upstream boundary and a constant water level of 0.5 m at the downstream boundary), except that a water-level difference of 2 cm was prescribed across the downstream boundary. Conditions at the end of the first simulation were used as initial conditions for this simulation. Simulations were performed with the higher water level on the north side of the channel, the higher water level on the south side of the channel, and with and without Coriolis force.

With the presence of a lateral water-level gradient, a cross-channel flow was simulated for the region near the downstream boundary. These effects were detected as far as about 8 km upstream of the downstream boundary, but effects were small at distances greater than 2 km. Upstream of the influence of the cross-channel circulation, results were identical to those obtained in the first test case with no lateral water-level gradient. The water-level gradient imposed across the channel at the downstream boundary was greater than the longitudinal gradient from the upstream to the downstream boundary.

As previously mentioned, gage datums were tied to a first-order network by a ground survey which achieved second-order vertical accuracy. It is possible that some small errors in gage datums exist which could lead to an apparent lateral water-level gradient at the downstream boundary. An additional confounding factor is that site WL4 is located essentially on the north shore of the estuary, whereas site WL5 is located in a small sheltered harbor along Goose Creek and about 2 km south of the south shore of the estuary (fig. 3). Subsequent simulations made with observed boundary conditions and with no lateral water-level gradient at the downstream boundary, however, do show distinct lateral circulation patterns in the downstream region of the estuary. Moreover, measured velocities near the downstream model boundary also indicate the presence of a lateral difference in currents (fig. 7). Between August 23 and September 6, 1989, the net velocity on the south side of the estuary was in the upstream direction, and the net velocity on the north side was in the downstream direction. For all of these reasons, data from only site WL4 were used as the downstream water-level boundary. Sensitivity tests were performed with the calibrated model to further evaluate the effects of the downstream lateral water-level gradient.

Pamlico River Model Calibration

Model calibration was achieved through adjustment of model parameters for a period with complete time-varying data at all boundaries and at interior checkpoints. The model was calibrated using data collected during June 14-30, 1991.

The mean water levels at the upstream (site WL1) and downstream (site WL4) boundaries were 0.325 m and 0.303 m, respectively, for the calibration period. These values are greater than the

mean water levels at sites WL1 and WL4 for the entire data-collection period (table 2) and greater than the monthly mean water level for June during the data-collection period (table 3). Highest water levels during the calibration period occurred between June 23 and 27 (fig. 15).

Mean salinities at the upstream (site S1) and downstream (site S5) boundaries were 3.7 ppt and 11.2 ppt, respectively, for the calibration period. The salinity at sites S1 and S5 during the calibration period was greater than salinities typically observed at those locations during June 1989-92. Near-surface monthly mean salinity at sites S1 and S5 for the month of June in 1989-92 were 1.2 and 8.8 ppt, respectively, and near-bottom values were 1.8 ppt and 9.8 ppt (table 5). There was some top-to-bottom salinity difference at site S1 from about June 19-24, and again during June 29-30 (fig. 16). The maximum difference between near-surface and near-bottom salinities was about 4 ppt during this period, in comparison with a monthly mean value of 0.7 ppt for June during 1989-92. During June 19-24, the salinity of the near-surface waters declined with time, while the near-bottom salinity remained relatively constant. At site S5, the estuary was generally well-mixed vertically during the calibration period, with the maximum difference between near-surface and near-bottom salinities seldom exceeding 1 ppt (fig. 16).

Wind measured at site W1 was primarily from the south-southwest (fig. 17) during the calibration period, which is typical for June (table 7). However, from about June 23-25, wind

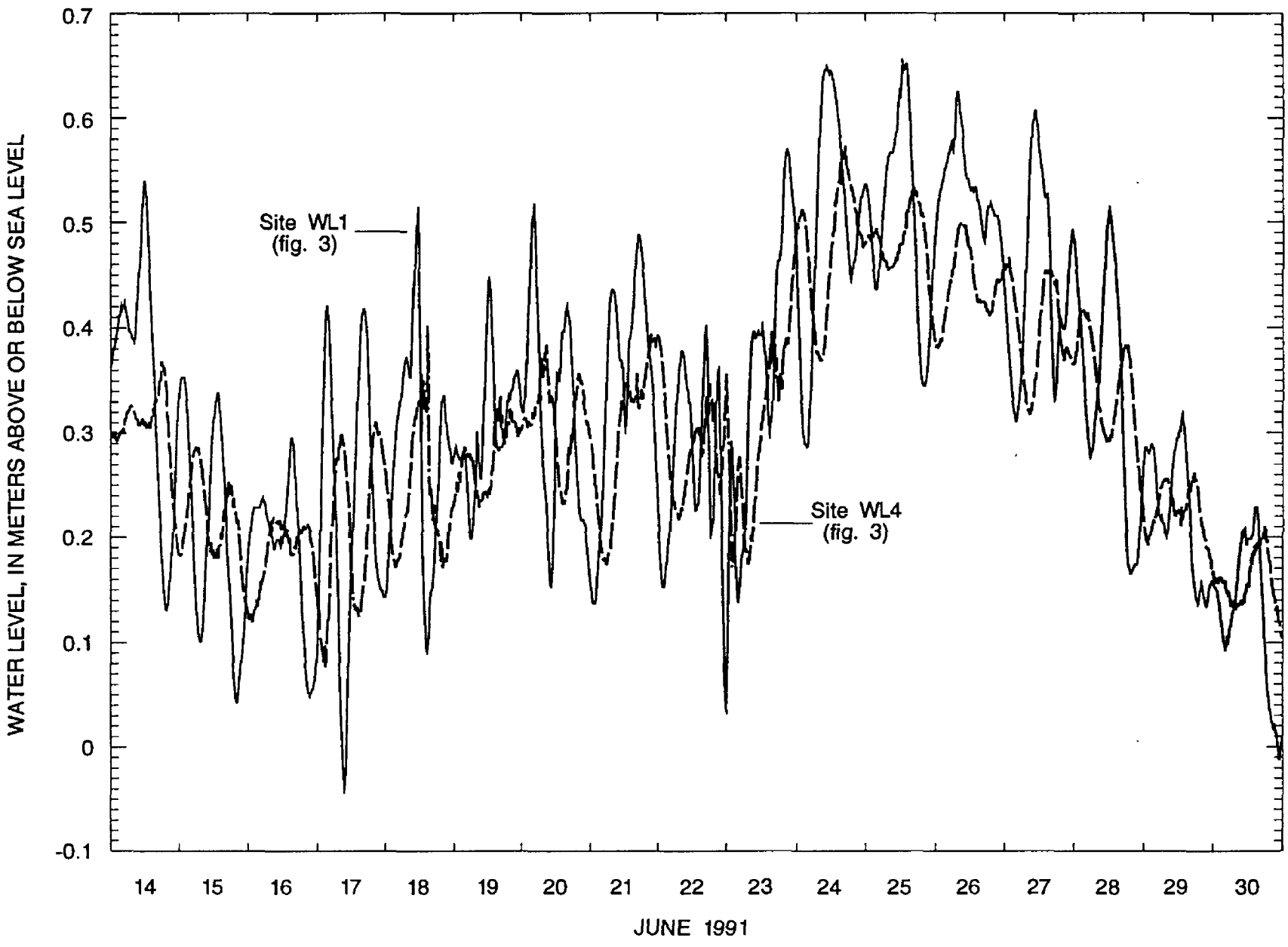

Figure 15. Water levels at model boundaries in the Pamlico River for calibration period.

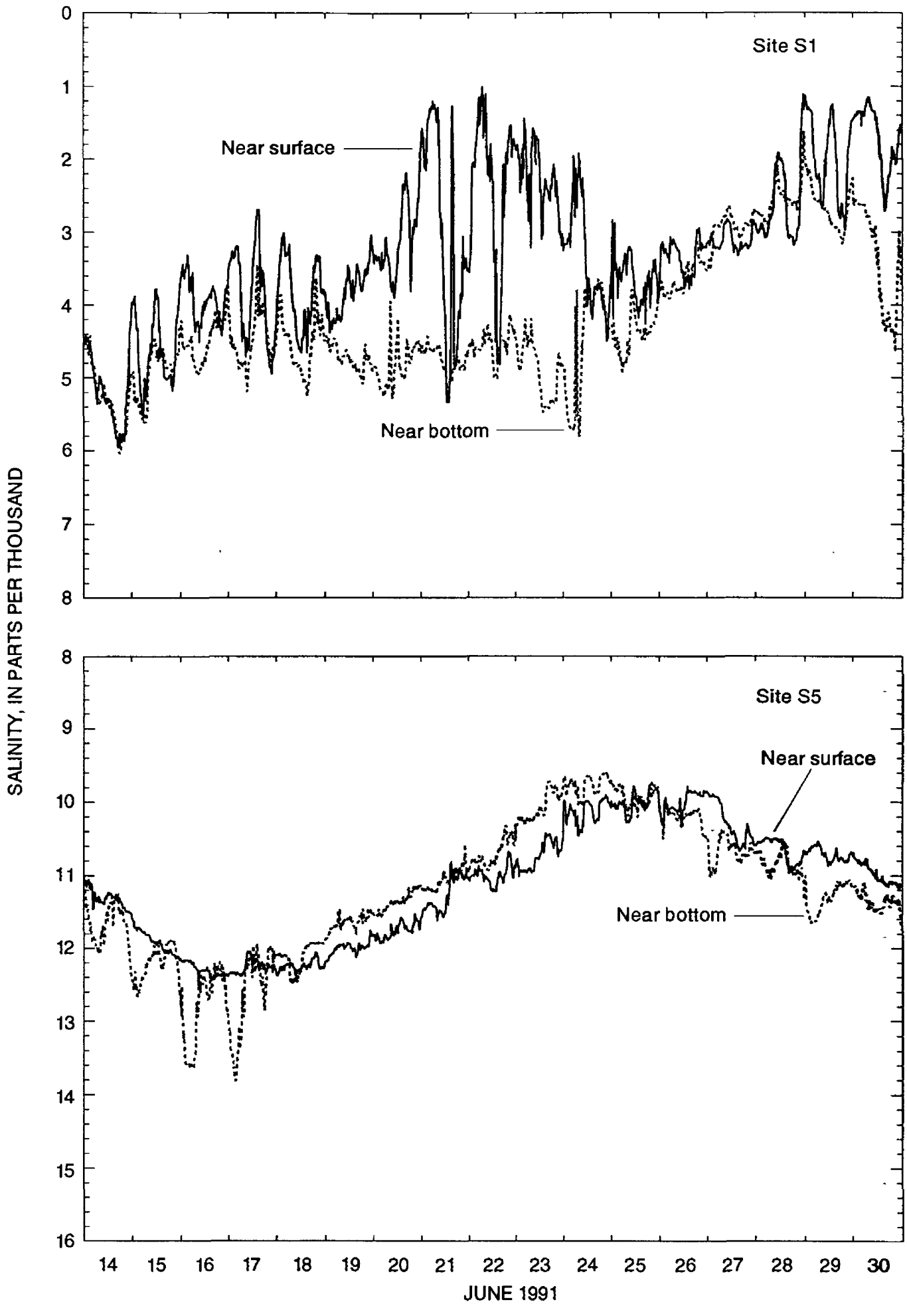

Figure 16. Near-surface and near-bottom salinity at model boundaries in the Pamlico River for calibration period.

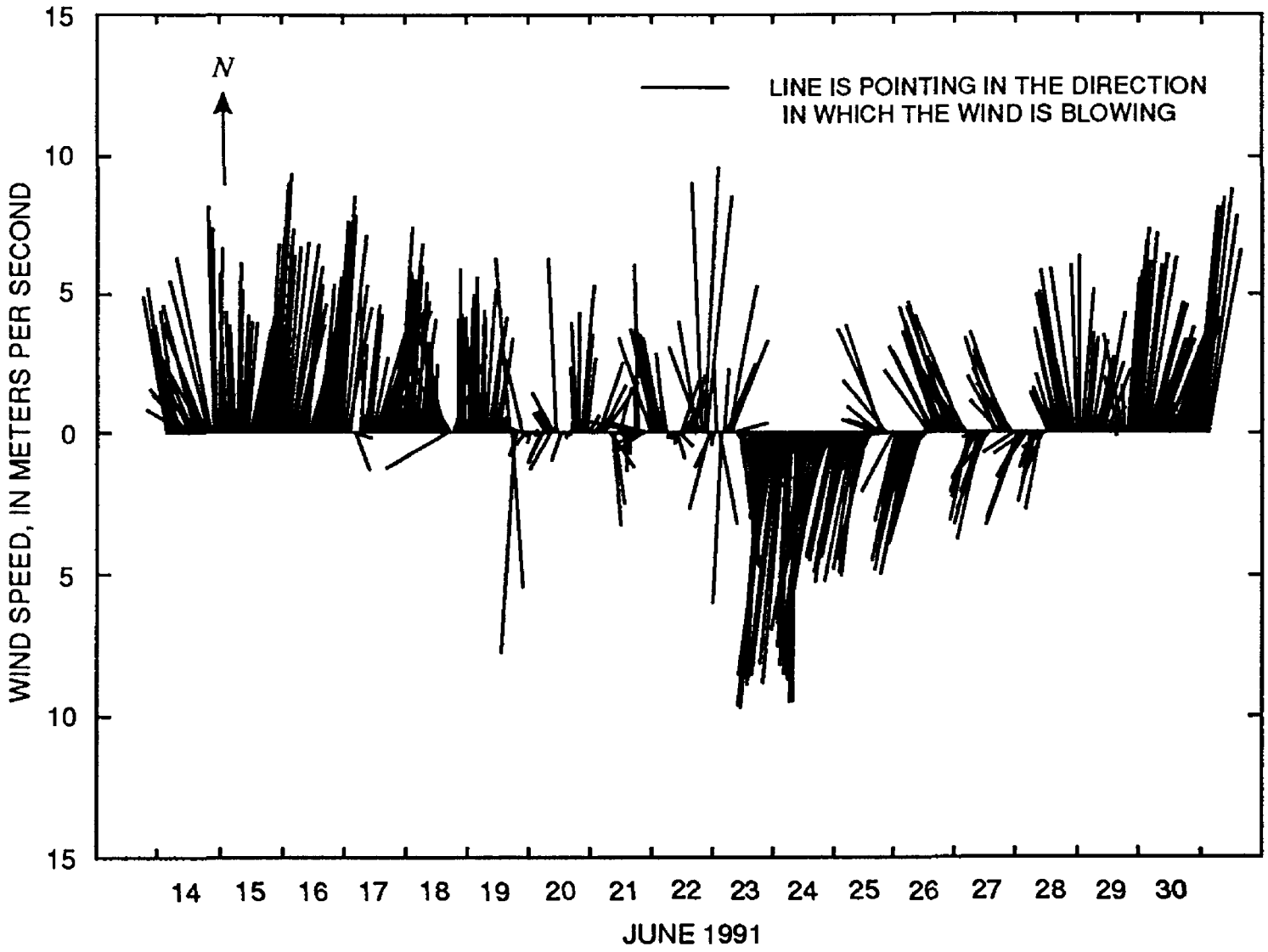

Figure 17. Wind speed and direction at site W1 in the Pamlico River for model calibration period.

blew from the east-northeast at speeds in excess of 5 m/s much of the time (fig. 17). This period was preceded by a time of relatively low wind speeds for a few days, as well as relatively large top-to-bottom salinity differences at site S1 (fig. 16). The increase in magnitude of wind and the change in direction apparently resulted in elimination of the vertical salinity gradient and an increase in water levels (fig. 15).

Simulations were made for the calibration period using different values of model parameters. The following model parameters provided the best agreement between observed and simulated data: (1) $\eta = 0.028$ (resistance coefficient); (2) $C_d = 0.001$ (wind-stress coefficient); $k' = 10$ m^2/s (unadjusted horizontal momentum mixing coefficient); (4) $D_i = 20$ m^2/s (isotropic mass-dispersion coefficient); and (5) $D_c = 14$ m^2/s (coefficient relating mass dispersion to flow properties).

Simulated and observed water levels and salinities were compared to quantify model performance. Mean-simulated minus observed values and the root mean square (RMS) of simulated minus observed values were calculated at water level (sites WL3 and WL5) and salinity (sites S2, S3, and S4) checkpoints using 15-minute values.

The mean difference between the simulated and observed water level at site WL3 was 1.2 cm (the positive value indicates that simulated values exceeded observed values) and the RMS value was 1.7 cm. These values are about 5 percent and 8 percent, respectively, of the mean daily water-level range for June. At site WL5, the mean difference between simulated and observed water levels was less than -0.1 cm, and the RMS error was 0.8 cm, representing about 1 percent and 4 percent, respectively, of the mean daily water-level range at site WL5 for June.

The absolute value of the mean difference between simulated and observed salinity at each of three model checkpoints (sites S2, S3, and S4) was less than 1 ppt. RMS values of simulated minus observed salinity were 0.7, 0.6, and 0.5 ppt at sites S2, S3, and S4, respectively. The mean differences in simulated and observed values and the RMS values are less than or equal to the observed monthly mean of the difference between near-bottom and near-surface daily mean salinity for June (table 6). Salinity was slightly over-predicted in the lower part of the estuary at site S4 and under-predicted in the upper and middle sections of the estuary at sites S2 and S3 (fig. 18).

Daily variations in simulated salinities were not as large as observed values. At least part of the smaller simulated variations could be due to the fact that the model salinity boundary conditions are an average of near-surface and near-bottom observed salinities. Averaging these values tends to reduce some of the natural variation in the boundary salinity, which in turn results in less variation in simulated results.

Pamlico River Model Validation

Model validation is the process used to evaluate a model by testing it with observed data that were not used in the calibration procedure. The model was validated using data collected during two separate periods. Simulations were made for August 30 through September 12, 1989, which included the time when recording current meters were moored in the estuary. The model also was validated using data from a longer period—July 4-28, 1991.

1989 Validation Period

Boundary conditions for the August 30-September 12, 1989, validation period were treated the same as for the model calibration period, with two exceptions. First, because near-bottom salinity data were unavailable at site S1 for this period, near-surface salinity measured at site S1 was used as the upstream salinity boundary condition. Second, hourly wind data measured at Cherry Point Marine Corps Air Station, located about 75 km due south of site S2, were used for the water-surface boundary condition because data from site W1 were incomplete.

The mean water levels at the upstream (site WL1) and downstream (site WL4) boundaries were 0.359 m and 0.349 m, respectively, for the 1989 validation period. These values are near the monthly mean for September (table 3), when monthly mean water levels were 0.344 m and 0.337 m at sites WL1 and WL4, respectively. Lower than average water levels were present for the first 2 days of the period, but water levels were relatively high for most of the remainder of the validation period (fig. 19).

Observed salinity at the upstream boundary (site S1) ranged from 0.1 to 3.6 ppt (fig. 20), with a mean value of 1.7 ppt, which is slightly lower than the average for September (table 5). Observed salinity at the downstream boundary (site S5) ranged from 9.6 to 11.9 ppt during the validation period (fig. 20), and the mean salinity during the period was 10.7 ppt. There were some vertical differences in salinity at the downstream boundary for much of the simulation period (fig. 20), and data at the other salinity measurement sites showed similar conditions. A change in wind direction on September 9 coincided with vertical mixing at site S5 (figs. 20 and 21A). Wind speeds during the period were less than 5 m/s about 95 percent of the time, with a maximum recorded speed of 7.5 m/s. Wind was from the north to northeast more than 50 percent of the time, with some periods of light southerly winds (fig. 21A).

In addition to water-level and salinity data, measured current speed and direction data were available for 8 days of the validation period. Observed data from seven recording current meters located along two cross sections in the estuary were compared with simulated data.

Initial simulations produced maximum velocities, which were generally less than half the observed maximums, and mean and median simulated velocities were less than the observed values shown in table 9. To identify the cause for underprediction of velocities, wind data measured at Cherry Point (on land) were compared with data from site W1 (measured over the open water) for a summer period in 1991. The comparison indicated that wind speeds were typically about three times greater at site W1 than at the Cherry Point station,

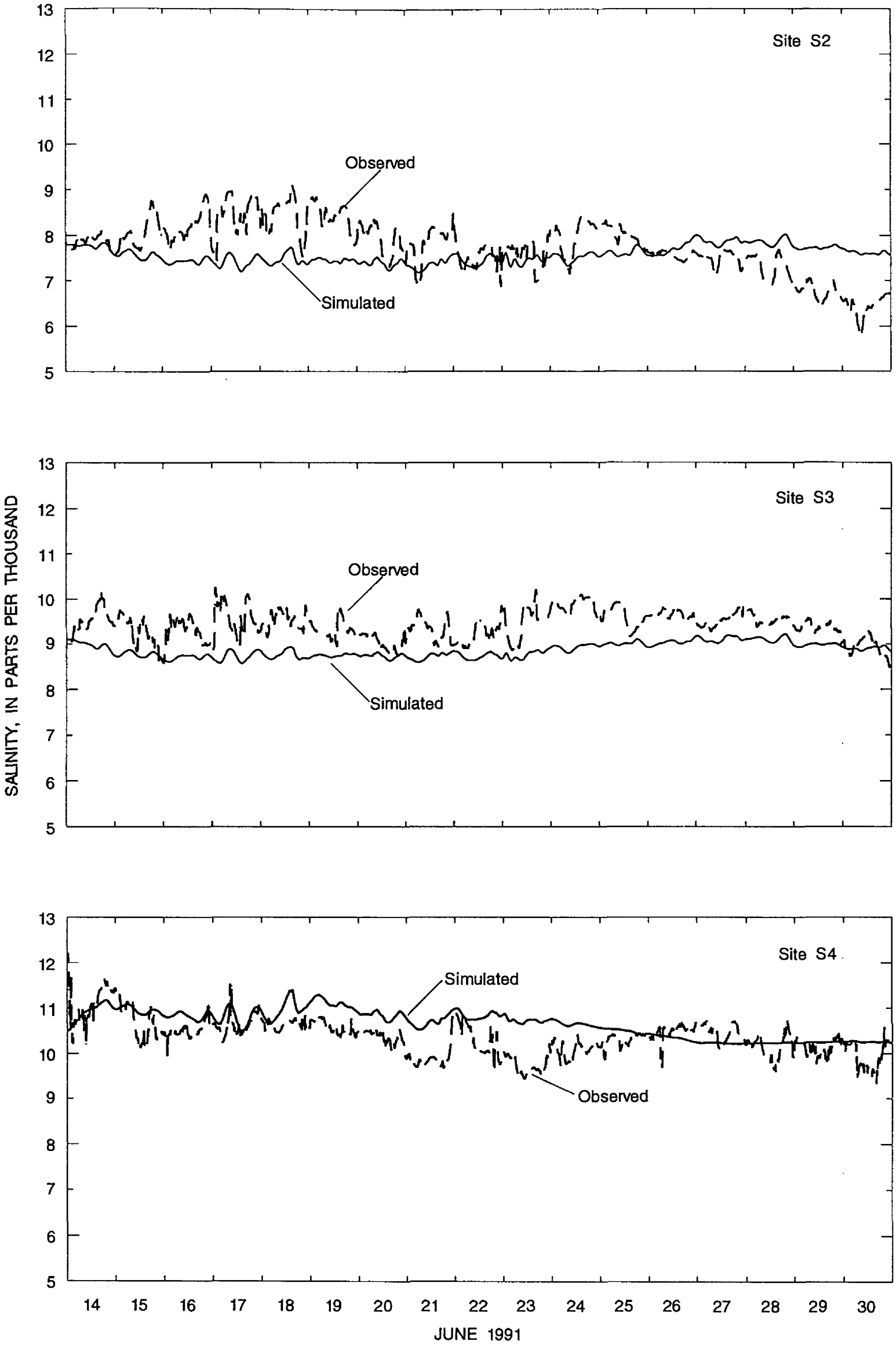

Figure 18. Simulated and observed salinity at sites S2, S3, and S4 in the Pamlico River for model calibration period.

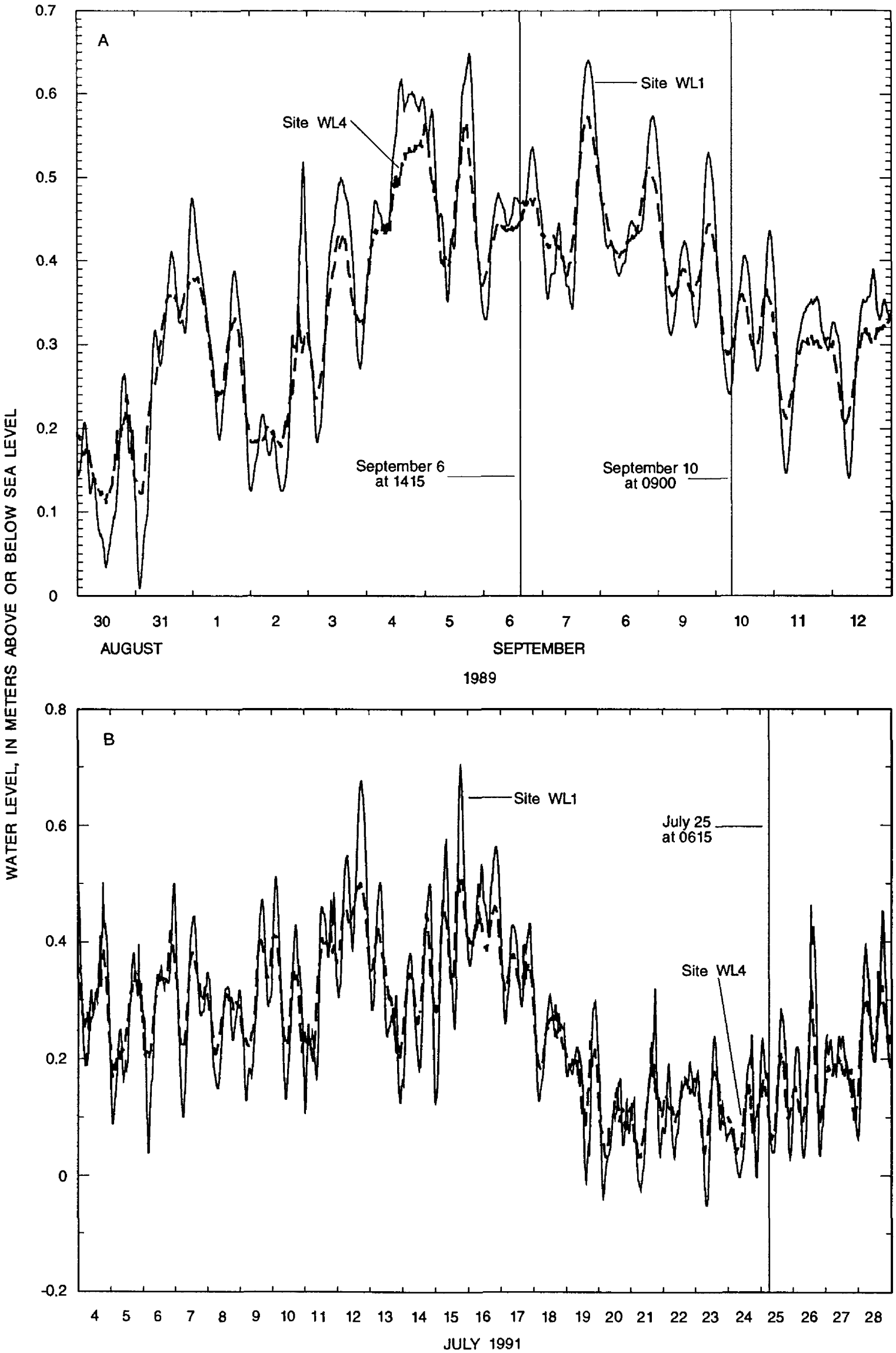

Figure 19. Observed water levels at upstream and downstream boundaries in the Pamlico River for two model validation periods: (A) August 30-September 12, 1989, and (B) July 4-28, 1991.

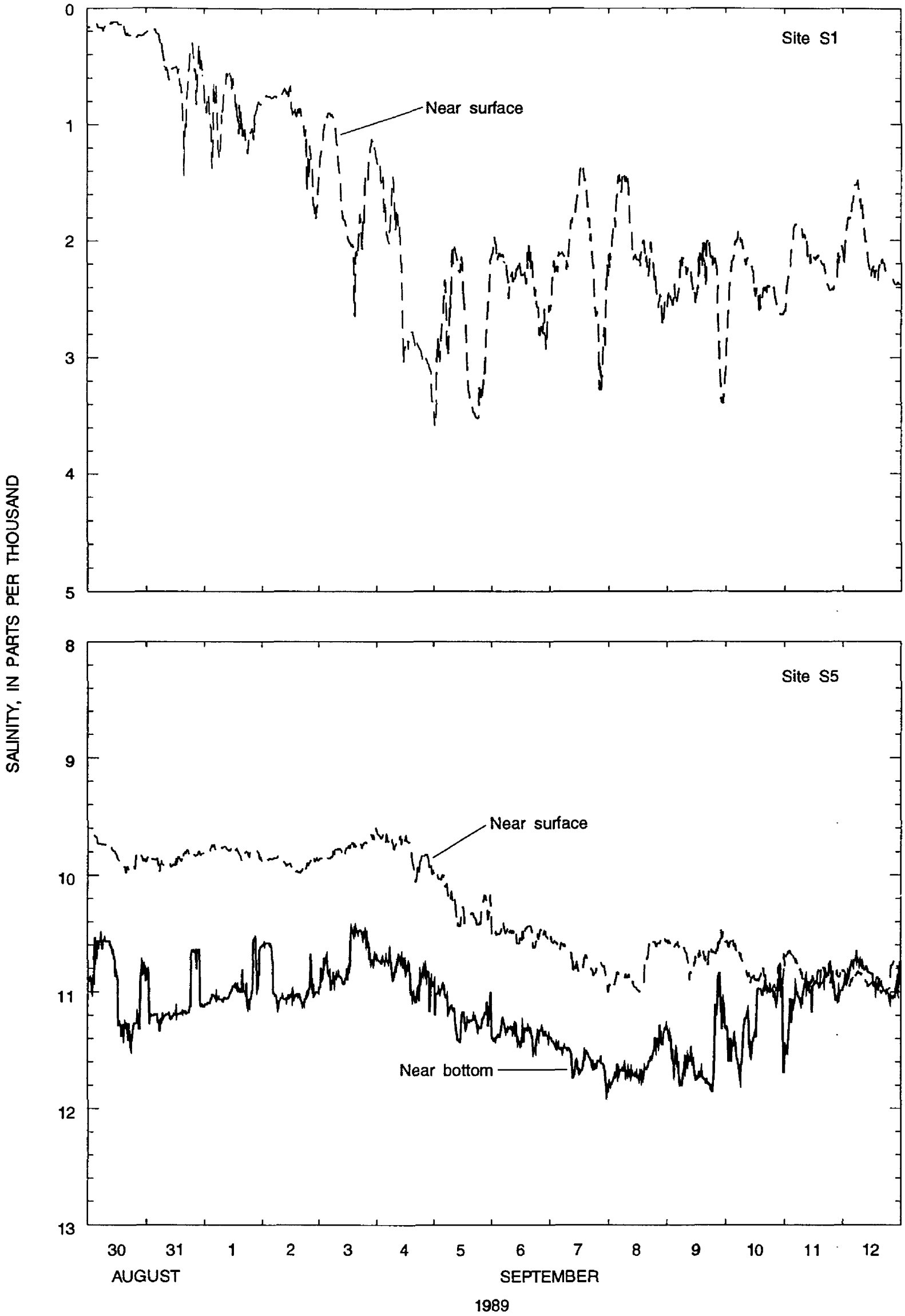

Figure 20. Observed salinity at sites S1 and S5 in the Pamlico River during August 30-September 12, 1989.

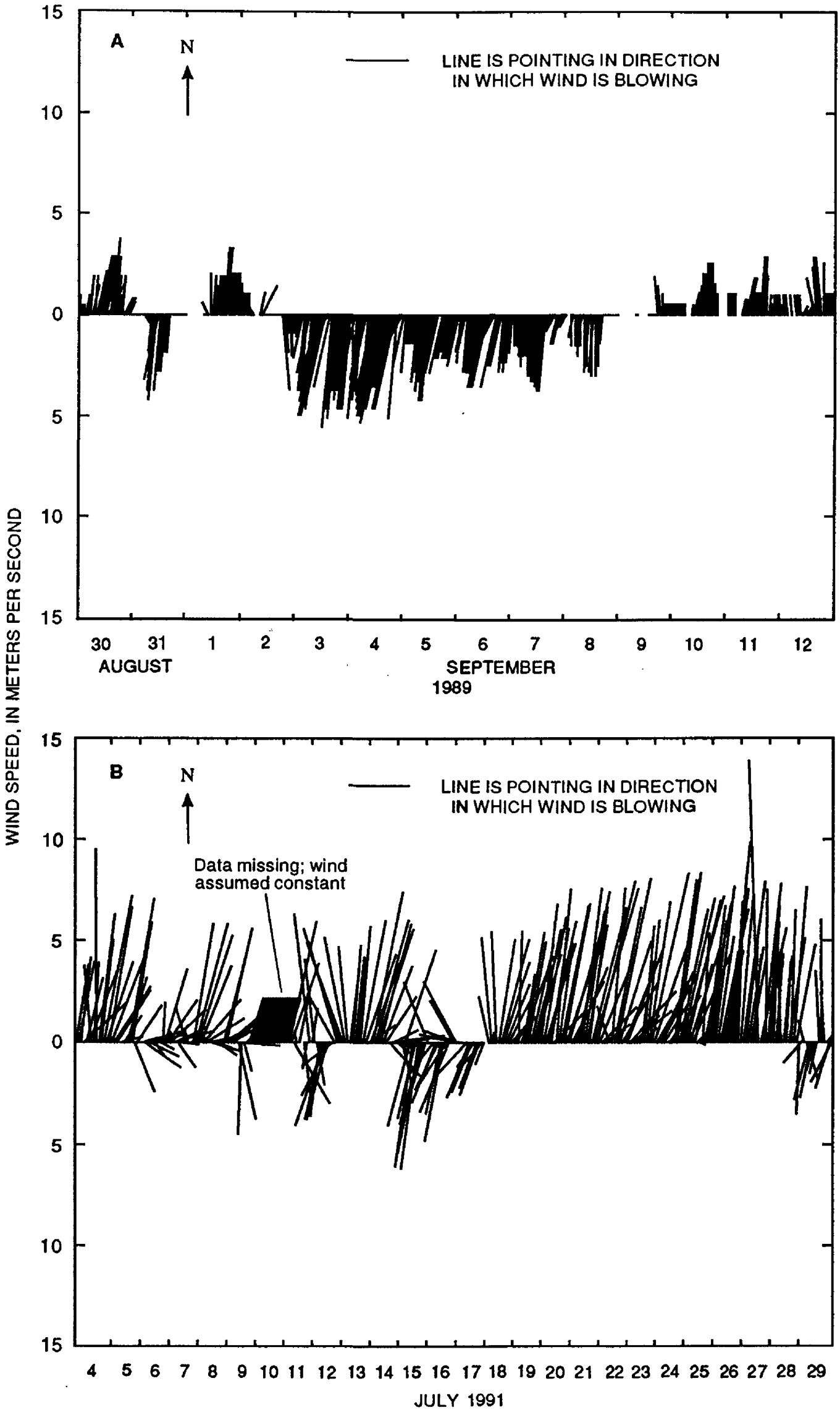

Figure 21. Wind speed and direction measured at (A) Cherry Point Marine Corps Air Station during August 30-September 12, 1989, and (B) Pamlico River site W1 during July 4-28, 1991.

but wind directions at the two sites were similar. Consequently, the simulation was repeated with the observed Cherry Point wind speed increased threefold. Mean wind speed increased from 2.5 to 7.5 m/s, and median wind speed increased from 2 to 6 m/s. As a result of this increased wind speed, the mean simulated velocity increased an average of 44 percent at the upstream measurement sites (sites V1, V2, and V3) and an average of 76 percent at the downstream measurement sites (sites V4, V5, V6, and V7). Because the winds at site W1 appear to be significantly greater than those measured at Cherry Point and because the higher winds resulted in simulated velocities which more closely agreed with observed values, the model was validated for the 1989 period using three times the observed Cherry Point wind speed for the water-surface boundary condition.

For the entire 14-day validation period, mean and RMS values of the difference between simulated and observed water levels were less than or equal to 3.4 cm (table 11). The mean and RMS values for each site were between 0.1 and 14 percent of the mean daily water-level range for September (table 3). With the exception of the RMS value for site S3, the mean and RMS values of the difference between simulated and observed salinity were less than the respective difference between near-bottom and near-surface salinity recorded in September (table 6). Because the initial salinity conditions were estimated, model performance was somewhat poor during the initial 4 days of the simulation period (fig. 22). Following this initial period, the model responded more to the observed salinity boundary conditions than to the estimated initial salinity conditions, and the simulated salinity was in very good agreement with observations (table 11; fig. 22).

Simulated vertical mean velocities were more laterally uniform than observed point velocities at the mid-estuary section (sites V1, V2, and V3, figs. 7 and 23). Simulated velocities at the mid-estuary section were also more nearly aligned with the longitudinal axis of the estuary than were observed velocities (figs. 7 and 23; table 12). The mean difference between observed point and simulated velocities for the period August 30-September 6 ranged from -0.05 cm/s at site V3, to -0.4 cm/s at site V2, to -4.5 cm/s at site V1. Observed point velocities were generally under-predicted, with the best performance occurring at site V3 (table 12).

Table 11. Results of model validations for 1989 and 1991 test periods

[cm, centimeter; --, no observed data available for comparison; ppt, parts per thousand; <, less than]

Site (fig. 3)	August 30-September 12, 1989		July 4-28, 1991	
	Simulated minus observed		Simuleted minus observed	
	Mean value	Root mean square value	Mean value	Root mean aquare value
WL2 (cm)	-1.1	3.4	--	--
WL3 (cm)	.1	3.1	0.8	1.4
WL5 (cm)	-1.2	1.7	-1.7	2.0
S2 (ppt)	.2	.7	-.9	1.1
S3 (ppt)[a]	.4	1.2	-.7	1.0
S4 (ppt)	.2	.4	<.1	.5

[a]Simulated salinity compared to near-surface salinity, because near-bottom values were not available.

At the downstream measurement section (sites V4, V5, V6, and V7), simulated velocities exhibited the lateral nonuniformity and the cross-channel flow (fig. 23) seen in the observed record (fig. 7). Overall, simulated and observed directions were in general agreement, although there are periods of poor agreement. Simulated and observed magnitudes were in better agreement than at the mid-estuary section, and there was no tendency toward over- or under-prediction. The mean difference between observed point and simulated velocities for the 8-day period was less than or equal to 1.1 cm/s at the four downstream measurement sites.

Current measured at a single point in the water column can be markedly different from the vertical mean current at that location (see section on Currents). Moreover, during periods when near-surface currents are downstream and near-bottom currents are upstream, a point velocity measured near the channel bottom is likely to be greater than the vertical mean current.

Differences of as much as 5 ppt existed between simultaneously measured near-surface and near-bottom salinity during the August 30-September 12 validation period. Consequently, it is not surprising that the vertically averaged simulated

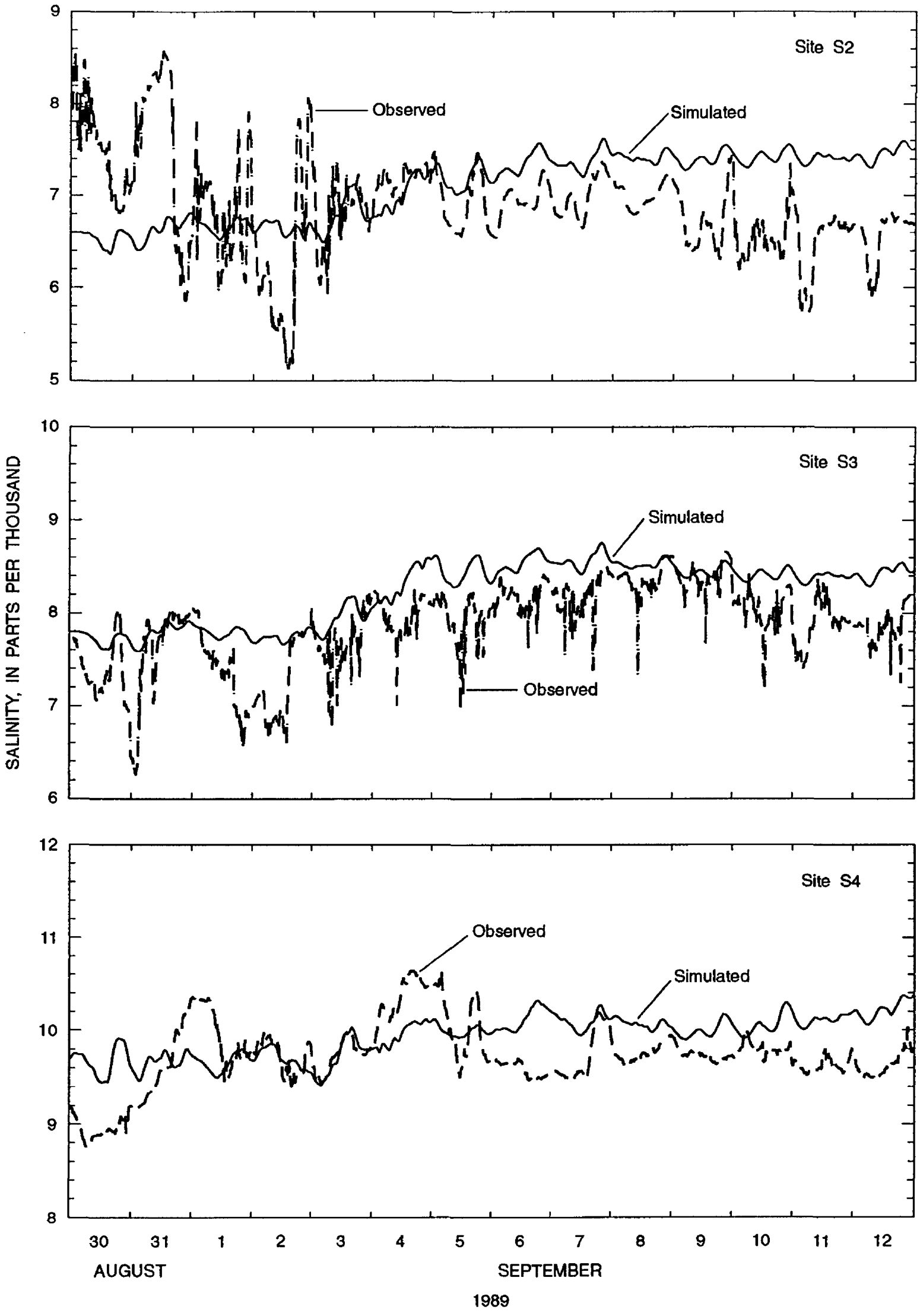

Figure 22. Simulated and observed salinity at sites S2, S3, and S4 in the Pamlico River for August 30-September 12, 1989.

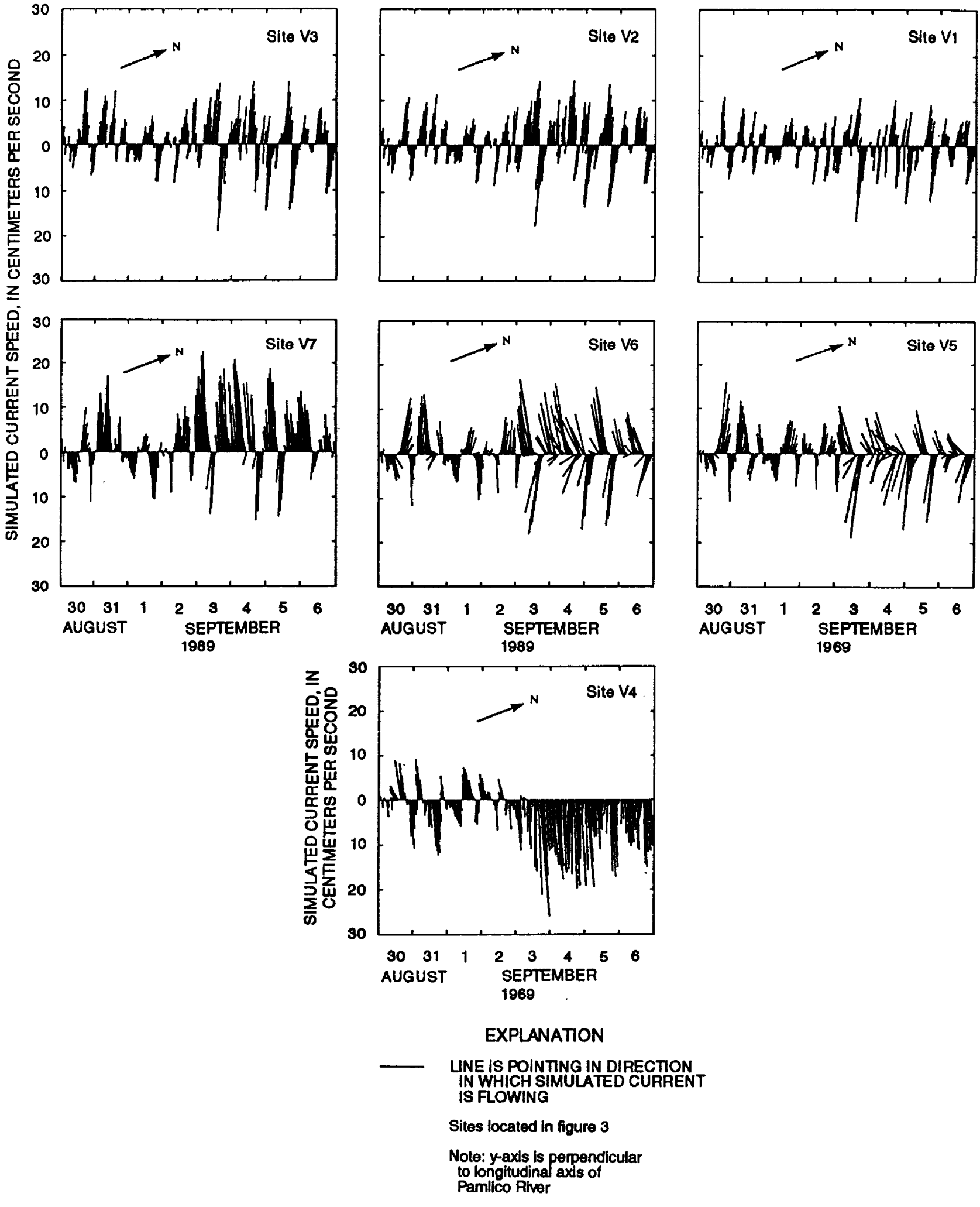

Figure 23. Simulated velocity at current meter sites in the Pamlico River for August 30-September 6, 1989.

Table 12. Summary of simulated and observed velocities at seven sites in the Pamlico River for August 30-September 6, 1989
[cm/s, centimeters per second)

Site (fig. 3)		Downstream current				Upstream current			
		Velocity (cm/s)			Direction (degrees E of N)	Velocity (cm/s)			Direction (degrees E of N)
		Mesn	Median	Maximum	Mean	Mean	Median	Maximum	Mean
V1	Observed	7.7	6	27	107	10.6	9	34	311
	Simulated	4.4	3.3	19.3	123	5.2	4.3	15	296
V2	Observed	5.5	5	25	101	5	3	22	298
	Simulated	4.3	3.3	18.2	127	5.2	4.4	15.3	296
V3	Observed	4.5	3	23	115	4.7	4	15	300
	Simulated	4.2	3.5	17.3	123	4	3.4	11.5	275
V4	Observed	7.8	5	27	129	5	4	17	264
	Simulated	5.2	4.6	15.9	111	8.6	7.7	23.6	279
V5	Observed	6.1	5	17	92	6.7	6	18	259
	Simulated	6.7	6	20.5	119	8.1	7.7	20.1	260
V6	Observed	4.9	4	15	74	5.8	5	19	275
	Simulated	6.5	5.5	20.2	130	6.5	6.3	17.5	271
V7	Observed	6.7	5	17	74	5.1	4	20	267
	Simulated	7.7	6.5	27	105	3.9	3.9	10.9	254

velocities were generally less than measured point velocities, particularly at the mid-estuary section where vertical salinity gradients were greater than those near the mouth of the estuary. Although the model performed better at reproducing observed water levels and salinities than measured point velocities, the fact that simulated and observed salinities are in good agreement (table 11) does indicate that transport characteristics are generally being simulated correctly.

1991 Validation Period

Boundary conditions during July 4-28, 1991, were treated as described for the model calibration. Mean daily water levels at the upstream and downstream boundaries were 0.256 m and 0.253 m, respectively, during this validation period (fig. 19B). These values are slightly higher than average mean July water levels at the sites (table 3). The mean salinity during the period was 5.8 ppt at the upstream boundary and 12.0 at the downstream boundary (fig. 24). These values are higher than the July mean salinity (table 5) and the mean daily maximum salinity for the data-collection period (table 4). Vertical salinity gradients existed at site S5 for part of the simulation period and were present for most of the simulation period at site S1 (fig. 24)

The wind speed measured at site W1 averaged about 6 m/s for the simulation period (fig. 21B). Winds blew from the south-southeast about 40 percent of the time. During the latter part of the simulation period, winds blew primarily from the south-southwest at speeds in excess of 5 m/s, corresponding to decreased water levels (fig. 19) and some slight top-to-bottom difference in salinity in the lower part of the estuary (fig. 24). Data were missing for site W1 from July 9 at 1600 to July 10 at 2300, so the wind speed and direction measured on July 9 at 1530 was applied to the 7 hours of missing record (fig. 21B).

For the 25-day simulation period, mean and RMS values of the difference between simulated and observed water levels ranged from 4 to 11 percent of the mean daily water-level range for July (tables 11 and 3). Mean and RMS values of the difference between simulated and observed salinities were less than or equal to the mean difference between near-bottom and near-surface salinity recorded in July for the 1989-92

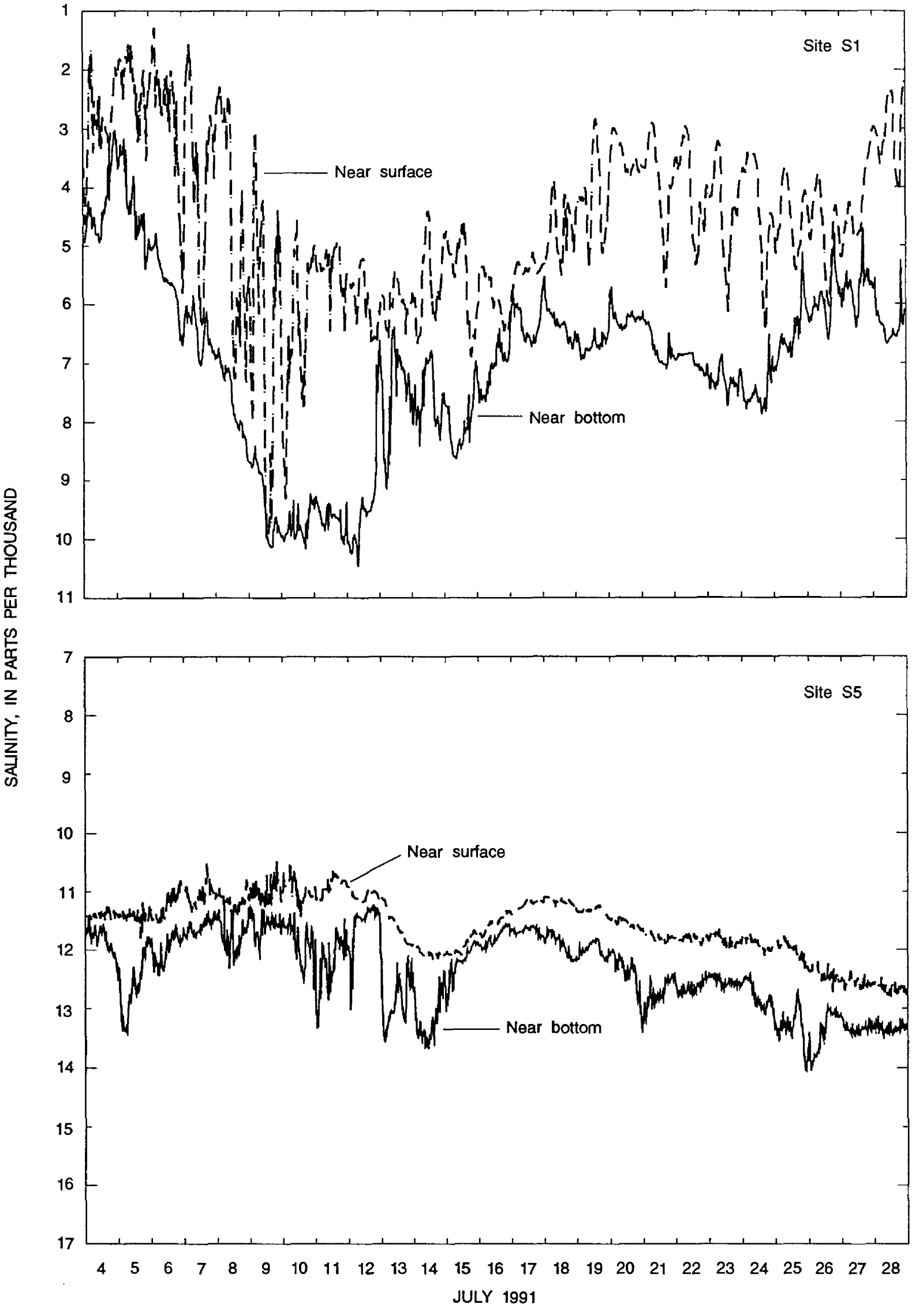

Figure 24. Near-surface and near-bottom salinity at sites S1 and S5 in the Pamlico River during July 4-28, 1991.

data-collection period (tables 11 and 6). Simulated salinity generally agrees with the observed average of near-surface and near-bottom salinity, with some slight underprediction at sites S2 and S3 (fig. 25).

In summary, the model was calibrated and validated for (1) water levels ranging from -0.052 m to 0.698 m, (2) salinities ranging from 0.1 ppt to 13.1 ppt, (3) and wind speeds ranging from calm to 22 m/s. The model was tested for periods with and without significant top-to-bottom differences in salinity. Simulated water levels were within 2 cm of observed values. Simulated salinities at three interior checkpoints were within 1 ppt of observed values. Daily variations in simulated salinities were typically not as large as observed variations. The magnitudes of simulated velocities generally matched observations at the downstream measurement section, but simulated magnitudes were generally less than observed values at the mid-estuary section.

Sensitivity Analysis

The sensitivity of model results to changes in model parameters and boundary conditions was analyzed. Model parameters which were included in the analysis were C_d, the wind-stress coefficient; η, the resistance coefficient; k', the unadjusted horizontal-mixing coefficient; and D_i, the isotropic mass-dispersion coefficient, which is used in the computation of the longitudinal mass-mixing coefficient. The parameter D_c was not included in the analysis because the effect of D_c on the magnitude of the longitudinal mass-mixing coefficient is generally minor relative to D_i (eq 20). Results from the calibration period, June 14-30, 1991, were used as the basis for comparison in the model parameter sensitivity analysis. Boundary conditions also were varied to evaluate sensitivity of model results to changes in forcing conditions. In particular, the presence of a lateral water-level gradient at the downstream open-water boundary was evaluated further, and the effects of open-water boundaries in tributary streams on circulation were characterized. Results from the August 30-September 12, 1989, validation period (using the observed Cherry Point wind speed) were used in evaluating sensitivity of model results to changes in boundary conditions.

Two simulations were made with the calibrated model using the June 14-30, 1991, boundary data. Wind-stress coefficient values of 0.0005 and 0.0015 were used for comparison with results from the calibrated model, in which a value of $C_d = 0.001$ was used. Wind speed during the period averaged about 6 m/s, and the wind direction was oriented across the channel for most of the period (fig. 17). The changes in C_d had a relatively significant effect on simulated flow and velocity magnitude in the estuary. In the western half of the estuary, mean flow during the period changed from the downstream direction ($C_d = 0.005$) to upstream ($C_d = 0.0015$). Mean velocities at sites V2 and V5 were less sensitive to changes in C_d than were maximum velocities (fig. 26). Also, the differences in mean simulated salinity at sites S2, S3, and S4 for the three values of C_d were negligible.

Results of simulations using the calibrated model, June 14-30, 1991, boundary data, and resistance coefficient values of 0.025 and 0.030 were compared with results using a resistance coefficient of 0.028. The range in flow (difference between the maximum upstream and maximum downstream flow) and velocity decreased as the resistance coefficient increased (fig. 26). The flow range decreased between about 4 percent at the upstream section and 15 percent at the downstream section as the resistance coefficient was increased from 0.025 to 0.030. Simulated maximum velocities at sites V2 and V5 decreased as much as 10 percent with the change in resistance coefficient from 0.025 to 0.030.

Values of the unadjusted horizontal momentum mixing coefficient, k', of 0 m^2/s and 100 m^2/s were used in simulations for comparison with results from the calibrated model in which $k' = 10$ m^2/s. Flow magnitude was essentially unchanged by the changes in k'. Circulation patterns in some areas of the estuary were, however, affected by changes in k'. Spatial variations in velocity direction and magnitude were slightly lower for $k' = 100$ m^2/s than for $k' = 10$ m^2/s, but the changes were observed primarily in the tributary streams, such as South Creek, rather than in the mainstem of the estuary.

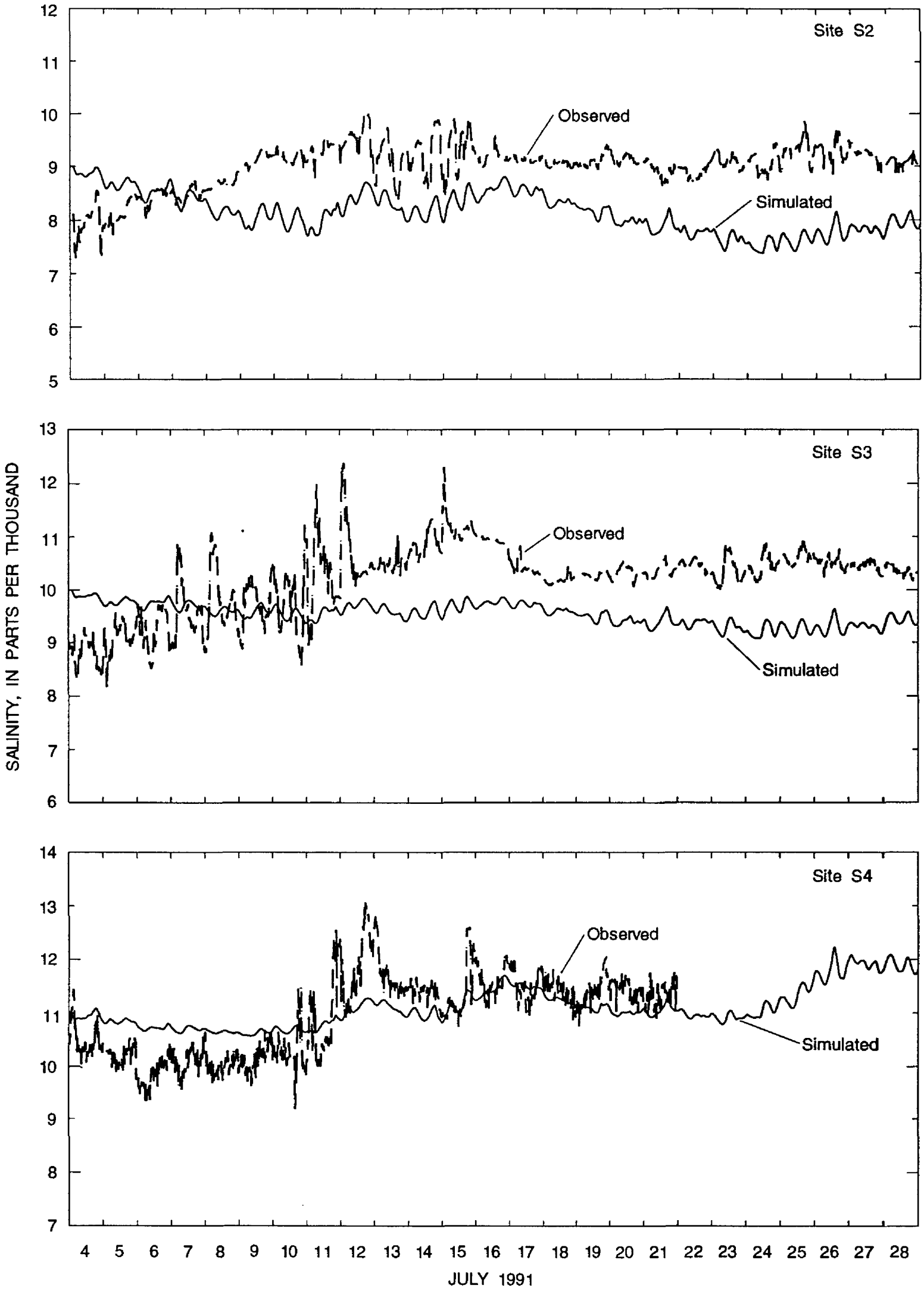

Figure 25. Simulated and observed salinity at sites S2, S3, and S4 in the Pamlico River for July 4-28, 1991.

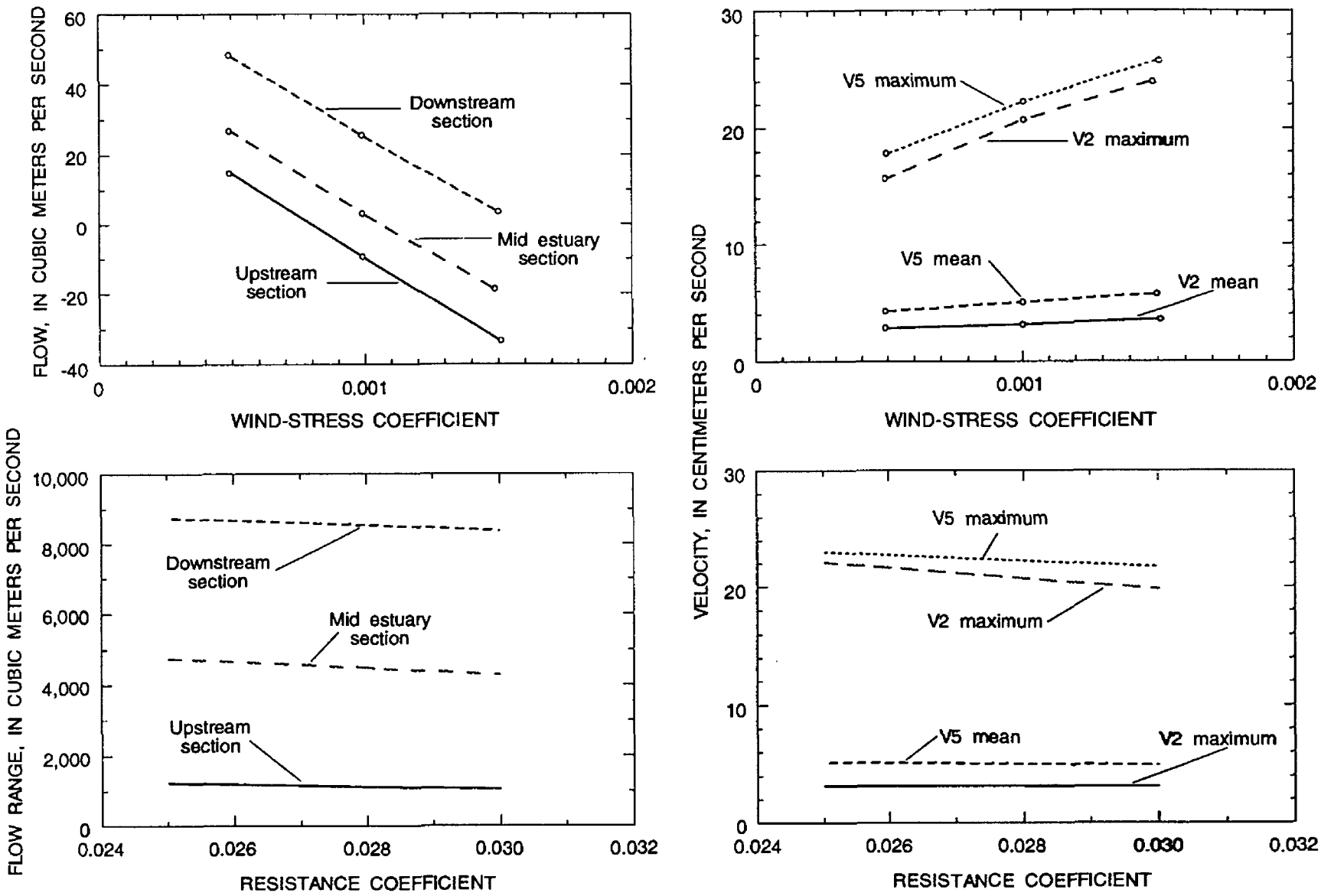

Figure 26. Effect of changes in wind-stress and resistance coefficients on flow and velocity.

Results from simulations using isotropic mass-dispersion coefficient, D_i, values of 5 m^2/s and 60 m^2/s were compared with results from the calibrated model with $D_i = 20$ m^2/s. The mean salinity at each of the sites S2, S3, and S4 for the simulation period showed little difference (less than 0.1 ppt) for the three values of D_i. Likewise, the daily variation in salinity was unaffected by changes in D_i. The spatial salinity distribution was, however, sensitive to the value of D_i (fig. 27). Because of the greater mixing produced by the higher value of D_i, the lateral distribution of salinity was more uniform for $D_i = 60$ m^2/s than for the lower values of D_i. The larger value of D_i also resulted in higher salinity in the upper reach of the estuary (fig. 27). Although detailed spatial distributions of salinity are not available for the June 14-30, 1991, simulation period, strong lateral salinity gradients are often observed in the Pamlico River, as previously discussed. Additional field studies which include dye tracking could provide information for better documentation of horizontal mixing of mass in the Pamlico River.

The effect of a lateral water-level gradient at the downstream boundary on flow and circulation patterns was evaluated further using boundary data for the period August 30-September 12, 1989 (figs. 19A, 20, and 21A). Simulations were made with and without the downstream lateral water-level gradient (previously described in the Pamlico River Model Validation section). Measured water levels at sites WL4 and WL5 were used for the simulation with the lateral water-level gradient. For the simulation period, the mean difference between

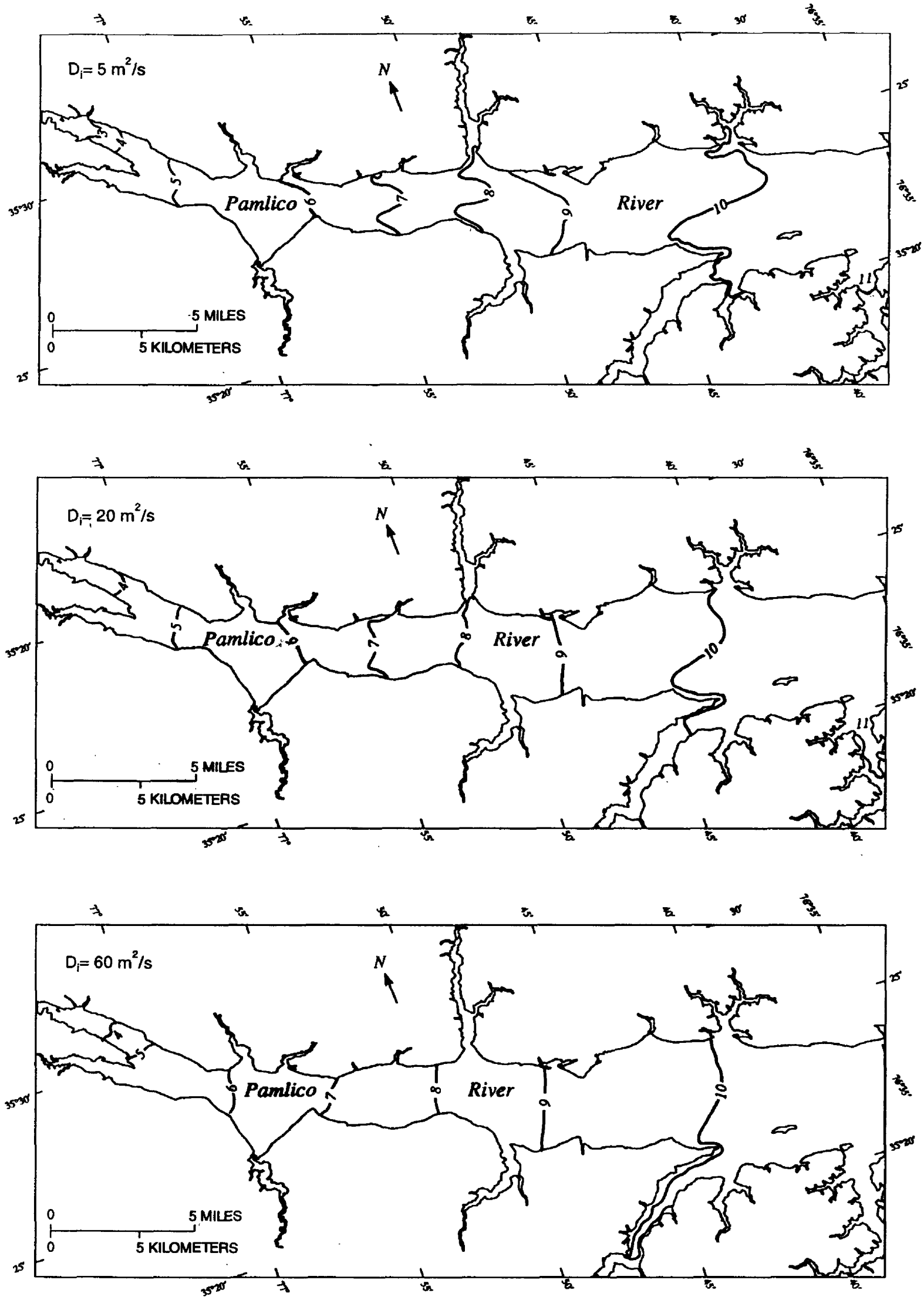

Figure 27. Lines of equal simulated salinity for June 26, 1991, at 1600 using the calibrated model and three values of the isotropic mass-dispersion coefficient, D_i.

observed water levels at sites WL4 and WL5 was about 2 cm, with water levels at site WL5 generally higher than at site WL4. In comparison, the mean difference in water level between sites WL1 and WL4 was 0.95 cm for the same period.

Only circulation patterns within about 2 km of the downstream boundary were affected by the lateral water-level gradient, which agrees with the results obtained from the preliminary simulations. The total range in flow for the simulation period (difference between maximum upstream and maximum downstream flow) decreased less than 3 percent throughout the model domain as a result of the downstream lateral water-level gradient. The mean flow for the period (which was upstream) increased about 34 m^3/s, or about 40 percent, at the downstream boundary. This change resulted from the decrease in the mean longitudinal water-level gradient through the addition of the higher downstream water-level boundary on the south side of the estuary. The relative sensitivity of model results near the downstream boundary further emphasizes the need for improved vertical control at all water-level gages. The provision for a ground survey loop around the estuary to reference all gages to a single datum is an important consideration for future model studies.

The effect of treating two of the larger tributary streams as open-water boundaries was characterized for the period August 30-September 12, 1989. Open-water boundaries were added at Bath Creek and South Creek. Observed water levels from sites WL2 and WL3 and an assumed constant salinity of 0.1 ppt were used as boundary conditions at the new open-water boundaries. Flow and circulation for this simulation were compared with those simulated when the streams were treated as closed-end embayments.

Mean flow for the period changed less than 10 percent throughout the estuary as a result of the new open-water boundaries. The change in the range of simulated flow was also small, with a decrease of less than 4 percent. As expected, the greatest differences were observed near the new open-water boundaries. Mean flow for the period changed from essentially zero to 10 m^3/s in Bath Creek, and from -1 to -21 m^3/s in South Creek (mean flow out of the estuary). Additionally, the range in flow more than tripled at Bath Creek and nearly doubled at South Creek. However, the effect on overall circulation in the estuary was primarily limited to the area around the mouths of the two creeks. Even when the direction of flow in the tributaries was reversed from the addition of the open-water boundary, circulation patterns in the main channel remained essentially unchanged (figs. 28 and 29). Because of the sensitivity of simulated flows in the tributaries to the type of boundary condition applied at the tributary (closed-end embayment with storage or open-water boundary), detailed analyses of tributary flows using the model should be made using measured water levels at these open-water boundaries.

Finally, it is apparent from figure 29 that results of any comparison of simulated and observed velocities is highly sensitive to the assumed position of the current meters. Because of the strong lateral and longitudinal velocity gradients, a difference of 2 or 3 computational cells in the assumed meter position could greatly affect the results of the comparison of simulated and observed currents. As previously noted, there was some uncertainty about the exact positioning of moored current meters used to collect velocity data between August 23 and September 6, 1989.

Model Application

The calibrated model was applied to the Pamlico River to simulate flow, circulation, and salinity distributions. Circulation patterns are shown using vector plots, particle tracking, and solute transport.

Flow Computation

Flows were simulated for the calibration period (June 14-30, 1991), the two validation periods (August 30-September 12, 1989, and July 4-28, 1991), and for August 7-29, 1991, which includes the period when Hurricane Bob passed near eastern North Carolina. Wind speed at site W1 reached a maximum of 14 m/s on August 18, and water level at site WL1 fell to -0.1 m on August 19, which is slightly less than the minimum value used in model calibration and validation.

During June 14-30, 1991, the simulated mean flow was in the upstream direction near Washington (-10 m^3/s), and in the downstream direction for the

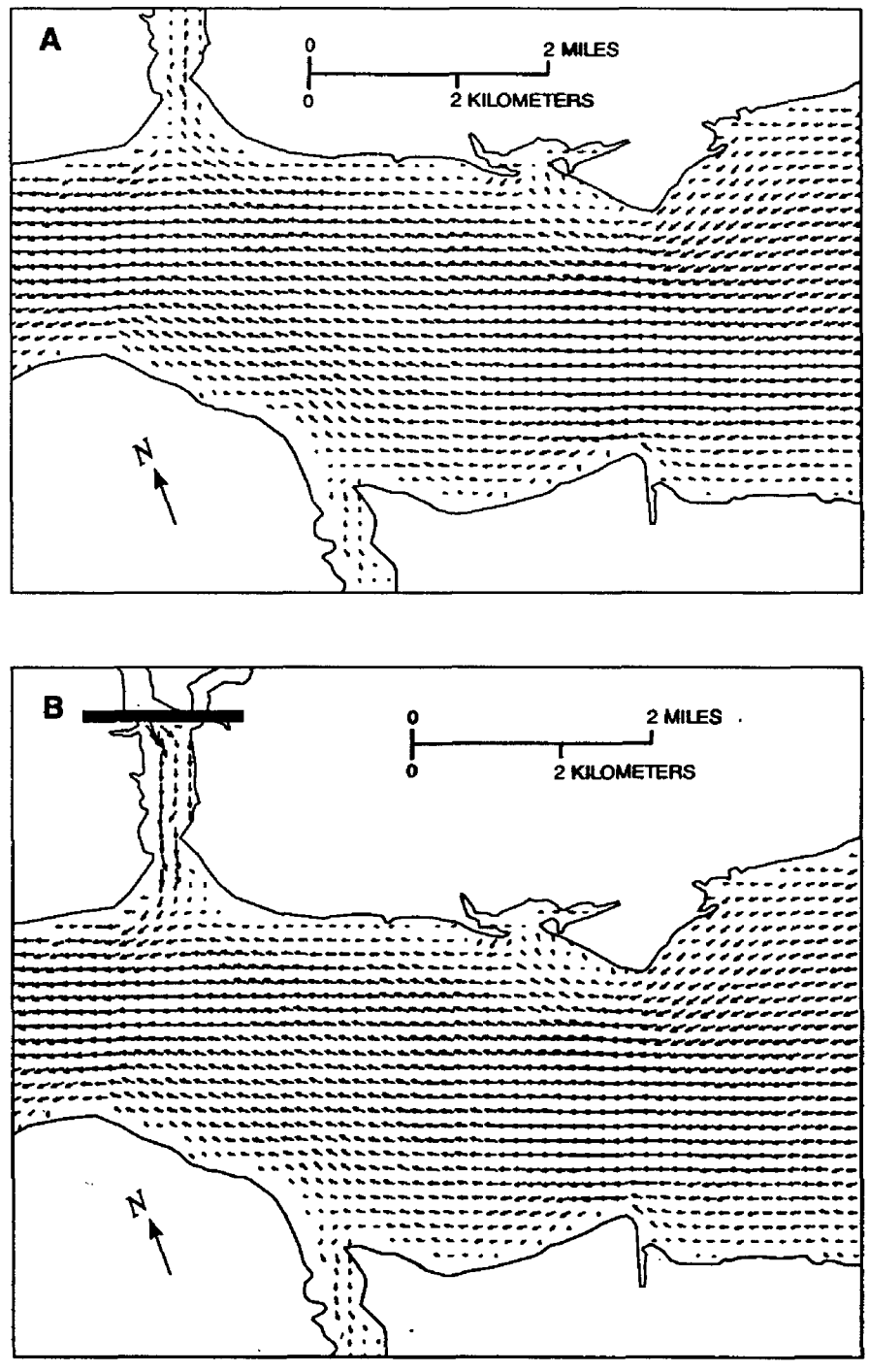

EXPLANATION

← VECTOR--Head points in flow direction. Greater vector length represents greater relative velocity

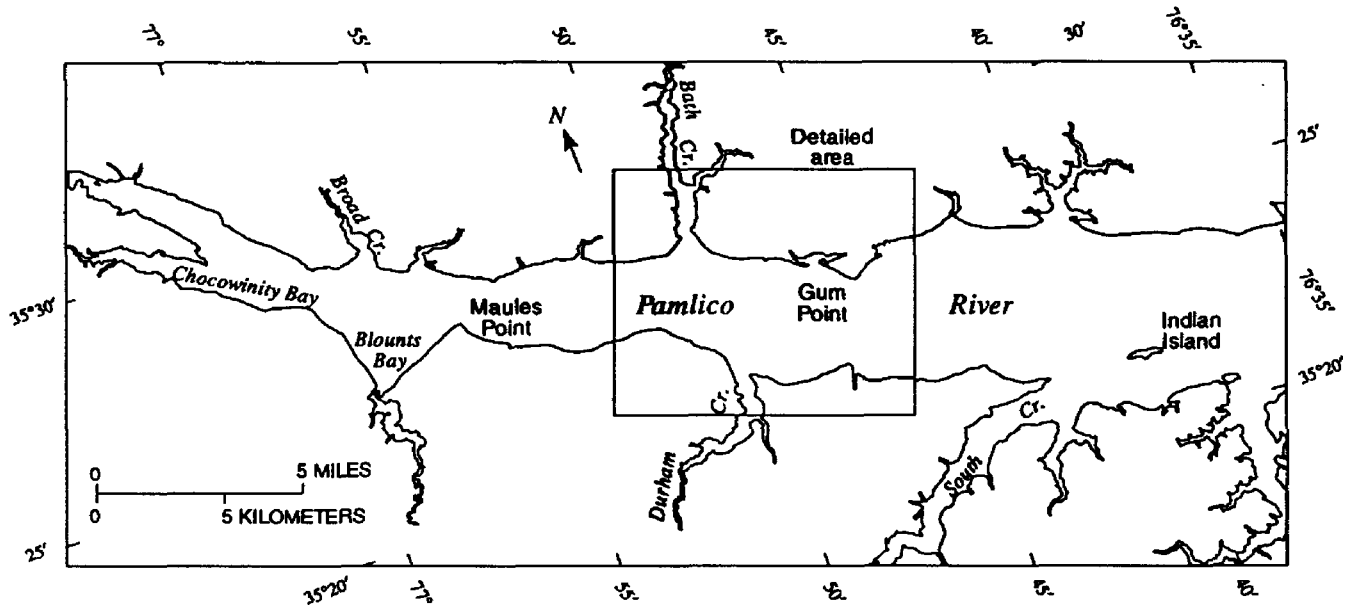

Figure 28. Simulated circulation patterns near Bath Creek for September 6, 1989, at 1410 with (A) Bath Creek as a closed-end embayment and (B) an open-water boundary in Bath Creek.

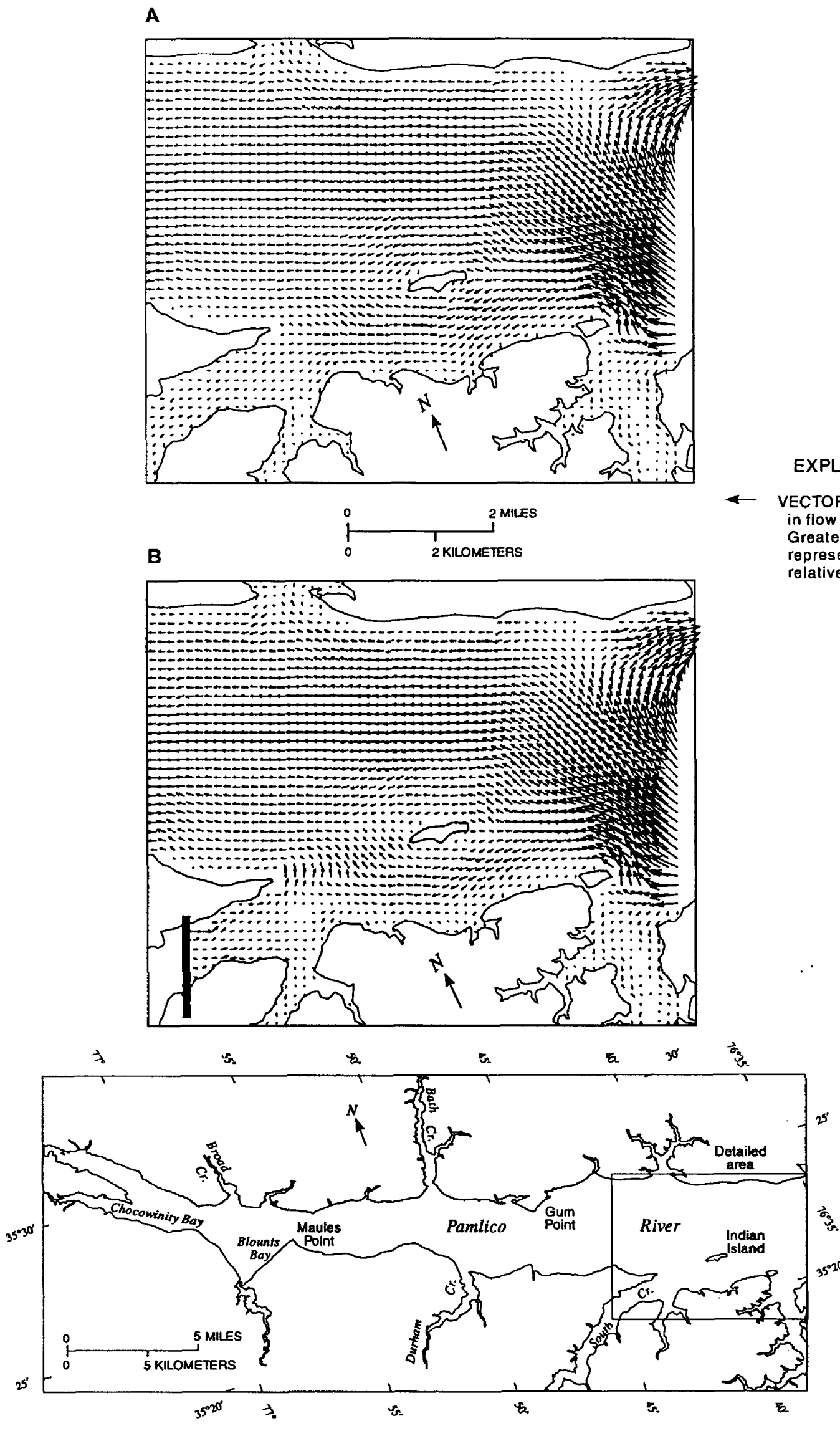

Figure 29. Simulated circulation patterns near South Creek for September 6, 1989, at 1410 with (A) South Creek as a closed-end embayment and (B) an open-water boundary in South Creek.

mid-estuary section (3 m^3/s) and downstream boundary (25 m^3/s) section. The maximum simulated instantaneous downstream flow ranged from 543 m^3/s near Washington to 4,910 m^3/s at the downstream boundary (table 13). Daily flow reversals occurred at all three sections during the simulation period (table 13). Flows during the other three simulation periods were generally similar to those during June 14-30, 1991. At Washington, instantaneous simulated flows during the four periods ranged from 610 m^3/s upstream to 543 m^3/s downstream; flows ranged from 5,930 m^3/s upstream to 6,970 m^3/s downstream at the downstream boundary.

Periods of several consecutive days during which the mean flow is in the upstream direction are not unrealistic. For example, observed mean flow near Washington was 53 m^3/s in the upstream direction during August 30-September 12, 1989. As a result of rising water levels in Pamlico Sound, the water level at the end of this 14-day period was about 0.17 m higher than at the beginning (fig. 19A). In comparison, a simulated steady upstream flow of 53 m^3/s for 14 days would increase the water level by 0.28 m throughout the model domain if all of the water remained within the model domain. During this period (August 30-September 12, 1989), however, tidal effects were observed 30 km upstream of Washington in the Tar River, where daily water-level fluctuations of between 0.17 and 0.29 m occurred.

These simulations of flow in the Pamlico River demonstrate the large variations in flow magnitude that can occur during a day, as well as variations that can occur from day to day. These simulations also demonstrate that flow is highly nonuniform throughout the estuary as reflected in the variation in daily maximum flows between the upstream and downstream sections. Finally, flow simulations such as these can be useful for

Table 13. Simulated daily maximum downstream and daily maximum upstream flow at three Pamlico River cross sections for June 14-30, 1991

[m^3/s, cubic meter per second. Negative flow is upstream (to the west). Section locations are shown in figure 3]

Data	Daily maximum downstream flow (m^3/s)			Daily maximum upstream flow (m^3/s)		
	Saction 1	Section 2	Section 3	Section 1	Section 2	Section 3
June 14	267	1,310	3,610	-499	-1,160	-2,130
15	333	707	2,260	-357	-671	-1,650
16	284	625	1,930	-308	-641	-1,280
17	469	1,380	3,920	-411	-1,230	-3,620
18	347	2,550	4,910	-347	-1,070	-2,240
19	373	495	1,080	-243	-708	-1,900
20	366	1,000	2,570	-381	-894	-1,850
21	431	681	1,730	-386	-940	-2,340
22	333	989	2,730	-438	-916	-2,500
23	442	2,010	4,200	-285	-1,920	-2,680
24	543	956	2,330	-426	-667	-2,520
25	317	914	2,830	-567	-1,130	-1,680
26	328	427	1,440	-452	-843	-1,410
27	465	818	2,070	-466	-847	-2,230
28	384	1,230	3,140	-494	-822	-1,950
29	254	648	1,840	-264	-374	-1,040
30	256	658	1,520	-290	-546	-878
Entire period	543	2,550	4,910	-567	-1,920	-3,620

determining instantaneous and mean constituent loadings throughout the estuary.

Circulation Patterns

One of the results of each model simulation is a time sequence of velocity magnitude and direction for each computational cell. Plots of these vectors can be used to examine detailed circulation patterns in areas of interest. As an example of the temporal and spatial complexity of circulation in the Pamlico River, simulated velocity vectors for selected times corresponding to three water-level conditions (fig. 30) during the August 7-29, 1991, simulation are shown in figures 31-34.

On August 22, 1991, at 0930 when water levels at sites WL1 and WL4 were at a daily minimum and water level at site WL4 exceeded that at site WL1 by 3.0 cm (fig. 30), simulated flow throughout the estuary was in the upstream direction (figs. 31A, 32A, 33A, and 34A). Currents were greatest in the upper reach of the estuary (fig. 31A), and there were large areas of essentially zero velocity in the lower middle (fig. 33A) and lower (fig. 34A) reaches. Velocities were higher near the shore than in the main channel, and were generally higher along the north than the south shore. This was particularly true near Broad Creek and Blounts Bay (figs. 31A and 32A), and Gum Point (fig. 33A) where topographic features affected circulation patterns. Flow was into Bath Creek (fig. 33A) and out of South Creek (fig. 34A) at this time.

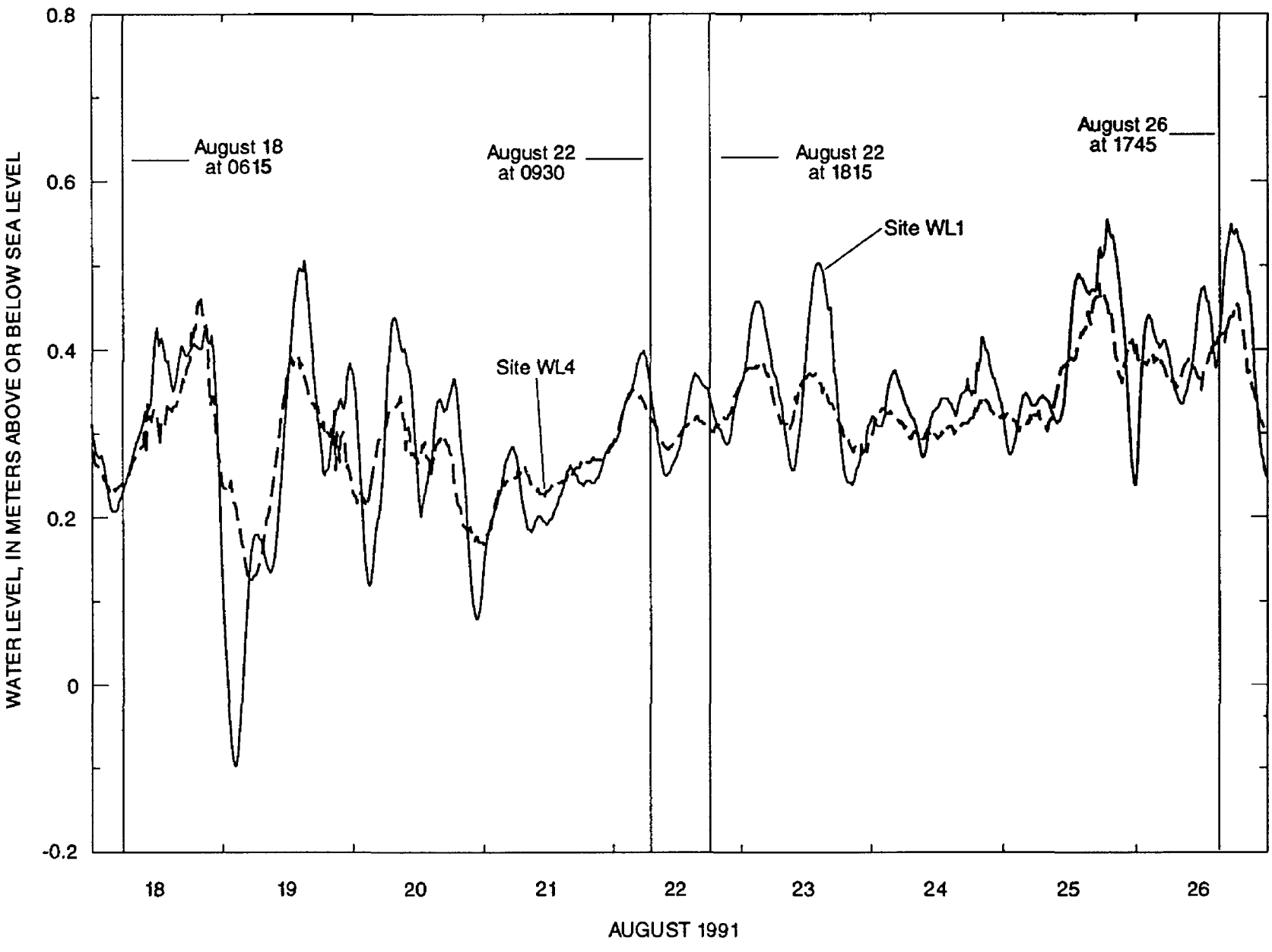

Figure 30. Water level at sites WL1 and WL4 in the Pamlico River during August 21-26, 1991.

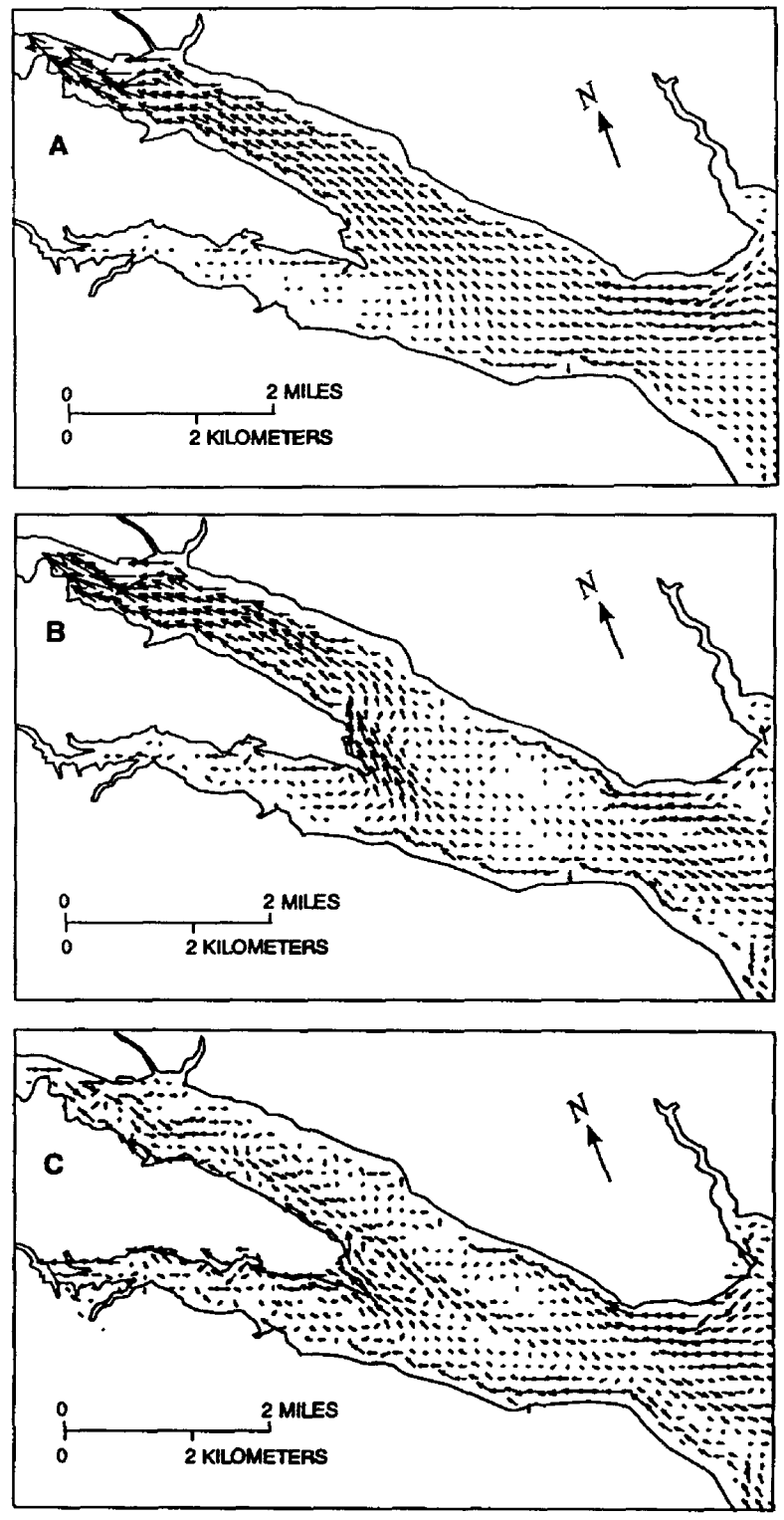

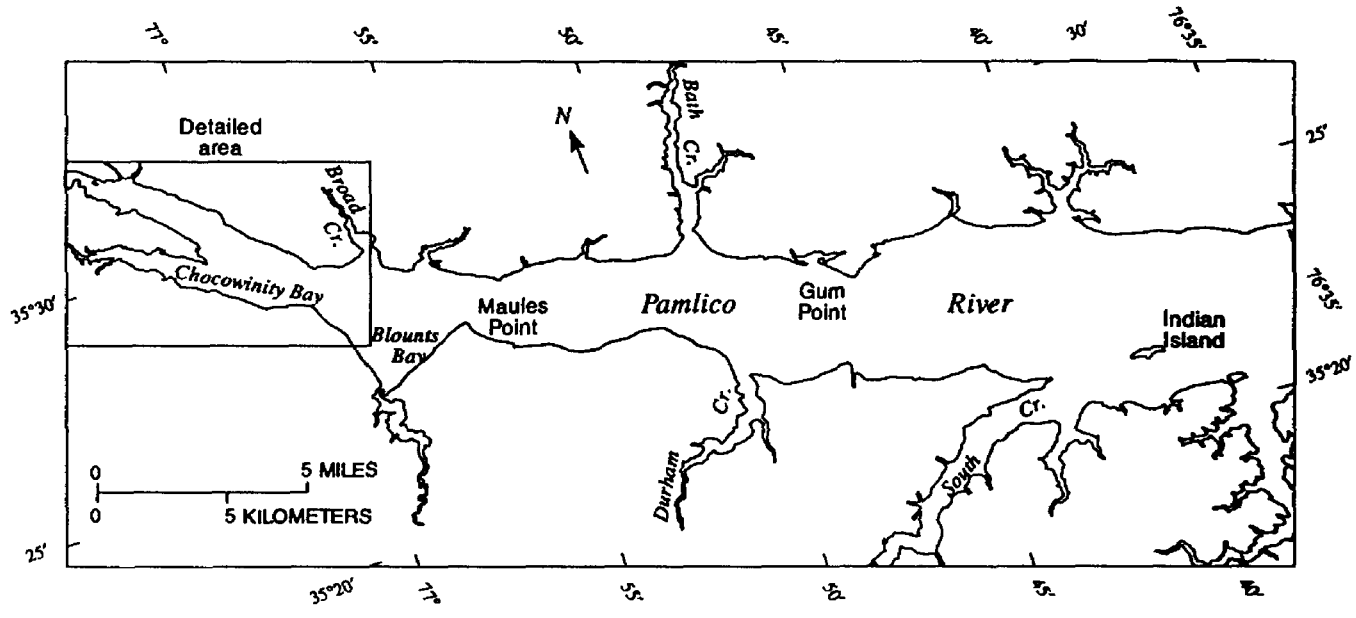

Figure 31. Simulated circulation patterns in the upper Pamlico River for 1991: (A) August 22 at 0930, (B) August 22 at 1815, and (C) August 26 at 1745.

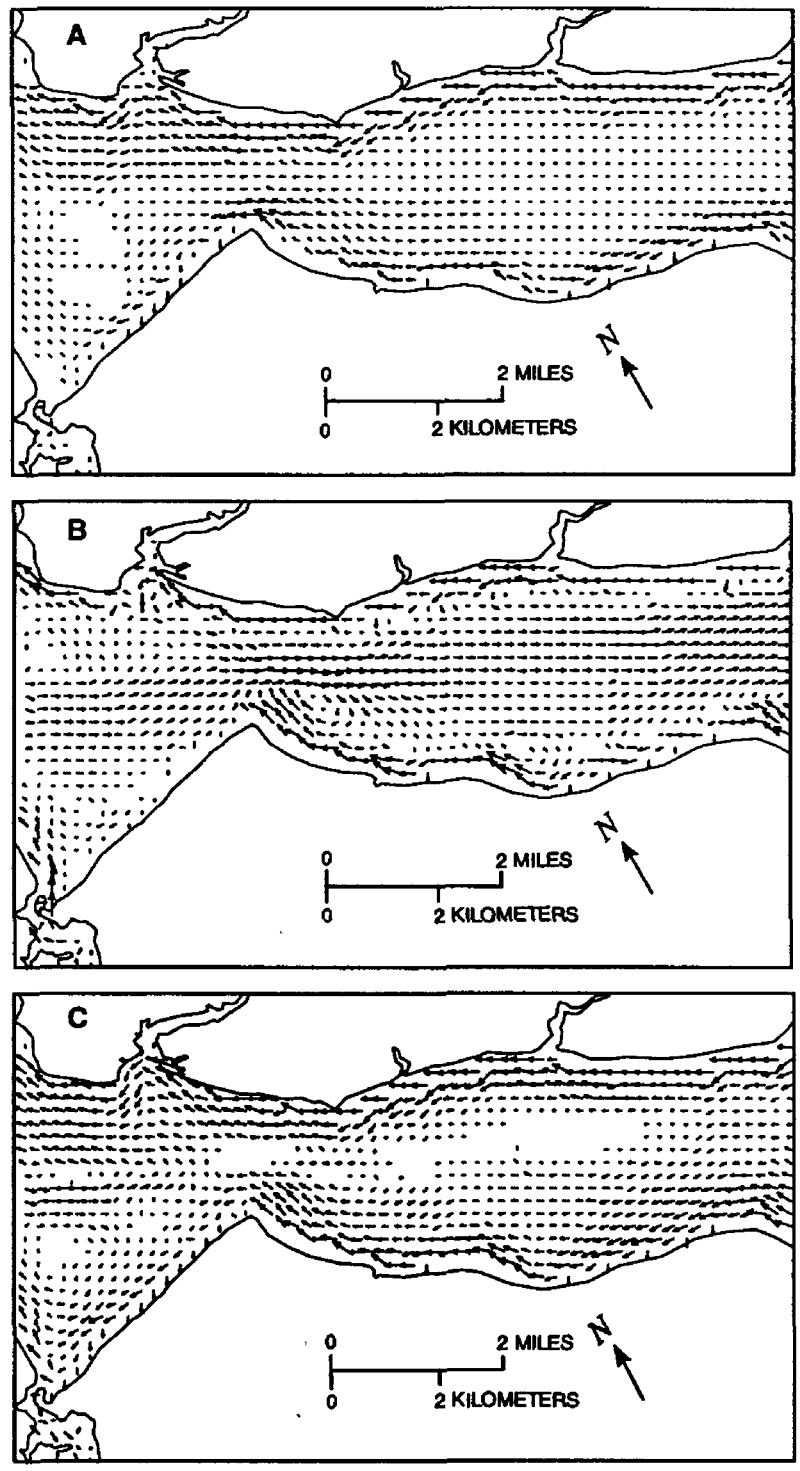

EXPLANATION

← VECTOR--Head points in flow direction. Greater vector length represents greater relative velocity

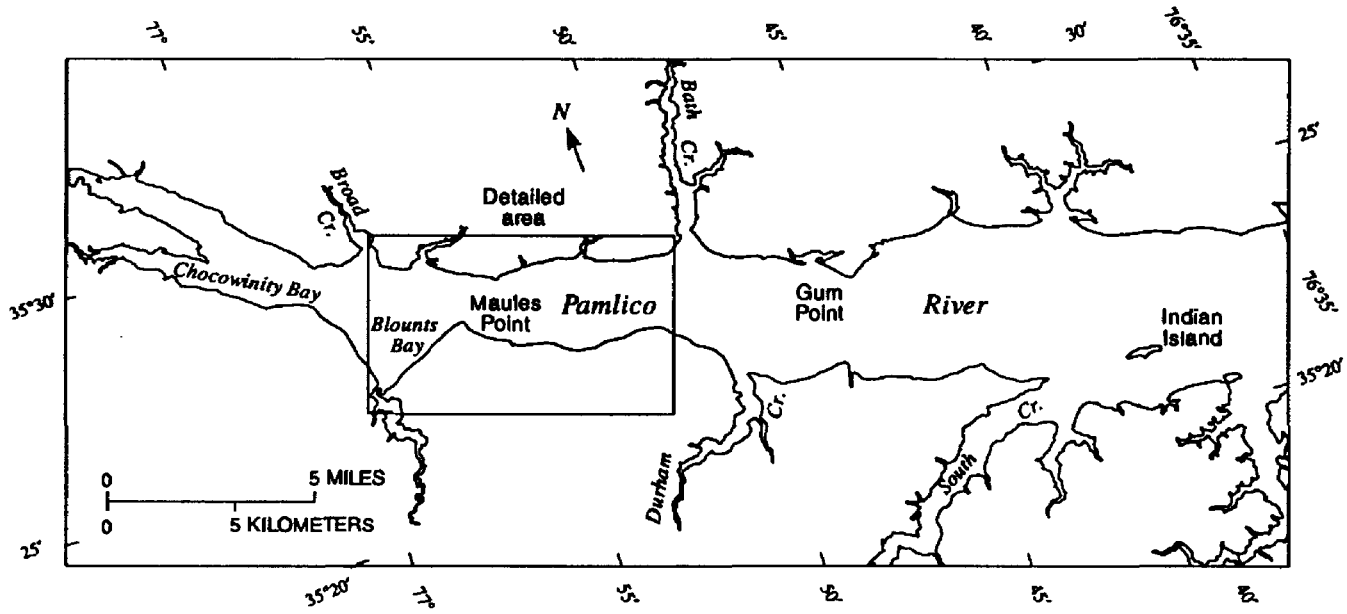

Figure 32. Simulated circulation patterns in the upper middle Pamlico River for 1991: (A) August 22 at 0930, (B) August 22 at 1815, and (C) August 26 at 1745.

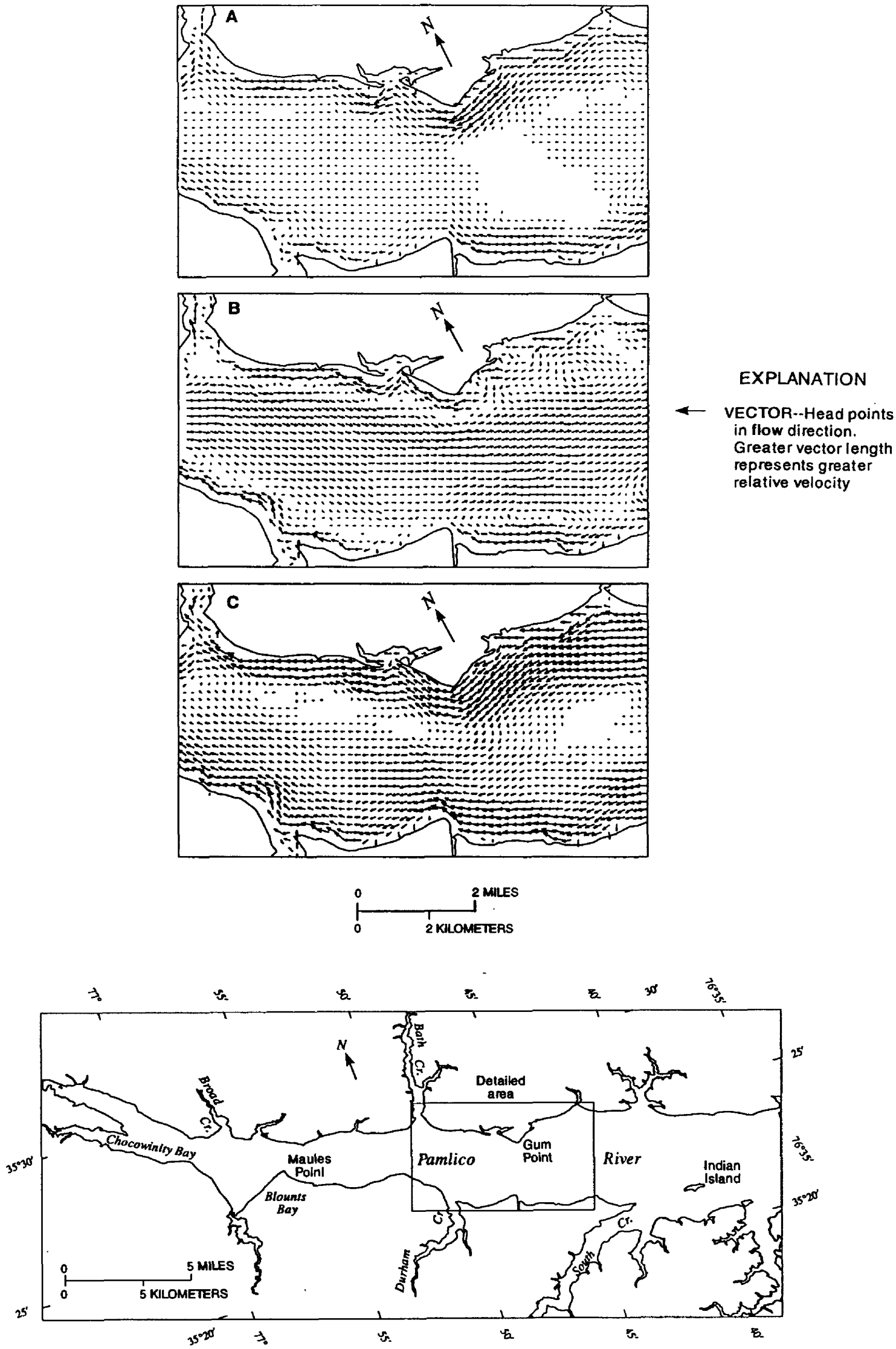

Figure 33. Simulated circulation patterns in the lower middle Pamlico River for 1991: (A) August 22 at 0930, (B) August 22 at 1815, and (C) August 26 at 1745.

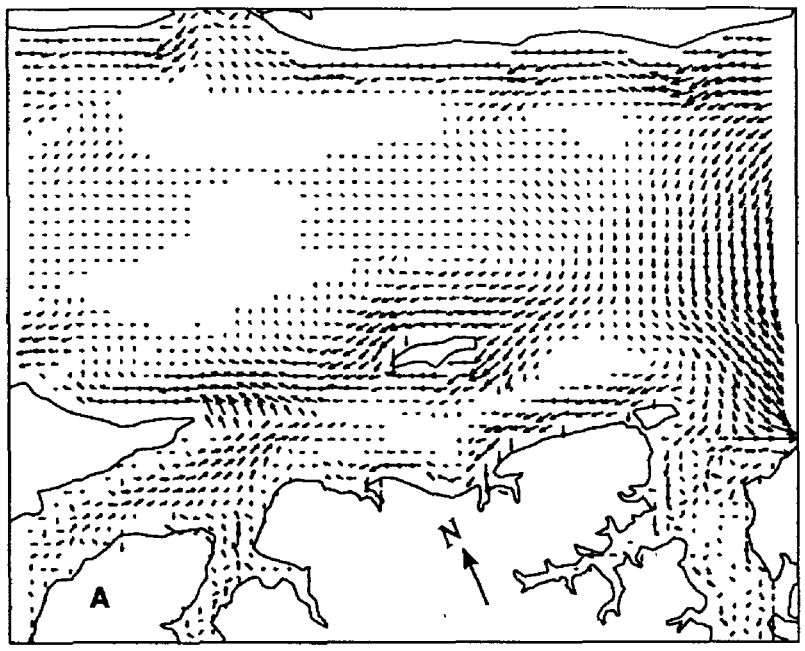

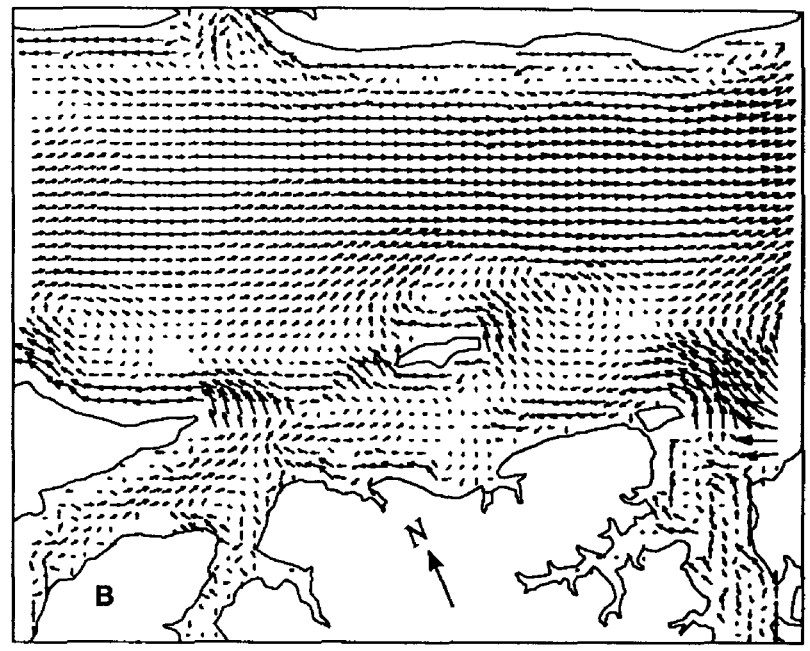

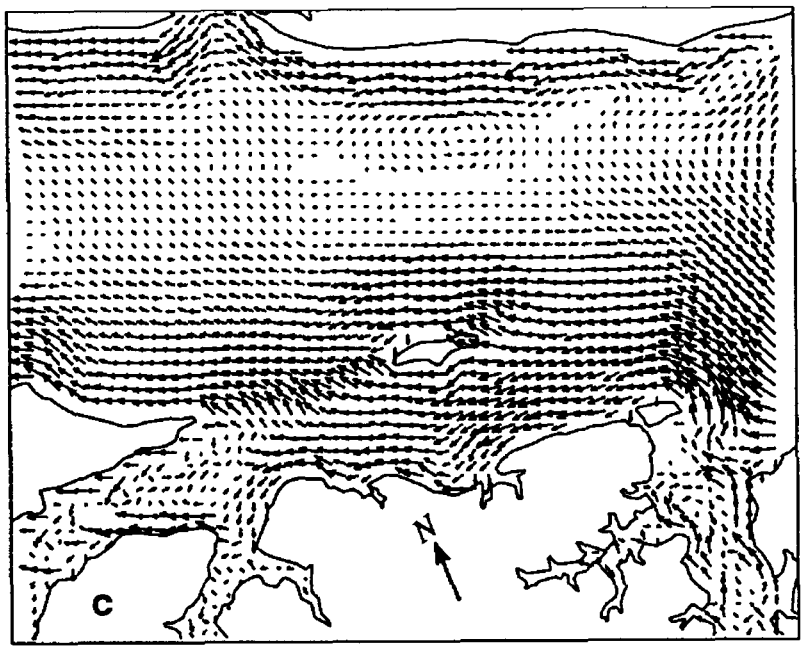

EXPLANATION

← VECTOR--Head points in flow direction. Greater vector length represents greater relative velocity

0 2 MILES
0 2 KILOMETERS

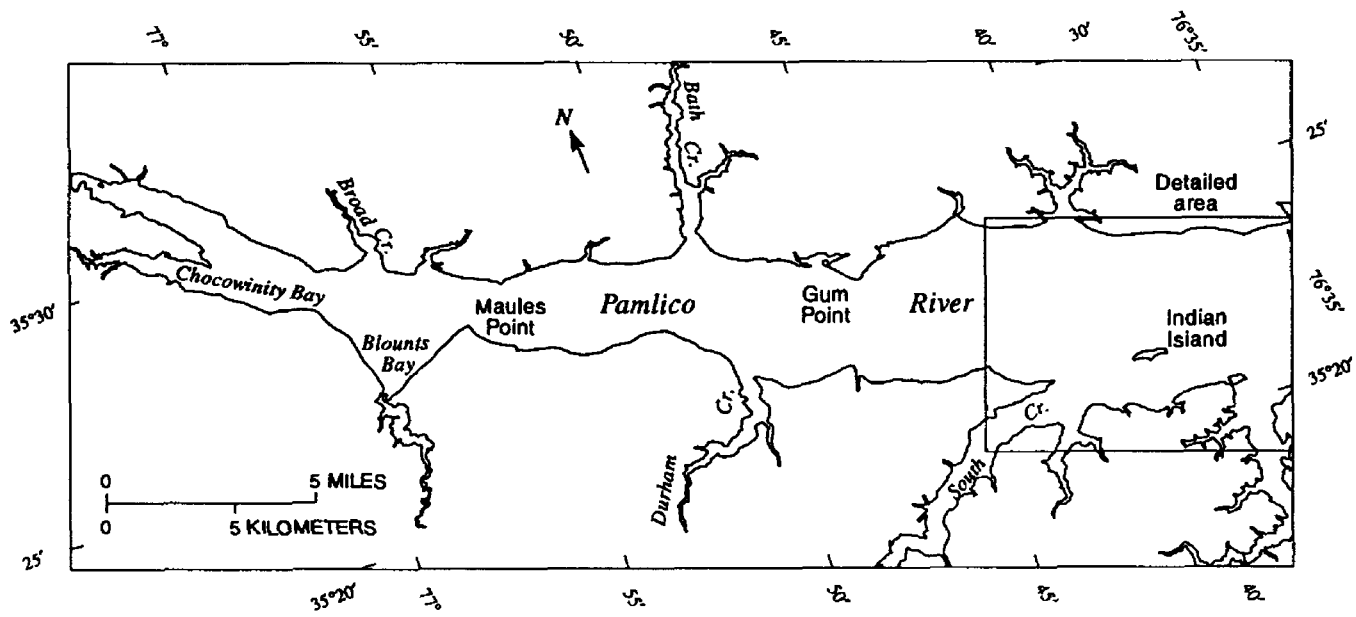

Figure 34. Simulated circulation patterns in the lower Pamlico River for 1991: (A) August 22 at 0930, (B) August 22 at 1815, and (C) August 26, at 1745.

Circulation patterns were more complex later on August 22 at 1815 (figs. 31B, 32B, 33B, and 34B). Water levels at sites WL1 and WL4 had been falling for about 3 hours, and water level at site WL1 exceeded that at site WL4 by 3.7 cm (fig. 30). Circulation patterns near the mouth of Chocowinity Bay (fig. 31B) indicate that water flowing out of the bay at this time moved upstream toward Washington. Downstream from the mouth of Chocowinity Bay, flow was generally directed downstream at mid-channel and upstream near both shores (figs. 31B, 32B, 33B, and 34B). Topographic gyres (or recirculation eddies) are evident at several locations, including (1) east of Maules Point near the south shore (fig. 32B), (2) near the mouth of Durham Creek (fig. 33B), (3) east of Gum Point on the north shore where currents are low (fig. 33B), and (4) west of the mouth of South Creek (fig. 34B). These recirculation eddies result when flow, which is upstream along the shore, is steered into the main channel and the downstream currents by a topographic feature of the shoreline, such as at a point or mouth of a creek. A double gyre is present on the north side of Indian Island (fig. 34B) as a result of the presence of the island coupled with the upstream flow to the south and downstream flow to the north of the island.

On August 26 at 1745, water levels were at a daily maximum and water level at site WL1 exceeded that at site WL4 by 10.1 cm (fig. 30). Flow was generally to the east upstream of Chocowinity Bay (fig. 31C). Downstream from Maules Point, flow was directed upstream (figs. 32C, 33C, and 34C), and between Chocowinity Bay and Maules Point, flow was downstream at mid-channel and upstream elsewhere. The low velocities in the center of the channel downstream from Maules Point indicate that flow was beginning to reverse from west to east.

A simulated particle having no mass and infinitesimal diameter was released at the center of the computational grid at each of seven locations in the model domain (figs. 35 and 36). The particles were released at the beginning of each of the four simulation periods and were tracked for the duration of the simulation. The resulting particle tracks characterize the transport of materials in the estuary under the hydrodynamic conditions present during the simulation periods.

In some cases, there was little net movement of the particles for the duration of the simulation (for example, particles 4 and 5, fig. 36A). In other cases, relatively small differences in the initial position of the particles resulted in a large difference in the final position of the particle (particles 4 and 5 and particles 6 and 7, fig. 35B). For the August 7-29, 1991, simulation, the net movement of particle 4 was downstream, but the net movement of particle 5, released approximately 1 km from particle 4, was in the upstream direction.

With the exception of particle 5 for the July 4-28, 1991, simulation (fig. 35B), none of the particles released at locations other than the downstream boundary (particles 6 and 7) moved downstream and out of the model domain. Particles 1 and 2 moved across the upstream boundary for the August 7-29, 1991, simulation, and particle 1 moved across the upstream boundary during the August 30-September 12, 1989, simulation.

These results demonstrate the extreme spatial variation in the flow field at any given time, as well as the large difference in circulation patterns which can occur under different forcing conditions. The results also demonstrate the difficulty in identifying a realistic "flushing time" or "residence time" for materials in the estuary because of great variations in circulation patterns and resulting transport. Similar particle tracks can be generated for any computational cell in the model domain and for any desired flow condition.

Solute Transport

The model is capable of simulating the transport of conservative constituents. To simulate solute transport in the Pamlico River and to further characterize circulation patterns, two continuous discharges were placed in the estuary. The first discharge point was on the north side of the estuary just upstream of the mouth of Broad Creek and was assigned a flow of 0.1 m^3/s. The second discharge point was located on the south side of the estuary about 4 km east of Durham Creek. The flow at the second discharge point was 1.0 m^3/s. Both discharges had an initial solute concentration of 1,000 ppt, had the same density as freshwater, and had a salinity of 0 ppt.

Solute transport was simulated for July 4-28, 1991 (figs. 19, 21, 24, and 25). As

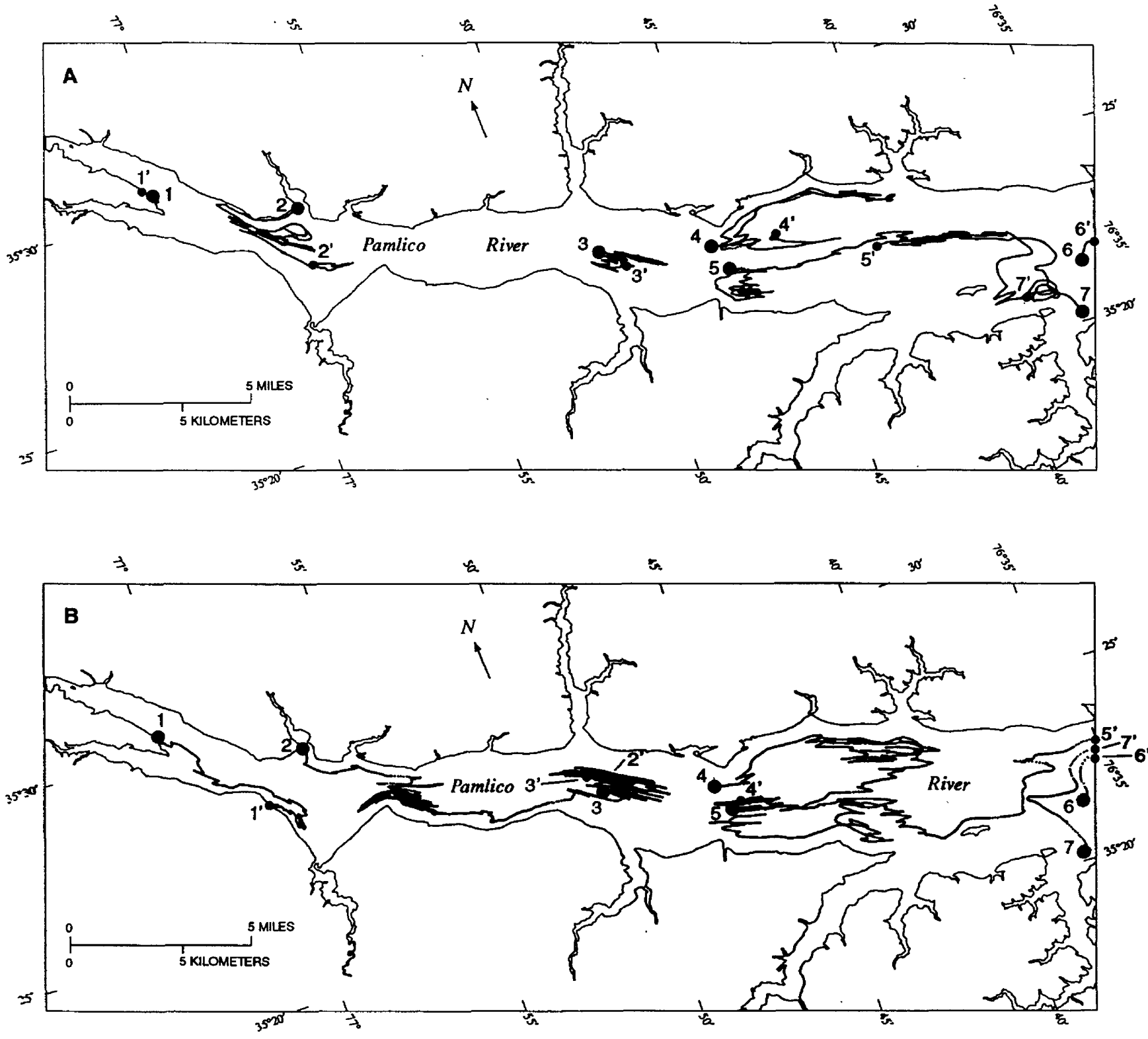

Figure 35. Simulated particle tracks for (A) June 14-30, 1991, and (B) July 4-28, 1991.

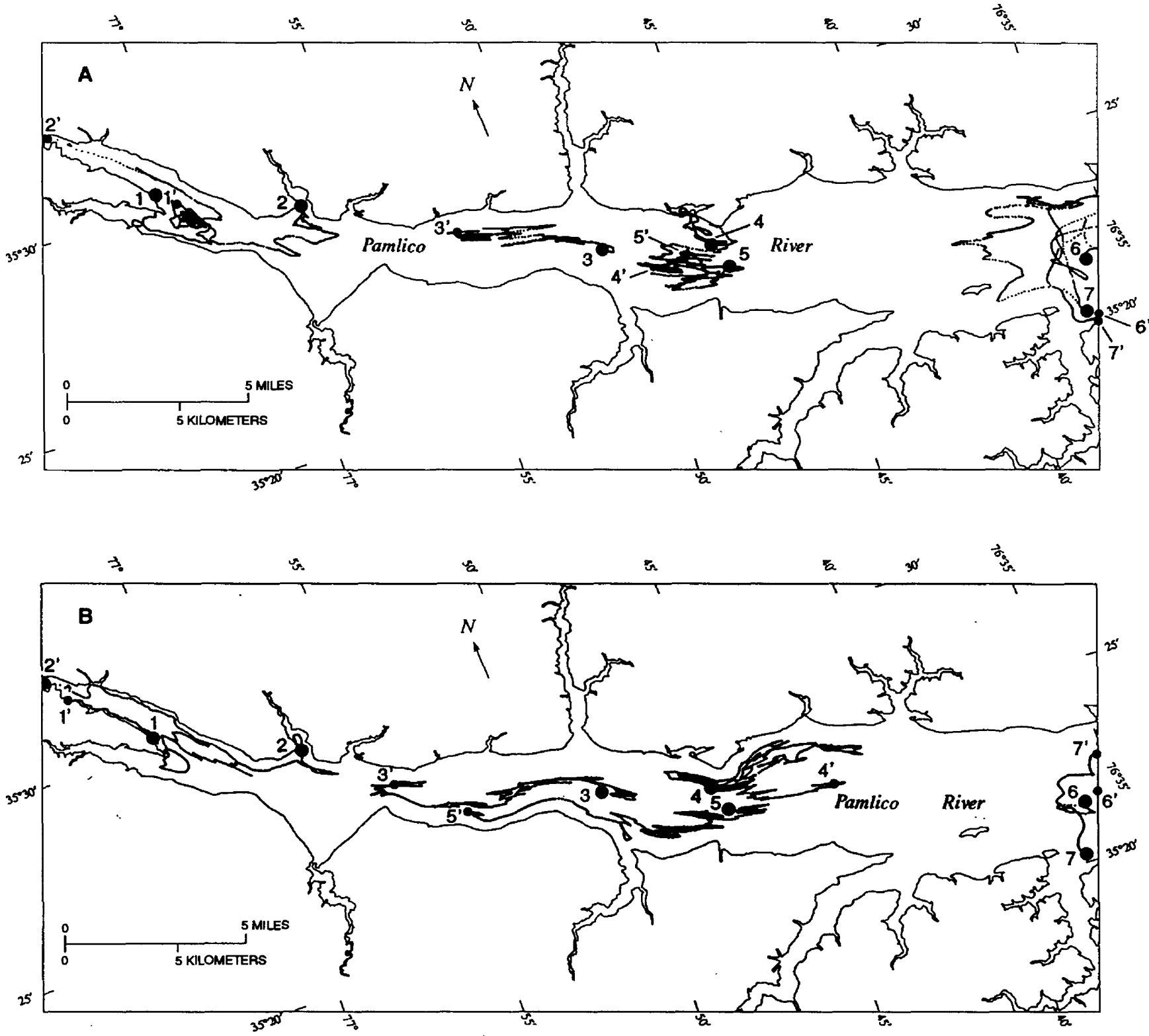

Figure 36. Simulated particle tracks for (A) August 30-September 12, 1989, and (B) August 7-29, 1991.

previously indicated, this was a period of near average water levels, relatively high salinity, and winds from the south-southeast. The upstream and downstream movement of the solute from the downstream release was relatively slow. After 5.5 days, the solute was present at a concentration of 2 ppt (or diluted 500 times from the original concentration) at the north bank across from the release point. After 19.3 days of continuous release, the solute was present at a concentration of 2 ppt along a 17-km reach of the estuary (fig. 37). After about 22 days of continuous release, the concentration along the north bank across from the release had increased to 6 ppt, or a dilution level of 167, but the transport of the solute out of the estuary was minimal.

At the upstream release point, nearly 20 days of continuous release was required before the concentration of the solute reached 2 ppt beyond the mouth of Broad Creek. The predominantly south-southeast winds during this period and the resulting circulation patterns served to enhance the transport of solute released on the south bank and impede the transport of solute released in Broad Creek. If Broad Creek were treated as an open-water boundary rather than as a closed-end embayment, it is likely that the simulated patterns for the Broad Creek release would be different from those presented. The 1 m^3/s discharge (which had a salinity of 0 ppt) on the south shore had no significant effect on salinity in the estuary. After 22 days of continuous discharge, the 10-ppt line of equal salinity was less than 500 m farther downstream than for the condition with no release (fig. 38). The shapes of the 9- and 10-ppt lines of equal salinity also were modified slightly by the discharge.

The transport of solutes released at other locations in the estuary and under different conditions can be simulated to further characterize mixing and transport. The transport of solutes from continuous and instantaneous releases (for example, chemical spills) can be simulated.

Salinity was simulated for each computational cell at each time step during all simulations. Lines of equal salinity were generated for two summer periods, August 30-September 12, 1989, and August 7-29, 1991, to show differences in salinity distribution patterns under differing hydrologic conditions. The 1989 period, as previously described, was a period of near average water levels and somewhat low salinity relative to the mean September values recorded during the period of data collection. By comparison, the 1991 period was characterized by lower water levels and higher salinity. The 1991 period also included the passing of Hurricane Bob near eastern North Carolina.

For the 1989 period, there was little change in salinity during the last 4 days of the simulation. There was only slight increase in salinity in the upstream direction in the upper part of the estuary (fig. 39). During August 18-26, 1991, however, there was significant upstream increase in salinity (fig. 40). Salinity distributions shown in figure 40 are for the minimum recorded water level (fig. 40A) and after a period of sustained easterly winds (fig. 40B).

The minimum water level occurred during Hurricane Bob and resulted in a 0.52-m water-level drop at Washington in a 4.5-hour period, which is about twice the August mean daily water-level range. This was followed by a period when winds were blowing from the east-southeast about 70 percent of the time. As a result of these combined effects, the simulated 10-ppt line moved upstream about 5 km, and the 7-ppt line extended to within 5 km of the upstream boundary (fig. 40B).

For all cases shown, lateral differences in salinity were present. The largest gradient occurred near the shore as a result of the lateral shear in the currents (for example, figs. 32B, 33B, and 34B).

Conclusions

Data and model results demonstrate the complexity of the Pamlico River flow field. Currents vary temporally (figs. 7, 8, and 9; table 9) and spatially. Currents can be simultaneously directed upstream in one segment of the estuary (fig. 31B) and downstream in another segment (fig. 32B). Likewise, currents vary laterally. For example, currents can be simultaneously upstream near the shore and downstream near the center of the channel (fig. 32C), or currents can be simultaneously upstream on the south side of the estuary and downstream on the north side (fig. 9A). And, at any given section in the estuary, currents can be simultaneously downstream near the surface and upstream near the bottom (site P5, fig. 9B). Ziegler and others (1994) showed that this two-layer flow,

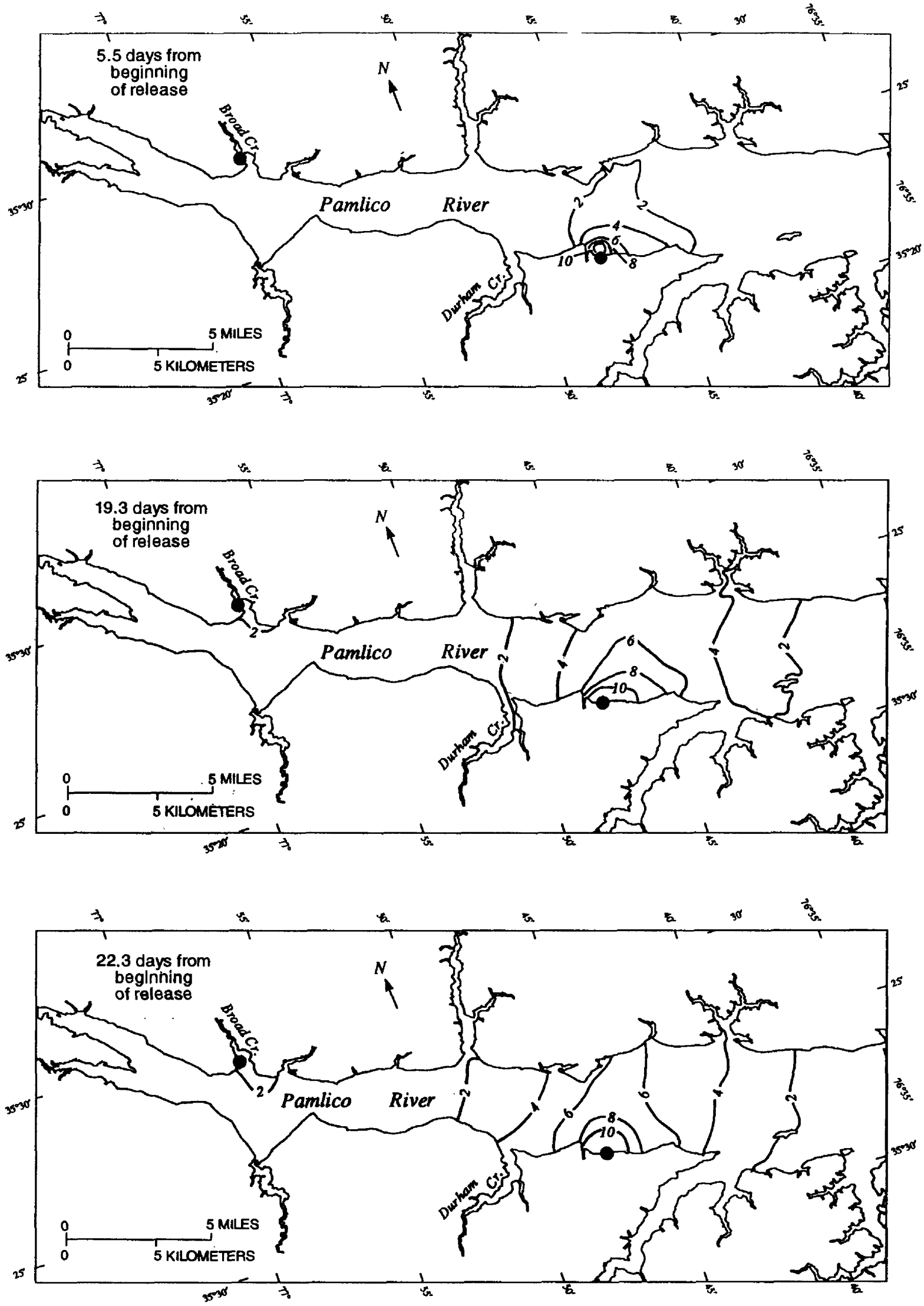

Figure 37. Simulated solute concentration from two continuous releases of water containing 1,000 parts per thousand solute concentration beginning on July 4, 1991, at 0000.

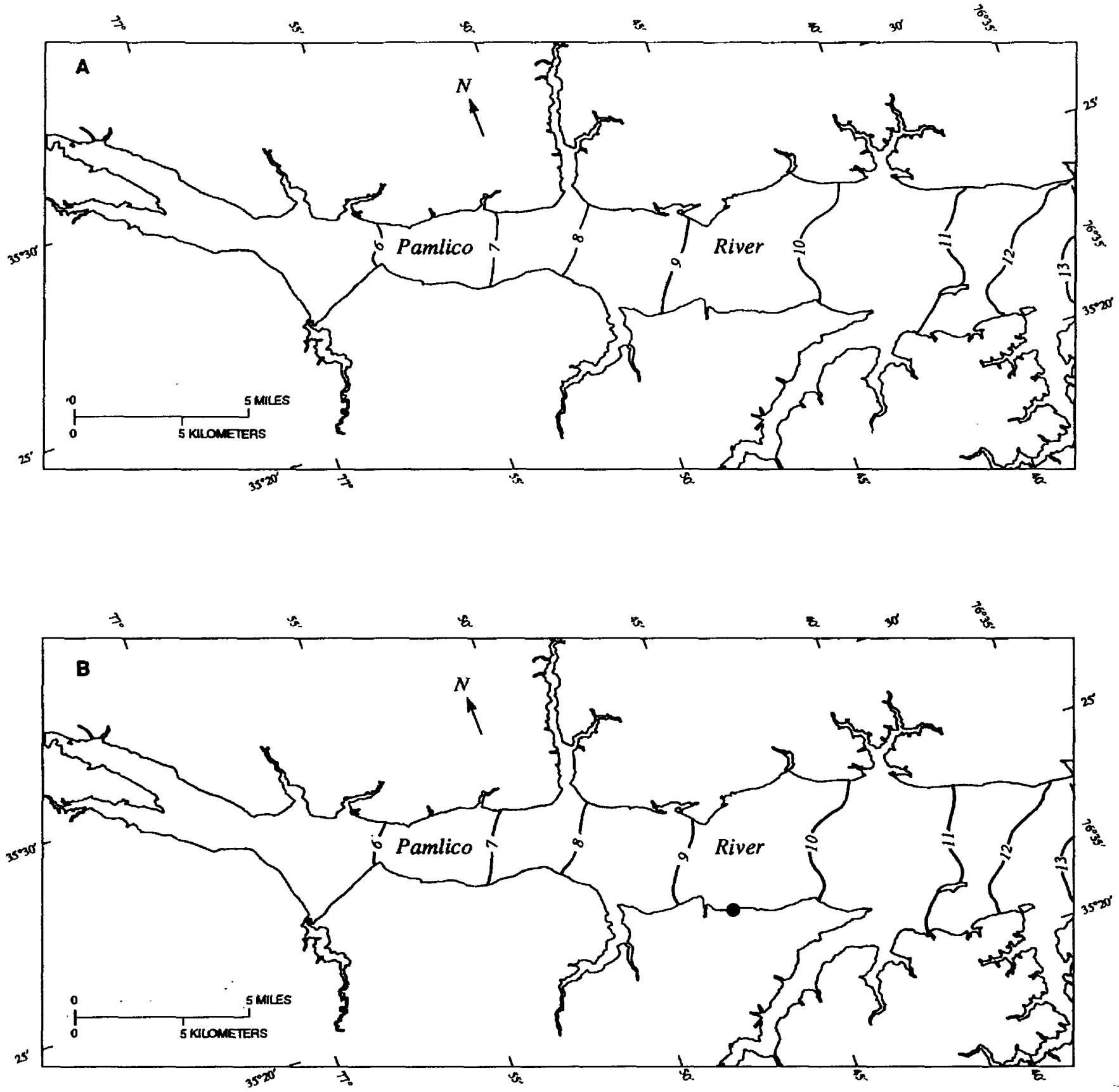

Figure 38. Lines of equal simulated salinity for July 25, 1991, at 0615 for (A) no discharge and (B) a discharge of 1 cubic meter per second with a salinity of 0 part per thousand on the south shore beginning on July 4, 1991.

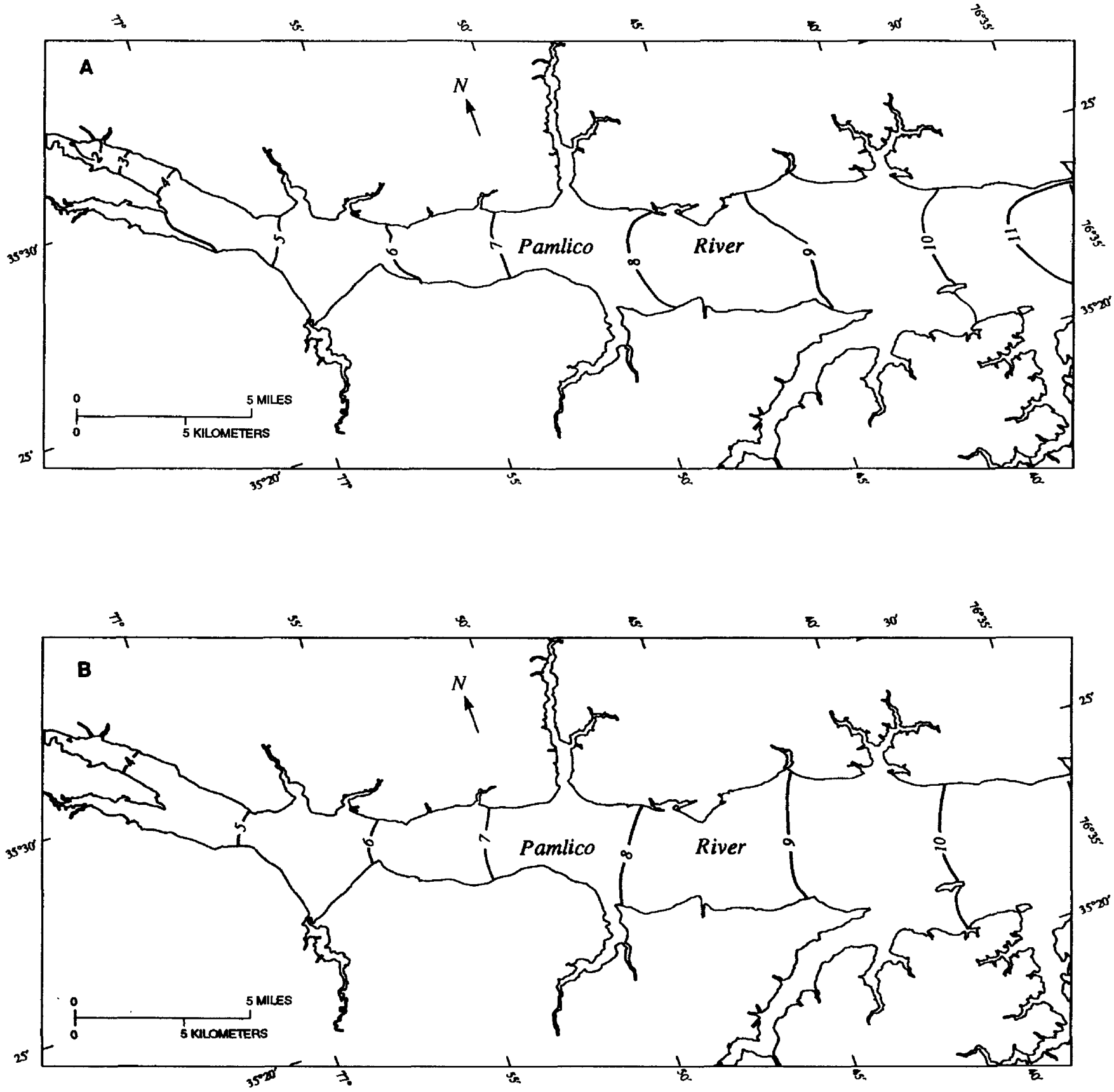

Figure 39. Lines of equal simulated salinity for (A) September 6, 1989, at 1415 and (B) September 10, 1989, at 0900.

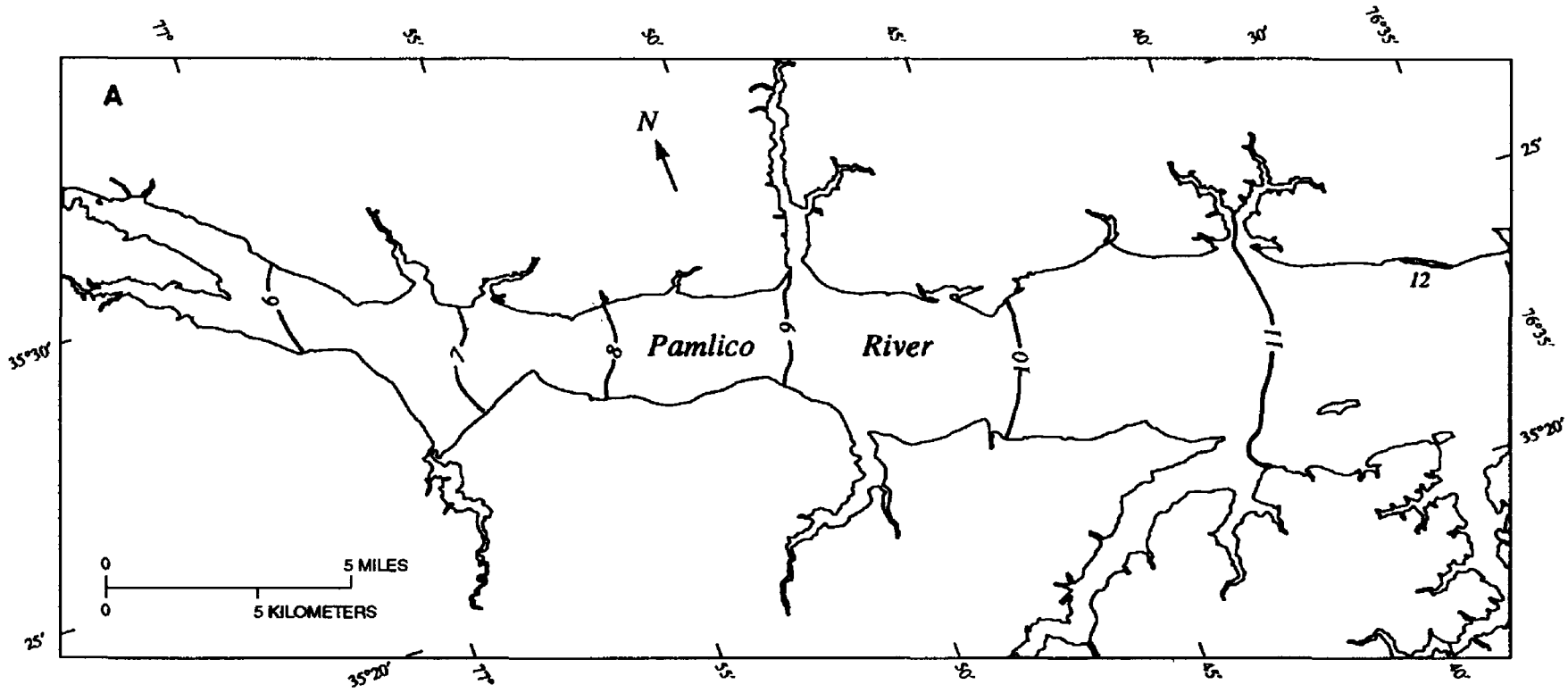

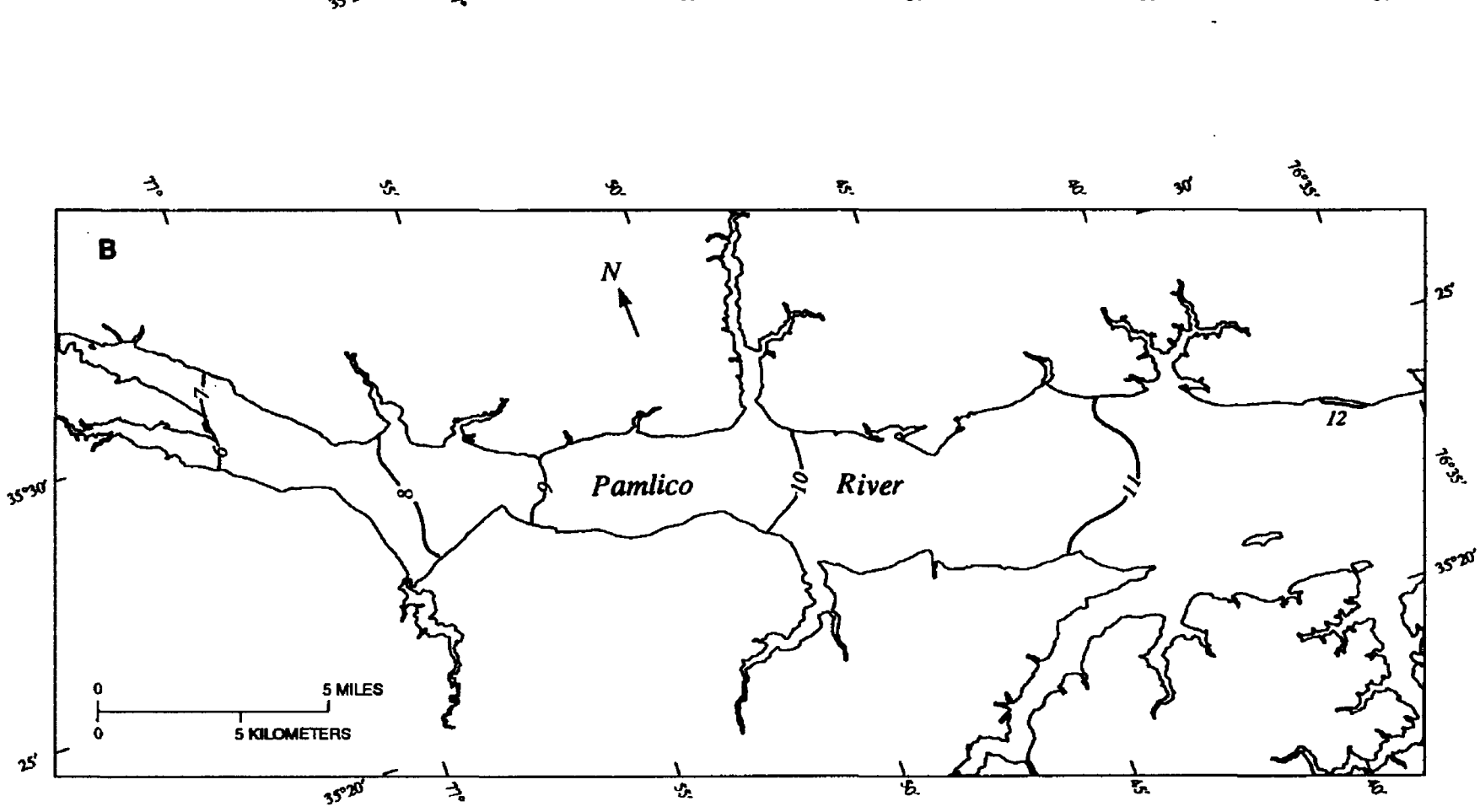

EXPLANATION

—6— LINE OF EQUAL SIMULATED SALINITY--
Interval 1 part per thousand

Figure 40. Lines of equal simulated salinity for (A) August 18, 1991, at 0615 and (B) August 26, 1991, at 1745.

which is driven primarily by the longitudinal salinity gradient, could exist even when vertical salinity gradients were essentially nonexistent.

Many of the characteristics of the flow field are related to the topographic features of the estuary. When flow reverses direction, currents near the shore, where depths are small, reverse direction before currents near the center of the channel, where depths and inertia are greater. Shoreline features also affect circulation patterns. Recirculation eddies form in the lee of points or promontories that extend into the estuary (for example, Maules Point, fig. 32B). Currents can often be greater near these topographic features because the flow must accelerate to move the greater distance around the point (for example, Gum Point, fig. 33C).

A spatially detailed hydrodynamic model is required to simulate the spatial heterogeneity of the Pamlico River flow field. The 200-m grid used in this study provides good lateral and longitudinal resolution of circulation, as well as solute transport. However, a spatially detailed three-dimensional model in which flow and transport are coupled is needed if the gravitational circulation in the estuary is to be accurately simulated. The lateral variation needs to be retained in the model if the effects of individual point- and nonpoint-source controls are to be evaluated.

Transport of solutes in the Pamlico River is generally quite slow. Materials can be retained in the estuary for several weeks with very little net movement during the period (for example, particles 3 and 4, fig. 35B). The net transport of a solute is very sensitive to the initial position (release point) of the material. Materials that are released at very nearly the same position can take entirely different transport paths and rates (for example, particles 4 and 5, fig. 36B).

Flow rates in the estuary are quite large relative to mean freshwater inflows. Consequently, dilution of materials released to the estuary also can be large, provided the concentration of the released material is initially low in the estuary. For example, the solute released continuously on the south shore of the estuary for more than 3 weeks (fig. 37) was diluted to less than 1 percent of the initial concentration except near the release point.

Although the model results presented in this report generally agree with observations, some features of the model can be enhanced to provide additional, or perhaps improved, simulation results. As previously discussed, a three-dimensional model is needed to simulate gravitational circulation, as well as vertical gradients, which govern selected water-quality processes.

Better vertical control is needed at water-level gages to ensure that circulation is forced by accurate water-level gradients. Relocating the western model boundary upstream and forcing the model with measured flow at the upstream boundary rather than water level might also improve results. A sophisticated flow measurement device, such as an ultrasonic velocity meter, would be required to obtain reliable flow records. Also, as previously discussed, inflows from tidal creeks need to be added to the model if water-quality processes in the estuary are to be simulated. These inflows, however, are generally small relative to flows in the estuary, and the inflows do not affect circulation patterns.

SUMMARY

The proper description of circulation is critical to the understanding and management of water quality, productivity, and distribution and abundance of biota in estuaries. Numerical models provide the capability to describe physical and biochemical processes with high spatial resolution throughout the entire estuary and to conduct experiments by evaluating estuarine response to a wide range of imposed conditions. The development of numerical models to characterize water circulation was identified as a high-priority goal of the Albemarle-Pamlico Estuarine Study. To address this need, the U.S. Geological Survey, in cooperation with the Albemarle-Pamlico Estuarine Study of the North Carolina Department of Environment, Health, and Natural Resources, conducted an investigation of hydrodynamics and transport in the Pamlico River. The investigation included a detailed field-measurement program and the development and application of a physically realistic model of hydrodynamics and transport.

This report documents development and application of a two-dimensional, unsteady hydrodynamic and transport model for a reach of

the Pamlico River which extends 48 km downstream (east) from the U.S. Highway 17 bridge near Washington. The approach leading to the development and implementation of the model consisted of data collection to characterize conditions in the study area and to implement and operate the model; model calibration, validation, and sensitivity testing; and model application.

To provide the required information for the Pamlico River estuary hydrodynamic model and to better define the physics of flow in the Pamlico River, water level, salinity and water temperature, wind speed and direction, current velocity, and bathymetric data were collected during the period March 1988 to September 1992. Data from pre-existing, continuous-record streamflow gaging stations and meteorological stations also were available during this period.

During the study period, the mean water level measured at the five water-level stations in the Pamlico River ranged from 0.226 m to 0.247 m in elevation. The highest and the lowest water levels were observed at the upstream (western) end of the Pamlico River. Water levels were generally highest in the late summer and early fall (August-October) and lowest during the winter (December-February). Although instantaneous differences in water level of as much as 0.3 m were observed throughout the study reach, the water-surface slope in the Pamlico River was generally small, on the order of 10^{-6}. The mean daily water-level range (difference between daily maximum and daily minimum water level) was 0.322 m at the upstream end of the study reach and 0.179 m at the downstream end. The daily water-level range was generally the greatest during April and May and typically at a seasonal minimum during the fall.

Mean near-surface salinities ranged from 2.2 ppt near Washington to 11.0 ppt at the downstream end of the study reach, and mean near-bottom salinities ranged from 4.7 ppt near Washington to 11.4 ppt at the downstream end of the reach. The difference between maximum observed and minimum observed salinity at each site ranged from 13.2 ppt to 20.4 ppt. High salinities also were observed at the upstream end of the estuary (13.2 ppt near the surface and 13.5 ppt near the bottom). Likewise, low salinities were observed at the downstream end of the estuary (2.1 ppt near the surface and 2.9 ppt near the bottom). Although overall observed variations in salinity were large at each site, daily variations were generally less than 2 ppt. Minimum monthly mean salinities generally occurred in April or May, and maximum monthly mean salinities were generally in November or December. Monthly means of the differences between simultaneously observed near-surface and near-bottom salinities ranged from less than 1 ppt to 5.7 ppt, with the highest values occurring in the upper reach of the estuary. Vertical salinity gradients were generally at a minimum between April and July and usually greatest from late summer through early winter.

Winds were generally from the south, southwest, and west during late spring and summer months. Wind speeds were greatest during the winter months. During December through May, wind speeds were greater than 9 m/s at least 10 percent of the time. Winds were typically light during June through August, with wind speeds less than 4.5 m/s about 37 percent of the time.

The long-term (1896-1992) annual average flow at Tarboro, the downstream-most continuous-record streamflow station on the Tar River, was 63.2 m^3/s. The estimated long-term annual average freshwater flow at Washington is 89 m^3/s. Estimated annual average freshwater flow at Washington during the study period ranged from 42.4 m^3/s in 1988 to 132 m^3/s in 1989. Estimated monthly mean inflows from the 1,230-km^2 basin, which drains to the study reach downstream from Washington, ranged from less than 0.1 m^3/s to 46.1m^3/s, which is about half of the estimated long-term average annual freshwater inflow at Washington. Estimated monthly mean freshwater inflows were less than 10 m^3/s 46 percent of the time and less than 20 m^3/s 66 percent of the time.

During the 15-day period when current meters were deployed in the study reach, velocities ranged from a maximum downstream velocity of 31 cm/s to a maximum upstream velocity of 34 cm/s. Highest mean and maximum velocities were generally observed on the north side of the estuary, although the mean upstream velocities were higher near the middle of the channel at the downstream end of the study reach. Even at the relatively narrow, mid-estuary section, where three meters were moored, there was a marked difference in velocity direction and magnitude across the estuary. Velocities were generally lower on the

south side of the estuary than on the north side at the mid-estuary measurement section. At the downstream end of the study reach, however, net water movement was upstream on the south side of the estuary, and net movement was downstream on the north side of the estuary.

A two-dimensional, vertically averaged modeling approach allowed discretization of the estuary into small computational cells to provide spatially detailed information on velocity, circulation, and transport so that longitudinal and lateral movement of materials within the estuary could be simulated. The effects of lateral water-level and salinity gradients, both of which have been observed, are included in the model. The vertically averaged approach, however, does not permit the direct simulation of vertical salinity gradients or the effects of these gradients on flow and transport. Implementation of the hydrodynamic and transport model for the Pamlico River included (1) development of the computational grid, (2) specification of model boundary conditions, (3) identification of initial conditions, and (4) selection of model parameters.

A 200-m x 200-m computational grid size was selected for the Pamlico River model. Boundaries of the Pamlico River model include the channel bottom, the shoreline and tributary streams, a downstream (or eastern) open-water boundary, an upstream (or western) open-water boundary near Washington, and the water surface. The channel bottom was assumed to be an impermeable and immobile boundary and was assumed to cause resistance to the flow and thereby extract energy from the mean flow. A "leak test" was performed to ensure that there were no unintentional openings in the shoreline boundary through which flow could leave the model domain. Tributary streams were treated as closed-end embayments in the model. Momentum was transferred to the estuary by wind blowing over the water surface. Measured wind speed and direction was used for the water-surface boundary condition. It was assumed that the wind was spatially invariant over the entire model domain, but that the wind varied with time.

Five model parameters were chosen prior to model simulations. These parameters include (1) the wind-stress coefficient, (2) a parameter that relates the direction of flow and the salinity gradient to the resistance coefficient, (3) the horizontal momentum mixing coefficient, (4) the isotropic mass-dispersion coefficient, and (5) a coefficient used to compute mass dispersion in the direction of flow. Because these parameters are generally empirical representations of a physical process, the parameters are not known with certainty and thus required some adjustment and testing during the calibration process.

Model calibration was achieved through adjustment of model parameters for a period with complete time-varying data at all boundaries and at interior checkpoints. The model was calibrated using data from the period June 14-30, 1991. The following model parameters provided the best agreement between observed and simulated data: (1) $\eta = 0.028$ (resistance coefficient); (2) $C_d = 0.001$ (wind-stress coefficient); (3) $k' = 10$ m^2/s (unadjusted horizontal momentum mixing coefficient); (4) $D_i = 20$ m^2/s (isotropic mass-dispersion coefficient); and (5) $D_c = 14$ m^2/s (coefficient relating mass dispersion to flow properties).

The model was validated using data collected during two separate periods. Simulations were made for August 30 through September 12, 1989, which included the time when recording current meters were moored in the estuary. The model also was validated using data from a longer period—July 4-28, 1991.

The model was calibrated and validated for (1) water levels ranging from -0.052 m to 0.698 m, (2) salinities ranging from 0.1 ppt to 13.1 ppt, (3) and wind speeds ranging from calm to 22 m/s. The model was tested for conditions with and without vertical salinity gradients. Simulated water levels were within 2 cm of observed values. Simulated salinities at three interior checkpoints were within 1 ppt of observed values. Daily variations in simulated salinities were typically not as large as observed variations. The mean magnitudes of simulated velocities were generally within 2 cm/s of mean observed velocities at the downstream measurement section, but simulated magnitudes were generally less than observed values at the mid-estuary section.

The sensitivity of model results to changes in model parameters and boundary conditions was analyzed. Results were sensitive to the value of C_d but relatively insensitive to changes in other parameters. Boundary conditions were also varied

o evaluate sensitivity of model results to changes in forcing conditions. The objectives of the modeling were to (1) provide a spatially detailed description of circulation and solute transport in the estuary, (2) develop the capability to compute flow rates, and (3) characterize the movement of passive materials in the estuary.

The calibrated model was applied to the Pamlico River to simulate flows, circulation, and solute transport. Flows were simulated for the calibration period (June 14-30, 1991), the two validation periods (August 30-September 12, 1989, and July 4-28, 1991), and for August 7-29, 1991, which includes the period when Hurricane Bob passed near eastern North Carolina. At Washington, instantaneous simulated flows during the four periods ranged from 610 m^3/s upstream to 543 m^3/s downstream; flows ranged from 5,930 m^3/s upstream to 6,970 m^3/s downstream at the downstream boundary.

A particle having no mass and infinitesimal diameter was released at the center of the computational grid at each of seven locations in the model domain. Particles were released at the beginning of each of four simulation periods and were tracked for the duration of the simulation. In some cases, there was little net movement of the particles for the duration of the simulation. In other cases, relatively small differences in the initial position of the particles resulted in a large difference in the final position of the particle. For one simulation period, the net movement of two particles initially located within 1 km of each other was in opposite directions. The results demonstrate the extreme spatial variation in the flow field at any given time, as well as the large difference in circulation patterns, which can occur under different forcing conditions. The results also demonstrate the difficulty in identifying a realistic "flushing time" or "residence time" for materials in the estuary because of the great variations in circulation patterns and resulting transport.

To simulate solute transport in the Pamlico River and to further characterize circulation patterns, the transport of a solute continuously released at two locations was simulated for a 25-day period. One solute discharge was on the north side of the estuary just upstream of the mouth of Broad Creek, and the second discharge was located on the south side of the estuary about 4 km east of Durham Creek. After 19.3 days of continuous release, the solute from the downstream release was present at a concentration of 2 ppt (or diluted 500 times from the original strength) along a 17-km reach of the estuary. After about 22 days of continuous release, the concentration along the north bank across from the release had increased to 6 ppt, or a dilution level of 167, but the transport of the solute out of the estuary was minimal. At the upstream release point, nearly 20 days of continuous release was required before the concentration of the solute reached 2 ppt beyond the mouth of Broad Creek.

Salinity is calculated for each computational cell at each time step during all simulations. Lines of equal salinity were generated for two summer periods, August 30-September 12, 1989, and August 7-29, 1991, to show differences in salinity distribution patterns under differing hydrologic conditions. For the 1989 period, there was little change in salinity during the last 4 days of the simulation. There was only slight displacement of lines of equal salinity in the upstream direction in the upper part of the estuary. During August 18-26, 1991, however, there was significant upstream displacement. As a result of the combined effects of a rising water level and east-southeast winds, the 10-ppt simulated lines of equal salinity moved upstream about 5 km, and the 7-ppt line extended to within 5 km of the upstream boundary. For all cases shown, lateral differences in salinity were present. The largest gradient occurred near the shore as a result of the lateral shear in the currents.

REFERENCES

Abbott, M.B., McGowan, A., and Warren, I.R., 1981, Numerical modeling of free-surface flows that are two-dimensional in plan, *in* Fischer, H.B., ed., Transport models for inland and coastal waters: New York, Academic Press, p. 222-283.

Amein, M., and Airan, D.S., 1976, Mathematical modeling of hurricane surge in Pamlico Sound, North Carolina: Raleigh, University of North Carolina Sea Grant College Program, North Carolina State University, Report No. UNC-SG-76-12, 102 p.

Anwar, H.O., 1983, Turbulence measurements in stratified and well-mixed estuarine flows: Journal of Estuarine, Coastal, and Shelf Science, v. 17, p. 243-260.

Anwar, H.O., and Atkins, R., 1980, Turbulence measurements in simulated tidal flow: Journal of the Hydraulics Division, American Society of Civil Engineers, v. 106, no. HY8, p. 1273-1289.

Arakawa, A., 1966, Computational design of long-term numerical integration of the equations of fluid motion: I. Two-dimensional incompressible flow: Journal of Computational Physics, v. 1, no. 1, p. 119-143.

Bales, J.D., and Nelson, T.M., 1988, Bibliography of hydrologic and water-quality investigations conducted in or near the Albemarle-Sounds region, North Carolina: U.S. Geological Survey Open-File Report 88-480, 148 p.

Beauchamp, C.H., and Spaulding, M.L., 1978, Tidal circulation in coastal seas, *in* Proceedings of the symposium on verification of mathematical and physical models in hydraulic engineering: New York, American Society of Civil Engineers, p. 518-528.

Bellis, V., O'Connor, M.P., and Riggs, S.R., 1975, Estuarine shoreline erosion in the Albemarle-Pamlico region of North Carolina: Raleigh, University of North Carolina Sea Grant College Program, North Carolina State University, Report No. UNC-SG-75-29, 67 p.

Benque, J., Cunge, J., Fevillet, J., Haugel, A., and Holly, F., 1982, New method for tidal current computation: Journal of the Waterways, Ports, and Coastal Ocean Division, American Society of Civil Engineers, v. 108, p. 396-417.

Chu, W.-S., Liou, J.-Y., and Flenniken, K.D., 1989, Numerical modeling of tide and current in central Puget Sound: Comparison of a three-dimensional and a depth-averaged model: Water Resources Research, v. 25, no. 4, p. 721-734.

Copeland, B.J., Hodson, R.G., Riggs, S.R., and Pendleton, E.C., 1984, The ecology of the Pamlico River, North Carolina—an estuarine profile: Washington, D.C., U.S. Fish and Wildlife Service, Report No. FWS/OBS-82/06, 83 p.

Creager, C.S., Baker, J.P., and North Carolina Division of Environmental Management, 1991, North Carolina's whole basin approach to water quality management—program description: Raleigh, North Carolina Department of Environment, Health, and Natural Resources, Water Quality Section, Report No. 91-08, 54 p.

Ditmars, J.D., Adams, E.E., Bedford, K.W., and Ford, D.E., 1987, Performance evaluation of surface water transport and dispersion models: Journal of Hydraulic Engineering, v. 113, no. 8, p. 961-980.

Douglas, J., 1955, On the numerical integration of $d^2u/dx^2 + d^2u/dy^2 = du/dt$ by implicit methods: Journal of the Society of Industrial Applied Mathematics, v. 3, no. 1, p. 42-65.

Eckert, C., 1958, The equation of state of water and sea water at low temperatures and pressures: American Journal of Science, v. 256, p. 240-250.

Elder, J.W., 1959, The dispersion of marked fluid in turbulent shear flow: Journal of Fluid Mechanics, v. 5, p. 544-560.

Garratt, J.R., 1977, Review of drag coefficients over oceans and continents: Monthly Weather Review, v. 105, p. 915-929.

Garrett, R.G., 1992, Water-quality data from continuously monitored sites in the Pamlico and Neuse River estuaries, North Carolina, 1990-91: U.S. Geological Survey Open-File Report 92-110, 196 p.

_____ 1994, Water-quality data from continuously monitored sites in the Pamlico and Neuse River estuaries, North Carolina, 1991-92: U.S. Geological Survey Open-File Report 94-27, 161 p.

Garrett, R.G., and Bales, J.D., 1991, Water-quality data from continuously monitored sites in the Pamlico and Neuse River estuaries, North Carolina, 1989-90: U.S. Geological Survey Open-File Report 91-465, 151 p.

Garvine, R.W., 1985, A simple model of estuarine subtidal fluctuations forced by local and remote wind stress: Journal of Geophysical Research, v. 90, no. C6, p. 11945-11948.

Giese, G.L., and Bales, J.D., 1992, Two-dimensional circulation modeling of the Pamlico River estuary, North Carolina, *in* Spaulding, M.L., Bedford, K., Blumberg, A., Cheng, R., and Swanson, C., eds., Estuarine and coastal modeling: New York, American Society of Civil Engineers, p. 607-619.

Giese, G.L., Eimers, J.L., and Coble, R.W., 1991, Simulation of ground-water flow in the Coastal Plain aquifer system of North Carolina: U.S. Geological Survey Open-File Report 90-372, 178 p.

Giese, G.L., Wilder, H.B., and Parker, G.G., 1985, Hydrology of major estuaries and sounds of North Carolina: U.S. Geological Survey Water-Supply Paper 2221, 108 p.

Goodwin, C.R., 1987, Tidal-flow, circulation, and flushing changes caused by dredge and fill in Tampa Bay, Florida: U.S. Geological Survey Water-Supply Paper 2282, 88 p.

Gordon, C.M., and Dohne, C.F., 1973, Some observations of turbulent flow in a tidal estuary: Journal of Geophysical Research, v. 78, no. 12, p. 1971-1978.

Hamilton, P., 1992, Modeling nearshore currents in the vicinity of the Endicott Causeway, Alaska, *in* Spaulding, M.L., Bedford, K., Blumberg, A., Cheng, R., and Swanson, C., eds., Estuarine and coastal modeling: New York, American Society of Civil Engineers, p. 227-239.

Hardy, A.V., and Hardy, J.D., 1971, Weather and climate in North Carolina: Raleigh, Agricultural Experiment Station, North Carolina State University, Bulletin 396.

Harned, D.A., and Davenport, M.S., 1990, Water-quality trends and basin activities and characteristics for the Albemarle-Pamlico estuarine system, North Carolina and Virginia: U.S. Geological Survey Open-File Report 89-11, 164 p.

Horton, D.B., Kuenzler, E.J., and Woods, W.J., 1967, Current studies in the Pamlico River and estuary of North Carolina: Raleigh, The University of North Carolina Water Resources Research Institute, Report No. 6, 21 p.

Hunter, J.R., and Hearn, C.J., 1987, Lateral and vertical variations in the wind-driven circulation in long, shallow lakes: Journal of Geophysical Research, v. 92, no. C12, p. 13106-13114.

Jarrett, J.T., 1966, A study of the hydrology and hydraulics of Pamlico Sound and their relation to the concentration of substances in the sound: Raleigh, North Carolina, M.S. thesis, Department of Civil Engineering, North Carolina State University, 156 p.

King, B., 1992, A predictive model of the currents in Cleveland Bay, *in* Spaulding, M.L., Bedford, K., Blumberg, A., Cheng, R., and Swanson, C., eds., Estuarine and coastal modeling: New York, American Society of Civil Engineers, p. 746-758.

Large, W.G., and Pond, S., 1981, Open ocean momentum flux measurements in moderate to strong winds: Journal of Physical Oceanography, v. 11, p. 324-336.

Lean, G.H., and Weare, T.J., 1979, Modeling two-dimensional circulation flow: Journal of the Hydraulics Division, American Society of Civil Engineers, v. 105, no. HY1, p. 17-26.

Leendertse, J.J., 1987, Aspects of SIMSYS2D, a system for two-dimensional flow computation: Santa Monica, Calif., RAND Corp., Report No. R-3572-USGS, 80 p.

_____1972, A water-quality simulation model for well mixed estuaries and coastal seas--volume IV, Jamaica Bay tidal flows: Santa Monica, Calif., RAND Corp., Report No. R-1009-NYC.

Leendertse, J.J., and Gritton, E.C., 1971, A water-quality simulation model for well mixed estuaries and coastal seas—volume III, Jamaica Bay simulation: Santa Monica, Calif., RAND Corp., Report No. R-709-NYC.

Leendertse, J.J., Langerak, A., and de Ras, M.A.M., 1981, Two-dimensional tidal models for the Delta Works, *in* Fischer, H.B., ed., Transport models for inland and coastal waters: New York, Academic Press, p. 408-450.

Masch, F.D., and Brandes, R.J., 1975, Simulation of tidal hydrodynamics—Masonboro Inlet, *in* Proceedings of the symposium on modeling techniques: New York, American Society of Civil Engineers, p. 220-239.

Mendelsohn, D.L., and Swanson, J.C., 1992, Application of a boundary fitted coordinate transport model, *in* Spaulding, M.L., Bedford, K., Blumberg, A., Cheng, R., and Swanson, C., eds., Estuarine and coastal modeling: New York, American Society of Civil Engineers, p. 382-417.

Miller, R.L., Bradford, W.L., and Peters, N.E., 1988, Specific conductance—theoretical considerations and application to analytical quality control: U.S. Geological Survey Water-Supply Paper 2311, 16 p.

North Carolina Department of Natural Resources and Community Development, 1987, Albemarle-Pamlico Estuarine Study work plan: Raleigh, North Carolina Department of Natural Resources and Community Development, 77 p.

_____ 1989, Tar-Pamlico River basin nutrient sensitive waters designation and nutrient management strategy: Raleigh, Division of Environmental Management, Report No. 89-07, 40 p.

Partch, E.N., and Smith, J.D., 1978, Time dependent mixing in a salt wedge estuary: Journal of Estuarine and Coastal Marine Science, v. 6, p. 3-19.

Peaceman, D.W., and Rachford, H.H., 1955, The numerical solution of parabolic and elliptic differential equations: Journal of the Society of Industrial Applied Mathematics, v. 3, no. 1, p. 28-41.

Pietrafesa, L.J., Janowitz, G.S., Chao, T.-Y., Wiesberg, R.H., Askari, F., and Noble, E., 1986, The physical oceanography of Pamlico Sound: Raleigh, University of North Carolina Sea Grant College Program, North Carolina State University, Working Paper 86-5, 125 p.

Rader, D.N., Loftin, L.K., McGee, B.A., Dorney, J.R., and Clements, T.J., 1987, Surface-water concerns in the Tar-Pamlico River basin: Raleigh, Division of Environmental Management, North Carolina Department of Natural Resources and Community Development, Report No. 87-04, 113 p.

Ridderinkhof, H., and Zimmerman, J.T.F., 1990, Mixing processes in a numerical model of the Western Dutch Wadden Sea, *in* Cheng, R.T., ed., Residual currents and long-term transport: New York, Springer-Verlag, Coastal and Estuarine Studies, v. 38, p. 194-209.

_____ 1992, Chaotic stirring in a tidal system: Science, v. 258, p. 1107-1111.

Riggs, S.R., Powers, E.R., Bray, J.T., Stout, P.M., Hamilton, C., Ames, D., Moore, R., Watson, J., Lucas, S., and Williamson, M., 1989, Heavy metal pollutants in organic-rich muds of the Pamlico River estuarine system—their concentration, distribution, and effects upon benthic environments and water quality: Raleigh, Albemarle-Pamlico Estuarine Study, North Carolina Department of Environment, Health, and Natural Resources, Project No. 89-06, 108 p.

Roache, P.J., 1982, Computational fluid dynamics: Albuquerque, N.M., Hermosa Publishers, 446 p.

Rodi, W., 1978, Mathematical modeling of turbulence in estuaries, *in* Nihoul, J.C.J., ed., Hydrodynamics of fjords and estuaries: Amsterdam, Elsevier Scientific Publishing Co., p. 14-26.

_____ 1987, Examples of calculation methods for flow and mixing in stratified fluids: Journal of Geophysical Research, v. 92, no. C5, p. 5305-5328.

Schaffranek, R.W., and Baltzer, R.A., 1988, A simulation technique for modeling flow on floodplains and in coastal wetlands, *in* Abt, S.R., and Gessler, J., eds., Hydraulic engineering—proceedings of the 1988 national conference: New York, American Society of Civil Engineers, p. 732-739.

Schmalz, R.A., 1985, User guide for WIFM-SAL—a two-dimensional vertically integrated, time-varying estuarine transport model: Vicksburg, Miss., U.S. Army Corps of Engineers Waterways Experiment Station, Instruction Report EL-85-1, 44 p.

Schwartz, F.J., and Chestnut, A.F., 1973, Hydrographic atlas of North Carolina estuarine and sound waters, 1972: Raleigh, University of North Carolina Sea Grant College Program, North Carolina State University, Report No. UNC-SG-73-12, 132 p.

Shankar, N.J., Cheong, H.F., and Chen, C.T., 1992, Modeling of coastal circulation in Singapore waters—a hybrid approach, *in* Spaulding, M.L., Bedford, K., Blumberg, A., Cheng, R., and Swanson, C., eds., Estuarine and coastal modeling: New York, American Society of Civil Engineers, p. 669-683.

Signell, R.P., 1992, Tide- and wind-driven flushing of Boston Harbor, Massachusetts, *in* Spaulding, M.L., Bedford, K., Blumberg, A., Cheng, R., and Swanson, C., eds., Estuarine and Coastal Modeling: New York, American Society of Civil Engineers, p. 594-606.

Signell, R.P., and Butman, B., 1992, Modeling tidal exchange and dispersion in Boston Harbor: Journal of Geophysical Research, v. 97, no. C10, p. 15591-15606.

Stanley, D.W., 1988, Water quality in the Pamlico River Estuary, 1967-1986—a report to Texasgulf Chemicals Company: Greenville, N.C., Institute for Coastal and Marine Resources, East Carolina University, ICMR Technical Report 88-01, 199 p.

Svendsen, H., Mikki, S.R., and Golmen, L.G., 1992, Frontal dynamics and circulation of the upper layer of a fjord system with complicated topography, *in* Spaulding, M.L., Bedford, K., Blumberg, A., Cheng, R., and Swanson, C., eds., Estuarine and coastal modeling: New York, American Society of Civil Engineers, p. 252-267.

Thomas, W.A., McAnally, W.H., and Letter, J.V., 1990, Generalized computer program system for open-channel flow and sedimentation; TABS system; volume 1: general overview; appendix f: user instructions for RMA-2V, a two-dimensional model for free-surface flows: Vicksburg, Miss., Waterways Experiment Station, U.S. Army Corps of Engineers, 54 p.

Thompson, D.B., 1992, Numerical methods 101—convergence of numerical models, *in* Jennings, M., and Bhowmik, N.G., eds., Hydraulic engineering; saving a threatened resource—in search of solutions: New York, American Society of Civil Engineers, p. 398-403.

Treece, M.W., Jr., and Bales, J.D., 1992, Hydrologic and water-quality in selected agricultural drainages in Beaufort and Hyde Counties, North Carolina, 1988-90: U.S. Geological Survey Open-File Report 92-498, 89 p.

van Dam, G.C., 1988, Models of dispersion, *in* Kullenberg, G., ed., Pollutant transfer and transport in the sea—volume I: Cleveland, Ohio, CRC Press, p. 91-160.

Watanabe, M., Harleman, D.R.F., and Vasiliev, O.F., 1983, Two- and three-dimensional mathematical models for lakes and reservoirs, *in* Orlob, G.T., ed., Mathematical modeling of water quality—streams, lakes, and reservoirs; New York, John Wiley & Sons, International Series on Applied Systems Analysis, v. 12, p. 274-336.

Weare, T.J., 1979, Errors arising from irregular boundaries in ADI solutions of the shallow-water equations: International Journal for Numerical Methods in Engineering, v. 14, p. 921-931.

Weisberg, K.H., and Pietrafesa, L.J., 1983, Kinematics and correlation of the surface wind field in the South Atlantic Bight: Journal of Geophysical Research, v. 88, no. C8, p. 4593-4610.

Wells, J.T., 1989, A scoping study of the distribution, composition, and dynamics of water-column and bottom sediments—Albemarle-Pamlico estuarine system: Morehead City, N.C., Albemarle-Pamlico Estuarine Study, North Carolina Department of Natural Resources and Community Development, Project No. 89-05, 39 p.

Westerink, J.J., and Gray, W.G., 1991, Progress in surface water modeling: Reviews of Geophysics, Supplement, U.S. National Report to International Union of Geodesy and Geophysics, 1987-90, p. 210-217.

Wilder, H.B., Robinson, T.M., and Lindskov, K.L., 1978, Water resources of northeast North Carolina: U.S. Geological Survey Water Resources Investigations 77-81, 113 p.

Williams, A.B., Posner, G.S., Woods, W.J., and Duebler, E.E., 1967, A hydrographic atlas of larger North Carolina sounds: Morehead City, N.C., Institute of Marine Sciences, University of North Carolina, Report No. UNC-SG-73-02, 129 p.

Winner, M.D., and Coble, R.W., 1989, Hydrogeologic framework of the North Carolina Coastal Plain aquifer system: U.S. Geological Survey Open-File Report 87-690, 155 p.

Wu, J., 1969, Wind stress and surface roughness at air-sea interface: Journal of Geophysical Research, v. 74, no. 2, p. 444-445.

Yeh, H.H., Chu, W.-S., and Dahlberg, O., 1988, Numerical modeling of separation eddies in shallow water: Water Resources Research, v. 24, no. 4, p. 607-614.

Ziegler, C.K., Bales, J.D., Robbins, J.C., and Blumberg, A.F., 1994, A comparative analysis of estuarine circulation simulation using laterally averaged and vertically averaged hydrodynamic models, *in* Spaulding, M.L., ed., Estuarine and coastal modeling: New York, American Society of Civil Engineers, 14 p.